Master Thesis, Department of Geosciences

Long-term observations of snow spatial distributions at Hellstugubreen and Gråsubreen, Norway

An investigation in winter balance, time stability, probing reliability, and reduced survey designs

Alexander Walmsley

UNIVERSITY OF OSLO

FACULTY OF MATHEMATICS AND NATURAL SCIENCES

Long-term observations of snow spatial distributions at Hellstugubreen and Gråsubreen, Norway

An investigation in winter balance, time stability, probing reliability, and reduced survey designs

Alexander Walmsley

Master Thesis in Geosciences

Discipline: Physical Geography, Hydrology and Geomatics

Department of Geosciences

Faculty of Mathematics and Natural Sciences

University of Oslo

July 2015

Supervisors: Dr Liss Marie Andreassen and Professor Jon Ove Hagen

This work is published digitally through DUO – Digitale Utgivelser ved UiO

http://www.duo.uio.no

It is also catalogued in BIBSYS (http://www.bibsys.no/english)

Cover image: Hellstugubreen, north-facing view. Photograph taken 16/05/2014. Photograph credit: author's own.

Abstract

Snow accumulation is the most spatially heterogeneous component of glacier mass balance calculations, yet it exhibits robust time stability in spatial distributions. This thesis examines the characteristics of time stability, the reliability and representativeness of snow probing locations, and the scope for reducing the snow measurement surveys at two glaciers. The Norwegian Water Resources and Energy Directorate's (NVE) long-term snow distribution archives at Hellstugubreen and Gråsubreen cover 48 and 44 years respectively, and provide a unique opportunity to investigate snow distributions on two proximate glaciers, allowing inter-comparisons. Throughout, data years are categorised into quarters, thus exposing variable snow spatial distribution patterns relative to overall precipitation levels.

Stability maps and statistics are computed on a cell-by-cell basis. Results find strong spatial heterogeneity in snow distributions, and increasing time stability with snow levels at both glaciers. Good time stability is also found at low precipitation levels at Gråsubreen. Overall, Hellstugubreen is more time stable than Gråsubreen. Reliability maps of representative probing locations are used to reduce survey designs, allowing resampling and reconstructions of winter balances. One index site for glacier-wide winter balance and one probing location per 50 m elevation interval are used. These calculations are done for all compiled data years, or combined quarters of data years.

Winter balance reconstructions produce records within <0.10 m w.e. and <0.15 m w.e. of official winter balances at Hellstugubreen and Gråsubreen. Mean percentage errors are <6.2 % and <13.7 % respectively. The most accurate winter balance reconstructions use one probing per 50 m elevation interval, and quartered data years. Using centreline only probings underestimates winter balance, most dramatically at Hellstugubreen. Several strongly irregular snow spatial distribution years are found, creating inconsistent results. These years are considered to be affected by localised irregular wind conditions.

Keywords: glaciological mass balance, winter balance, snow spatial distribution observations, time stability, reliability, representativeness, survey design.

Acknowledgements

Supervision from Dr Liss Andreassen (NVE) and Professor Jon Ove Hagen (University of Oslo) is gratefully acknowledged. Their kind mentoring, support and patience throughout have made this project possible. Both supervisors provided insightful and productive discussions, as well as techning me fieldwork techniques, for which I am thankful. Trond Eiken, Oda Røyset, Mathieu Tachon and Odd are acknowledged for their fieldwork assistance. Dr Liss Andreassen is thanked for providing valuable feedback on an earlier manuscript of this thesis. Data were received with thanks from NVE, and to all those who assisted in creating and compiling the datasets since the 1960s. Meteorological data were received from eKlima.

Fieldwork costs were covered by the University of Oslo, and a further fieldwork campaign I participated on was funded by NVE. Dr Liss Andreassen is thanked for arranging my part-time employment as a department engineer at the Snow, Ice and Glaciers Section at NVE. I express gratitude to the Norwegian state and the Ministry for Education and Research (KD) for funding higher education tuition.

During my masters studies I was able to study the course AT-329, Cold Region Field Investigations, at the University Centre in Svalbard (UNIS), and am appreciative of the tuition. I was fortunate to partake in the International Summer School in Glaciology in McCarthy, Alaska, with the support of GlacioEX funding.

I would like to acknowledge my undergraduate thesis supervisor, Dr Ian Willis, who first suggested I consider studying at the University of Oslo. I am grateful for the camaraderie from fellow Physical Geography masters students at the University of Oslo. Lowri Richards and my family are thanked for their kind support and encouragement throughout the course of the masters studies.

Oslo, July 2015

Table of contents

List of figures

Appendix

List of tables

List of acronyms

AAR ……..Accumulation area ratio
AD ...…….Anderson-Darling normality test
B_a ……....Glacier-wide specific annual balance
B_s …….…….…….Glacier-wide specific summer balance
b_s …….……...Summer balance at one point location
B_w ……...……..……Glacier-wide specific winter balance
b_w ……..Winter balance at one point location
CSDP ……...….Climatological snow distribution pattern
CV …….Coefficient of variability
DTM ……...Digital terrain model
GIS ……...Geographical information system
IPCC ……..The Intergovernmental Panel on Climate Change
IQR ……...Interquartile range
LOP ……..Lots of points
m a.s.l. ……Metres above sea level
m w.e. .…….Metres water equivalent
NAO ……...North Atlantic Oscillation
NVE .……The Norwegian Water Resources and Energy Directorate
RMSE ……...Root mean square error
SWE ……Snow water equivalent
UTC …….Coordinated universal time
WGMS ……..The World Glacier Monitoring Service
WS ……...Weather station

1. Introduction

Mass balance measurements determine annual changes of glacier mass in response to climatic and environmental forcing, and form an integral part of cryospheric knowledge. Traditional mass balance monitoring has been largely developed in the early-mid twentieth century (Zemp *et al*., 2009; Braithwaite, 2002), and contributes scientific information to a number of fields. This includes climate change indicators (see IPCC, 2013), humanitarian causes such as water security (see Scheffran and Battaglini, 2010), and water resource monitoring for economic enterprises such as hydropower (Grünewald *et al*., 2010; Lehning *et al*., 2008). This diversity has led to glacier mass balance monitoring taking on a vital role in cryospheric sciences.

Traditional glaciological mass balance monitoring consists of measuring the water equivalent of winter snow accumulation and the level of summer ablation at glaciers using discrete point data. Data is interpolated across the glacier area, and results summed to calculate the contiguous net mass balance for an annual period (Cogley *et al*., 2011). Snow accumulation is considered to vary in space to a greater degree than either snow densities (Boorman *et al*., 2013; Mizukami and Percia, 2005) or ablation (Schirmer *et al*., 2011). In calculating mass balance, snow spatial distributions on glaciers are a factor that must be accounted for in traditional mass balance monitoring techniques, in order to fully understand and evaluate snow distributions and masses (McKay and Gray, 2004; Pelto, 2000).

Despite strong spatial heterogeneity, many studies report a robust degree of time stability in snow spatial distribution patterns (Winstral and Marks, 2014; López-Moreno *et al*., 2011; Sturm and Wagner, 2010; Deems *et al*., 2008; Jansson and Pettersson, 2007). Consistent time stable snow spatial distributions at the end of accumulation seasons may aid in fully evaluating mass balance measurements. Time stability is geographically unique to individual glaciers, both in terms of distribution patterns, and the degree of time stability (Pelto, 2000), and is not without inconsistencies and irregularities (Winstral and Marks, 2014; Sturm and Wagner, 2010). These snow spatial distribution characteristics warrant further academic exploratory investigations where suitable data series exist.

The accuracy of snow accumulation estimates can be influenced by monitoring survey designs (Jansson and Pettersson, 2007; Kronholm and Birkeland, 2007; Pelto, 2000). Time stability introduces the potential for annual snow accumulation surveys to take advantage of repeat spatial distribution patterns. Specific areas on a glacier may be both representative of winter balances for a wider region of the glacier, and stable through time. Where these factors are synchronous, winter accumulation survey designs may constructively use the attributes of well-developed time stable areas, and reliable and representative snow measurement areas, to introduce reduced survey networks whilst maintaining accuracy.

Relationships within snow distribution patterns must be explored to evaluate *where* and *how* snow distributions vary, based on long-term extensive monitoring programmes. Multivariate relationships may influence snow distribution on a range of spatial and temporal scales to produce end of accumulation season snow distributions (Erickson *et al*., 2005). By using NVE's extensive archives of snow distribution on two mountain glaciers in southern Norway, Hellstugubreen and Gråsubreen, this thesis attempts to uncover some of the characteristics of snow distribution time stability; to locate representative point measurement locations; and to assess the scope and implications for reduced winter balance measurement surveys.

1.1 Thesis structure

This thesis follows a conventional structure, with five main sections: Introduction, Methodology and Data Processing, Results, Discussion, and Summary and Conclusions. Terminology and definitions referred to in this thesis are first set out to inform readers of specific nomenclature. Key concepts of the thesis are then outlined, before explaining the motivation, aims and objectives of the thesis. A scientific background is given to mass balance measurements, time stability, reliable and representative data, survey designs, and controls on snow distributions. The study areas are then described. The Methodology section concerns both the historical field methodologies, and data processing techniques and tools used in this thesis. The Results section is split between Hellstugubreen and Gråsubreen, with

results from each glacier separately outlined. For each glacier, first the statistical distributions of data are given, before the stability, reliability, and survey design results are described. In the Discussion section, both glaciers are examined together, with comparisons and explanations explored for causes and implications of findings. Attention is given to the differences and similarities of the glaciers, relative to appropriate literature. The Summary and Conclusions section outlines the findings, their explanations and implications, with recommendations for further research.

1.2 Terminology and definitions

This thesis complies with the 2011 publication the *Glossary of Glacier Mass Balance and Related Terms* (Cogley *et al*., 2011), where possible. This undertaking has aligned and clarified previously uncertain terms and techniques, many of which were previously accredited to Anonymous (1969), whereby nomenclature had been added to in a piecemeal fashion. Here, B_w is used to refer to the glacier wide specific winter balance, and b_w refers to the winter balance at one point. B_s and b_s represent the same respective features for summer balances. B_a refers to the glacier-wide specific annual balance, the sum of B_w and B_s, given that B_s is negative. All glacier-wide mass balance measurements in this thesis are specific, meaning they are relative to glacier area thus allowing glacier inter-comparison. All figures and calculations in this thesis use the metres water equivalent unit (m w.e.).

Further terminology is specific to this thesis. *Data year(s)* refers to all of the b_w points for one annual accumulation period, in snow water equivalent (SWE). The term *all years of data* refers to the agglomeration of all available b_w data from all years. This is often used in comparison to B_w *quarter(s)*, which refers to the agglomeration of data years which fall only within a specified quarter of the total B_w range. For example, if all recorded B_w values at a glacier ranged between 1 and 2 m w.e., B_w quarter 1 would refer to the data years where B_w ranged between 1 and 1.25 m w.e., etc.

Distributions of data are commented on extensively. A distinction is given between *statistical data distributions*, which refers to the statistical nature of data years, for example normal (Gaussian), bimodal, etc. and the *snow spatial distributions*, which refers to the physical locations in x, y, z coordinates, of snow on a glacier.

Stability maps are given in sections 3.1.3ii and 3.2.3ii, and are discussed in section 4.2.2. *Stability* is a measure of one cell's winter balance variation through time, and the term *time stability* is also used. *Variability zones* are contiguous areas of stability in adjacent cells, which fall in the same set range.

Survey reliability maps in sections 3.1.4 and 3.2.4, and mass balance reconstructions based on resampling these maps found in sections 3.1.5 and 3.2.5, are computed using either one b_w index site location, or a b_w location in every 50 m elevation interval. Reconstructions are computed for all years of data, and B_w quarters. Where B_w quarters are used, the data is compiled for all B_w quarters in order to gain a full dataset. Four reliability datasets are made: $B_w one_{all}$ means the B_w for the entire glacier based on one b_w location, using all years of data. $B_w one_q$ uses one b_w location, using the combination of all B_w quarters. $B_w ele_{all}$ means the B_w for the entire glacier based on one b_w location per 50 m elevation interval, using all years of data. $B_w ele_q$ means the B_w for the entire glacier based on one b_w location per 50 m elevation interval, using the combination of all B_w quarters.

The key concepts stability, reliability, precision and accuracy are further outlined in section 1.3 below.

1.3 Key concepts: Stability, reliability

Optimal winter balance measurement surveys should comply with two key characteristics: they should sample areas that are stable in time, and are reliable and representative. Both of these concepts can occur independently or synchronously; they are not mutually exclusive. The ability of these concepts to overlap is shown figuratively in Figure 1.3.1.

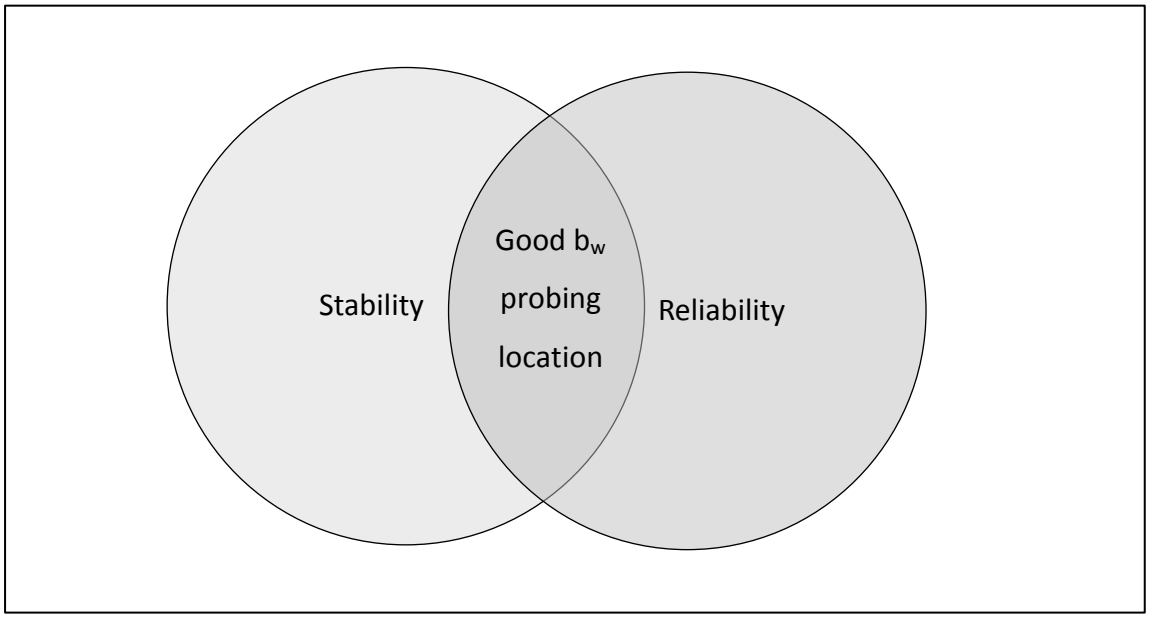

Figure 1.3.1 Venn diagram (used to show possible logical relationships between a set of characteristics) for key concepts: Stability and reliability.

Stability is a measure of how a specific area remains at a set level through time. The set level can be a relative measure. 'Time stability' clarifies that the temporal aspect of stability is measured. Variability is a measure of the range of stability. Variability zones are contiguous areas where variability ranges are similar within a set boundary. Time stability is important in snow spatial distribution evaluation because it is a measure of how probable it is for a specific area to give precise results from year to year. Here, stability is synonymous with precision.

Reliability is a measure of how accurate and representative a measurement is: for winter balance, this means that a snow depth measurement is at or near the values for the wider area. For example, a reliable measurement at 1925 m a.s.l. may fall within 10 % of the mean value of all average measurements for the elevation interval 1900-1950 m a.s.l. Reliability is important in survey optimisation because it is a measure of how representative and accurate a given measurement is. Here, reliability is synonymous with accuracy.

A stable area may produce consistent results every year, however, if this is unreliable, the results can be entirely inaccurate. Conversely, a specific location may produce reliable

results for one year, yet may produce entirely inappropriate results in a different year, again producing inaccuracies. Ideally, when considering reduced survey designs both stability and reliability should be fulfilled to a satisfactory extent.

1.4 Motivation

Whilst NVE operates one of the most successful and long-lived glaciological mass balance monitoring programs and contributes extensively to mass balance literature (see Andreassen and Oerlemans, 2009; Andreassen *et al*., 2007; Rasumssen and Andreassen, 2005; Andreassen *et al*., 2002; Haakensen, 1986), relatively little detailed attention has been given to the measurement surveys themselves. Indeed, the field methodology of glaciological mass balance recording has remained largely consistent through the greater part of the twentieth century, and into the twenty-first century (Kjøllmoen, 2011; Andreassen *et al*., 2005). The survey designs of long-term glaciological mass balance measurements in Norway have not been spatially evaluated beyond the heuristic interpretation that with ample measurements using the 'lots of points' (LOP) spatial coverage technique (Sturm and Wagner, 2010, Grayson *et al*., 2002), accurate and precise results will be produced. This is used regardless of the snow spatial distribution stability, or the reliability and representativeness of b_w point measurements. Accumulation measurements are understood to vary in space to a high degree, creating spatial heterogeneity of snow distribution (Mott *et al*., 2008; Machguth *et al*., 2006). Stable snow distributions could, however, facilitate simplified snow measurement surveys.

In order to investigate the precision and accuracy of winter balance measurements, the time stability of snow spatial distribution and the reliability of measurement locations should be quantified, and appropriate survey designs produced and tested. As noted above in section 1.3, stability and reliability are independent, yet potentially synchronous properties, each requiring space specific testing. Many commentators posit that snow distribution patterns feature time stability (Wistral and Marks, 2014; Schirmer *et al*., 2011; Sturm and Wagner, 2010; Deems *et al*, 2008; Balk and Elder, 2000; Jansson, 1999). The degree of stability is

not, however, constant (Sturm and Wagner, 2010; Jansson and Pettersson, 2007). Investigations have, in general, considered overall spatial patterns, however, they have not quantified inconsistencies well. Nor have they attempted to group and categorise different snow precipitation levels to further evaluate the causes and effects of variable time stability in spatial snow distribution patterns.

Time stable areas are important for mass balance measurements, however, this does not account for the representativeness of results obtained. Jansson and Pettersson (2007) attempt to quantify the representativeness of probing results for winter balance measurements on Storglaciären, Sweden. They consider the correlation of b_w probing measurements to B_w overall mean measurements. This technique measures the relative correlation to a mean value, and does not account for the raw probing value. Here, this thesis aims to investigate snow probing representativeness by seeking reliable probing locations and developing multiple survey designs based on these locations.

The number of b_w point measurements is often dictated by field conditions, resulting in variable coverage between data years. Where a limited number of measurements can feasibly be taken, random errors can be magnified. The number of b_w probings taken in a given year show significant variation, between 29-240 and 36-158 for Hellstugubreen and Gråsubreen respectively. Similarly, the average nearest distance between adjacent probings varies between 42.7-147.1 m and 50.4-109.8 m at Hellstugubreen and Gråsubreen. These inconsistencies highlight the variable data collected each year, and demonstrate the need for reliable data collection, especially when few probings can feasibly be taken.

Many studies attest that snow probing surveys can be reduced and attain similarly accurate results (Winstral and Marks, 2014; López-Moreno *et al.*, 2011; Cogley, 1999; Jansson, 1999), however, few studies have attempted this in reality, and tested the output results. This investigation re-samples survey data, based on multiple survey designs, in order to reconstruct and compare the results relative to the NVE official B_w result reference values.

1.4.1 Aims and objectives

This thesis will investigate the long-term observations of snow distribution patterns on two Norwegian glaciers, Hellstugubreen and Gråsubreen. Two main criteria will be used in investigating long-term snow spatial distribution observations: stability through time, and reliability of snow survey measurement locations. By working on two glaciers, this thesis aims to draw out comparisons in time stability of snow distributions, and the reliability of snow surveys at different sites, and better understand the geographical contexts of these differences.

By using these criteria as guidelines, this thesis first aims to assess the degree of time stability observed in snow distributions through creating stability maps, snow spatial distribution error assessments, and spatial correlations. Time stability will be assessed relative to winter balance levels, to explore how stable distribution patterns co-vary with B_w quarters. This technique assesses both whether high or low B_w data years are more or less stable, and the spatial patterns of such stabilities.

The thesis then aims to investigate whether reliable snow probing locations can be found on the glaciers to measure winter balance. These locations are then used in attempts to reduce the survey size whilst maintaining accurate and precise measurements. Survey reductions operate on three levels: first, one index site is sought to represent the B_w of an entire glacier; second, a b_w probing in every 50 m elevation interval is sought to represent that area-elevation region; third, centreline only probings are assessed. The first two reduced survey designs are created using all data years, or an agglomeration of B_w quarters. The thesis then aims to reconstruct B_w values based on the reduced survey designs, to test their accuracy relative to the reference official B_w record.

The thesis aims to discuss possible causes and controls of variable snow spatial distributions. In particular, comparisons between the geographical and topographical settings of the glaciers will be discussed as potential controls on snow spatial distribution patterns. Wind frequency distribution data from weather stations (WSs) will be used to investigate wind as a potential control on snow spatial distributions.

1.5 Scientific background

This thesis is grounded in the scientific context of mass balance reporting, observations of snow spatial distribution, time stability, and snow survey design reliability and representativeness. These broad themes are all related by their roles in fully understanding winter balance characteristics and processes on mountain glaciers, and accurately reporting mass balance measurements. The scientific background of mass balance reporting is first outlined, before considering literature in time stability of snow in alpine environments. Further, the concepts of representative and reliable snow sampling are discussed. Finally, an overview of the mechanisms controlling snow spatial distributions is offered; first by mechanisms operating at varying spatial scales, and then by mechanisms functioning at varying temporal scales.

1.5.1 Mass balance

Mass balance reporting is a central theme in glaciology as a discipline, and is highly valued in its own right, with results reported to the World Glacier Monitoring Service (WGMS). Mass balance measurements have dominated many of the advancements in technology adopted by glaciology, namely in remote sensing using laser, radar and gravimetric methods (Tedesco, 2015; see Bamber and Rivera, 2007, for a review of remote sensing applications to glacier mass balance), and recently drone operated photogrammetry and structure-from-motion post-processing (Carrivick *et al*., 2013). Despite these advances, the traditional glaciological mass balance techniques developed in the early-mid twentieth century still play a central role in reference mass balance assessments (Zemp *et al*., 2009).

Glaciological methods have used the LOP heuristic assessment concerning the appropriate numbers of discrete point data of both b_w and b_s to calculate B_w and B_s, and thus B_a. b_w values have been converted to m w.e. values using a depth-density conversion based on density pit data. Conventionally, mean b_w and b_s values have been calculated for 50 m

elevation intervals, and multiplied by their area-elevation values to calculate volume balances. Glacier-wide specific mass balance can be computed by dividing the sum of area-elevation volume balances by the area of the glacier, thereby making mass balance records at different glaciers comparable (Cogley et al., 2011).

The method outlined above has come under increased scrutiny in recent years, with concern over cumulative systematic errors in mass balance calculations (Zemp *et al*., 2010; 2013). Reanalysis has been used to re-calculate, and if necessary, adjust mass balances (Zemp *et al*., 2010; Thibert *et al*., 2008; Holmund *et al*., 2005). Error analysis has been concerned with possible errors in the representativeness and reliability of results obtained using the LOP method. Multiple studies have attempted to evaluate the accuracy and necessary sample size of traditional glaciological mass balance measurements (Winstral and Marks, 2014; Jansson and Pettersson, 2007; Pelto, 2000; Cogley, 1999; Fountain and Vecchia, 1999). Further, potential errors in density measurements have been identified, which may significantly affect B_w values (Funk *et al*., 1997). The important reference traditional glaciological mass balance technique is not infallible, and should be evaluated to the greatest possible extent to understand the rigorousness and reliability of mass balance reporting results.

1.5.2 Time stability

Time stability refers to a repeated, or otherwise, pattern of spatial distribution. Time stability in snow spatial distributions are observed in multiple studies (see Sturm and Wagner, 2010; Deems *et al*., 2008; Jansson and Pettersson, 2007; Erickson *et al*., 2005) and is readily attributed to environmental controls, most significantly wind re-distribution by snow-drift (Doorschot and Lehning, 2002). Wind sheltering on initial precipitation is also a major factor in time stable snow spatial distributions (Erickson *et al*., 2005). Whilst time stable patterns in snow distributions dominate in alpine environments, this does not preclude highly spatially heterogeneous snow distributions themselves (Machguth *et al*., 2006).

Time stable snow spatial distribution patterns have, however, been found to exhibit a number of exceptions, and irregular data years. This is particularly the case in long time series

observation records, such as the record held at Storglaciären, Sweden (Jansson and Pettersson, 2007). Here, numerous b_w points of data fitted poorly with the prevailing glacier-wide conditions, leading to zero or negative correlation coefficients. Further, Winstral and Marks (2014) find a breakdown of time stable relationships at particularly high precipitation levels. They remark that controlling obstacles to wind distributions may be less effective if surrounding snow levels are sufficiently high to limit the wind field divergences found at lower precipitation levels. Time stability is then a central feature to alpine environments, and has numerous causes, many of which are further examined in section 1.5.4; however, time stability also has nuances and complexities requiring site specific evaluation.

Time stability patterns have implications to both snow modelling, and to snow distribution monitoring. Sturm and Wagner (2010) successfully utilise a climatological snow distribution pattern (CSDP) to feed the SnowModel distribution model, with improvements in model outputs of up to 60 %. Further, where greater stability is found, fewer probings may be required, as Pelto (2000; p. 9) notes:

> *"If a glacier has large homogeneous areas, this reduces the measurement density…; if it has many small unique mass balance zones, a higher measurement density is required."*

Reduced survey designs may however be problematic given the possibility of not being able to identify irregular snow distribution years, increasing the potential for random errors.

1.5.3 Representativeness and reliability of snow surveys

Potential snow survey sampling reductions that take advantage of time stability must also be representative of the SWE in the area they are probing. Pelto (2000) advocates a reduction in snow sampling surveys, owing to the decrease in effectiveness of increasing probing densities beyond a specific threshold. Interestingly, this threshold is not uniform across the

two glaciers Pelto (2000) investigates: at Columbia Glacier, Alaska, > 100 points km^{-1} do not significantly increase B_w calculation accuracy; at Lemon Creek Glacier, Alaska, the threshold figure is 10 points km^{-1}. Here the representativeness of probings is markedly different between the glaciers, creating a geographically specific problem. At the alternative extreme, an overly dense probing survey network may, in fact, produce less reliable results. Where probings are spaced regularly 50-100 m apart across a glacier surface, the snow probing measurement errors themselves can be higher than the error caused by incomplete spatial coverage of the glacier, a paradox referred to as *reductio ad absurdum* (Cogley, 1999).

Reduced survey designs are important to consider, and can significantly reduce survey costs (Watson *et al.*, 2006). Some studies have found good agreement with reference results using reduced surveys. Rasmussen and Andreassen (2005) find strong linear mass balance gradients at ten Norwegian glaciers for B_a, B_w and B_s, suggesting that balances near the centre of glacier can be representative for glacier-wide balances. Winstral and Marks (2014) use one index site to compare to basin wide snow depths, and find generally good agreement. However, this is reduced in years with irregular snow distribution patterns. Jansson (1999) finds reducing a probing network from 100x100 m to 400x400 m calculated B_w to within an average 7 % difference from reference results. This does not clarify the potential for irregular snow distribution years.

Reduced snow survey designs must then account for the representativeness and reliability of probing locations in addition to good time stability, in order to accurately produce B_w records.

1.5.4 Snow distribution mechanisms

At macro, landscape scales (linear 10^4-10^5 m), the processes causing snow formation, dependent on temperature lapse rates and orographic features, are highly influential on snow distribution. Precipitation forms as a result of moisture in the air reaching saturation vapour pressure, often enhanced by condensation nuclei, resulting in moisture condensation.

Collision of water particles allows water droplet growth, which fall as precipitation when the updraft holding the droplets in suspension is overcome by their increased mass. Cooler air has a reduced water capacity due to a lower saturation pressure threshold, resulting in precipitation on cooling (McKay and Gray, 2004). Orographic boundaries result in air parcels lifting, causing cooling, saturation, and precipitation. As such, elevation is directly correlated to snow distribution at macro-scales. The characteristics of air masses is largely dependent on the parent source, for instance the influence of travel over water masses and maritime conditions will increase the moisture content of air parcels, with associated increased precipitation.

Another such macro-scale process is the influence of winds over ridge environments causing 'preferential deposition', coined by Lehning *et al.* (2008). This process acts by accelerated uplift due to a funnelling confluence of air as it attempts to overcome largescale obstacles with the least altitude rise. This acceleration affects near surface wind patterns, reducing precipitation opportunity (Dadic *et al*., 2010a; Mott *et al*. 2008). By contrast, on the leeward side of ridges, air diverges and windspeeds decelerate, allowing condensation and precipitation.

At meso-scale (linear 10^2-10^3 m), the interaction of landscape and basin scale processes take place. Snow-drift, defined as the movement of previously fallen snow, is the dominant control of snow distribution at this scale (Mott *et al*., 2010; Tarboton *et al*., 2000). Glaciers are flatter than surrounding mountains, and may create fewer obstacles for wind-blown snow to accumulate on; however, this is dependent on the glacier geometry.

Snow can drift by three mechanisms: creep, whereby snow rolls at speeds < 5 ms^{-1}; saltation, where snow lifts and falls repeatedly between 1-10 cm at speeds 5-10 ms^{-1}; and suspension, where snow is lifted and carried by updrafting between 1-100 m at speeds > 10 ms^{-1}. Creep is considered to be insignificant in terms of snow volume redistribution relative to saltation and suspension (Lehning *et al*., 2008). Saltation can take place due to aerodynamic entrainment, whereby the shear velocity at the snow surface is greater than the surface shear strength threshold; rebound, where snow bounces along a surface; or ejection, where a landing snow particle causes another to lose surface friction and enter saltation movement (Doorschot and Lehning, 2002). Aerodynamic entrainment can also result in suspension

movement, and is controlled by the friction velocity of wind at the surface interface, causing a non-linear increase in snow transport (Doorshot and Lehning, 2002).

Importantly, when snow is carried and its mass is overcome by updrafts, either temporarily in saltation, or continuously in suspension, it is exposed to enhanced sublimation and mass loss (Mott *et al*., 2010; Lehning *et al*., 2008), thus affecting overall redistribution patterns. The extent of enhanced sublimation is a variable of the energy exchange components (see Hock, 2005). A generalised relationship states that there is a logarithmic loss of mass transported with distance covered.

Whilst redistribution is central to snow distribution at this scale (McKay and Gray, 2004; Dadic *et al*., 2010b), it is dependent on many factors. Higher density snow is less transportable due to increased surface shear strength. This is partly influenced by the surface energy balance (Hock, 2005). Aspect influences exposure to radiation, whilst surface albedo influences the energy exchange and degree of snow hardness and metamorphosis. Wind itself can break snow's dendritic crystalline shape, increasing hardness and density by snow packing (Doorschot and Lehning, 2002). Temperature at the time of snowfall also influences its dryness, hardness and crystal structure, with cooler temperatures facilitating dryer, lighter and erodible snow. Older snow with a higher degree of metamorphosis has a higher threshold wind speed required for the shear velocity to overcome the surface shear strength threshold.

Micro-scale (linear 10-10^2 m) factors are dominated by surface roughness. The rougher a surface, the greater its ability to hold fine particles in location and reduce snow redistribution by snow-drift (Lehning *et al*., 2011; Mott *et al*., 2010). On mountain glaciers, this applies to crevasse type features, however, a temporal influence occurs as these features may become smoothed through time.

On annual timescales, glaciers have changing mass accumulation patterns, however, it is well established that known areas are likely to feature prevailing snow accumulation patterns that repeat annually (Deems *et al*., 2008; Erickson *et al*., 2005). Snow distribution on annual timescales is also known to be disproportionately influenced by accumulation patterns preferentially to ablation patterns (Schirmer *et al*., 2011; Dadic *et al*., 2010b; Grünewald *et al*., 2010; Erickson *et al*., 2005). Doorschot and Lehning (2002) contribute the majority of

consistent snow distribution patterns in alpine environments to prevailing winds and the redistribution of snow by saltation.

At sub-annual timescales, often influential individual events take place affecting snow distribution. Large storms occupy small time-scales in the order of hours to days, yet are capable of the highest volume of snow redistribution by high winds (Schirmer *et al*., 2011; McKay and Gray, 2004). In a separate example, repeated storms from the North West were shown to have a strong influence on snow spatial distributions at a study site near Davos, Switzerland, and contributed most towards the overall snow accumulation pattern (Schirmer et al., 2011).

Here, a range of spatial and temporal interacting factors affecting snow distribution patterns have been described, demonstrating what Tarboton *et al*. (2000; p. 1) call the,

> *"interrelated and multiscale nature of the processes involved [in snow spatial distribution]."*

1.6 Study areas

The investigated glaciers are part of NVE's longstanding measurement programme, and are considered reference glaciers by the WGMS (WGMS, 2013). Both are continental glaciers located in the mountainous Jotunheimen region in southern Norway.

1.6.1 Hellstugubreen

Hellstugubreen, also referred to as Hellstugubrean on official maps (61º34' N, 8º 26' E) (Figure 1.6.1) is a valley glacier in central Jotunheimen ranging from 1482-2229 m a.s.l.

with an area of 2.89 km^2 (Andreassen and Winsvold, 2012; Andreassen, 2011a). The glacier is polythermal (Tachon, *pers. comm.*), and shares a border with Vestre Memurubrean to the south. There are two cirque areas to the south-west of the glacier, where steep headwalls are found. Glaciological mass balance measurements have taken place annually since 1962. Mass balance has shown a negative trend, with the cumulative mass balance of -19 m w.e between 1962-2010 (Andreassen, 2011a). This negative mass balance is dictated by prevailing negative summer balances, whilst winter balances have no trend, as shown in Figure 1.6.2.

Five outline measurements and elevation maps have been produced in 1962, 1968, 1980, 1997 and 2009. Maps from 1962, 1968 and 1980 were produced by analogue airborne photogrammetry; 1997 maps used digital airborne photogrammetry; 2009 maps used digital airborne laser scanning and photogrammetry. Digital terrain models (DTMs) have been constructed from the above data. Geodetic and traditional glaciological mass balance techniques have shown generally good agreement in results (Andreassen *et al*., 2002). The contour maps and DTM for 1962 are of poor quality, and shows significant errors when compared to off-glacier ground control points (Andreassen, *pers. comm.*). For this reason, it is regarded as highly uncertain. In mass balance measurements, the maps are used from their inception year to the year of replacement, and are not adjusted for annual changes in glacier geometry. The glacier has reduced in area from 3.38 km^2 in 1962 to 2.89 km^2 in 2009 (NVE reports, 1965-2010). Hellstugubreen has retreated 1135 m between 1901-2014, including 575 m since the first mass balance measurement season in 1962 (NVE, 2015).

Extensive glaciological investigations have been carried out at Hellstugubreen, including Pytte's (1964) thorough mass balance investigation, which included excellent spatial coverage across the glacier. Mapping and mass balance results have also been analysed by Haakensen (1986), finding good agreement between cartographic and traditional glaciological mass balance results. Further, sensitivity to climatic changes at Hellstugubreen has been evaluated using energy balance modelling (Oerlemans, 1992).

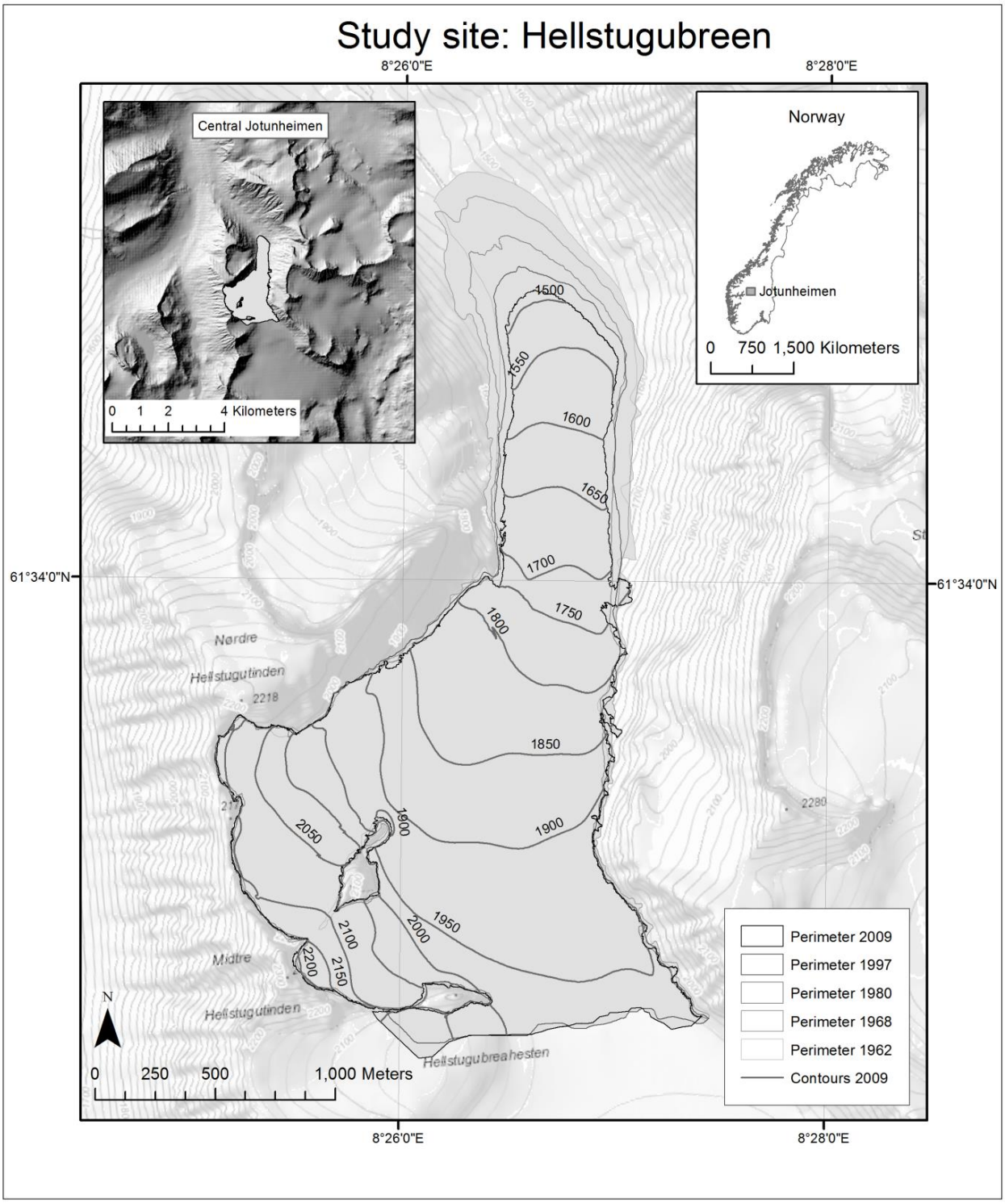

Figure 1.6.1. Hellstugubreen and surrounding topography, southern Norway.

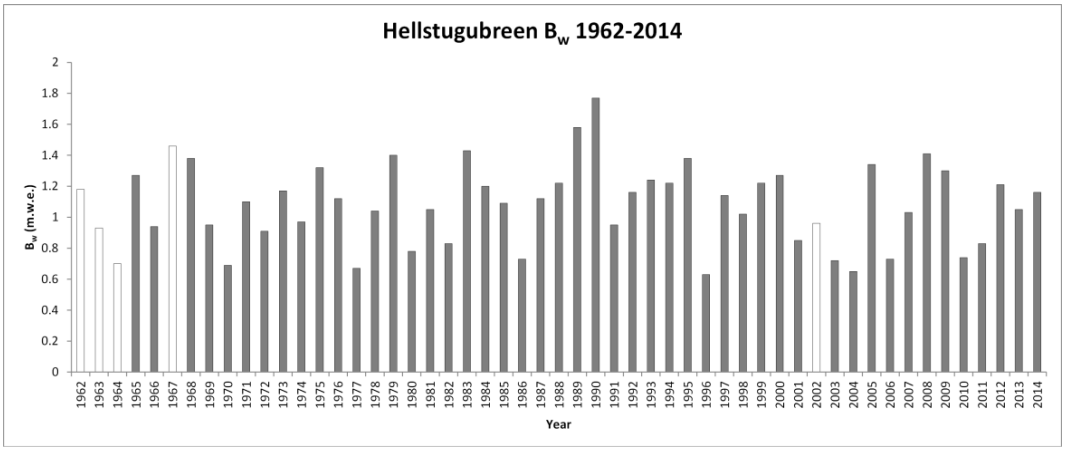

Figure 1.6.2. Hellstugubreen B_w 1965-2014. White bars represent years where b_w data are not available. No trend can be seen through time.

1.6.2 Gråsubreen

Gråsubreen also referred to as Gråsubrean on official maps (61°39' N, 8°37' E) (Figure 1.6.3) is a polythermal glacier in eastern Jotunheimen ranging from 1833-2283 m a.s.l. with an area of 2.12 km^2 (Andreassen, 2011b). Gråsubreen and the adjacent Glitterbreen, Austre Grotbreen and Vestre Grotbreen form the Glittertind massif. The central part of the glacier features superimposed ice caused by snowdrift creating a thin snow pack (Sørdal, 2013; Andreassen, 2011b). For the data years 1971, 1976, 1977, 1980, 1982 and 1986, partial snow absence in the central area was recorded. Glaciological mass balance measurements have taken place annually since 1962. Mass balance has shown a negative trend, with the cumulative mass balance of -17.7 m w.e between 1962-2010 (Andreassen, 2011b). This negative mass balance is dictated by prevailing negative summer balances, whilst winter balances have no trend, as shown in Figure 1.6.4.

Four outline and elevation maps have been produced in 1968, 1984, 1997 and 2009. The maps from 1968 and 1984 were produced using analogue airborne photogrammetry; 1997 maps used digital airborne photogrammetry; 2009 maps used digital airborne laser scanning and photogrammetry. DTMs have been constructed from the above data. Geodetic and traditional glaciological mass balance techniques have shown good agreement between results, with the exception of the 1968 maps, which are considered uncertain (Andreassen *et al*., 2002; Haakensen, 1986). In mass balance measurements, the maps are used from their

inception year to the year of replacement, and are not adjusted for annual changes in glacier geometry. The glacier has reduced in area from 2.57 km^2 in 1968 to 2.12 km^2 in 2009 (NVE Glaciological Investigations in Norway reports, 1965-2010).

Glaciological investigations including energy balance analyses have been carried out at Gråsubreen (Messel, 1985; Klemsdal, 1970). Net radiation and local weather variations are considered central to energy balances at Gråsubreen (Klemsdal, 1970). Further, a mapping and geomorphological assessment was made over Jotunheimen, with a detailed analysis of ice-cored moraines at Gråsubreen by Østrem (1961).

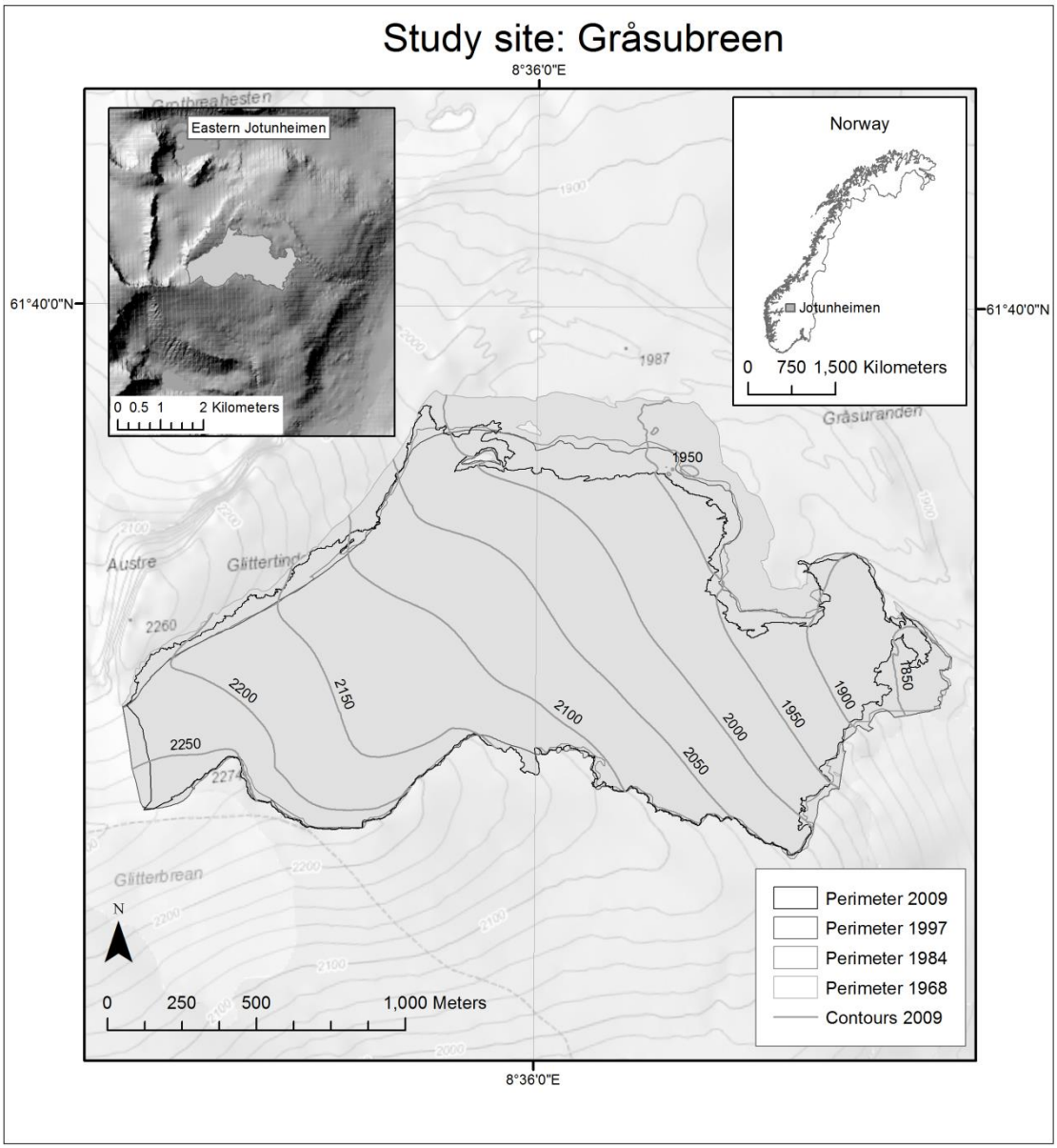

Figure 1.6.3 Gråsubreen and surrounding topography, southern Norway.

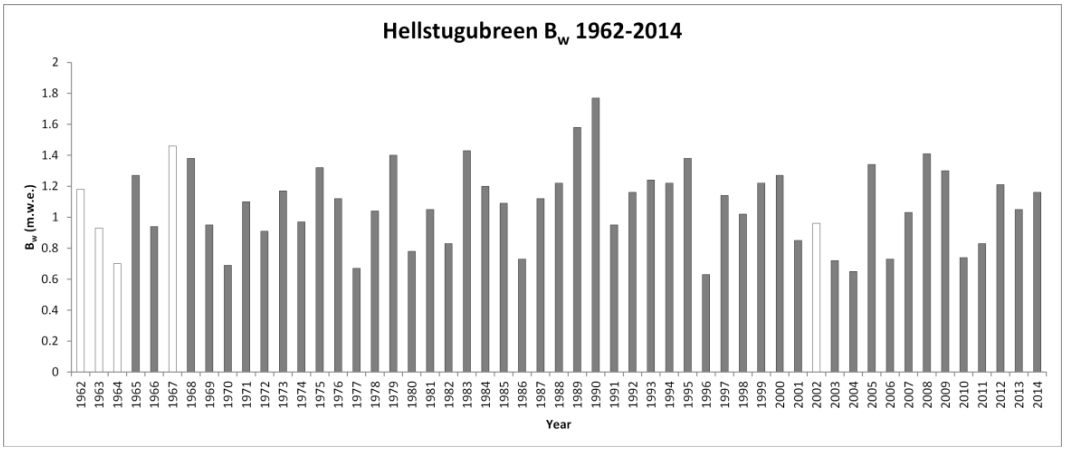

Figure 1.6.4. Gråsubreen B_w 1962-2014. White bars represent years where b_w data are not available. No trend can be seen through time.

1.7 Climate

Hellstugubreen and Gråsubreen lie in central and eastern Jotunheimen, a mountain region of southern Norway. Climate characteristics are dominated by elevation and orographic precipitation patterns. Dominant south-westerly winds transport moisture from the Atlantic, with greatest orographic precipitation in the western Jotunheimen mountains (Sørdal, 2013). Further east, precipitation levels are reduced, reflecting a transition from maritime to continentally dominated climatic characteristics. Temperature inversions are not uncommon in valley regions during calm winter periods (Isaksen *et al*., 2002). Snowfall levels have shown significant inter-annual variation, as shown in Figure 1.6.2 and Figure 1.6.4, however, little overall trend is visible. A period of high snowfall occurred in the late 1980s, dominating net mass balance for those years. Energy balance measurements have been reported at Hellstugubreen (see Andreassen and Oerlemans, 2009; Andreassen *et al*., 2008) and Gråsubreen (see Messel, 1985; Klemsdal, 1970).

2. Methodology and data processing

2.1 Field methodology and NVE's data

Winter balance measurements are undertaken once annually by NVE between April and June using the floating data traditional stratigraphic glaciological mass balance method (Andreassen *et al*., 2005; Østrem and Brugman, 1991). This measures differences between successive summer surfaces. The author took part in the 2014 fieldwork campaigns at Hellstugubreen and Gråsubreen. Snow probings are taken across the glacier using metal probes, as shown in Figure 2.1.2. The LOP approach (Sturm and Wagner, 2010; Grayson *et al*., 2002) is employed to collect data across a broad spatial area. There is no set pattern for snow depth probing, and consequently different spatial patterns are covered each year. An average of c. 100 probings are taken along transects between stakes in a given year, and snow depths recorded. The actual number of probings per year, and the average distance to the next nearest probing are shown in Table 2.1-1. Variations demonstrate the compelling case for a snow spatial distribution investigation to assess survey designs.

Table 2.1-1. Number of probings and average nearest distance to the next closest probing.

	Hellstugubreen		Gråsubreen	
Year	**Number of probings**	**Average nearest probing distance (m)**	**Number of probings**	**Average nearest probing distance (m)**
1965	136	79.6	-	-
1966	171	60.8	-	-
1967	-	-	-	-
1968	198	71.3	107	65.9
1969	240	42.7	-	-
1970	151	75.8	-	-
1971	129	74.2	112	78.2
1972	127	82.4	104	87.8
1973	106	93.1	94	85.1
1974	137	78.1	105	82.5
1975	108	81.9	118	78.4
1976	121	85.9	70	85.9
1977	80	121.1	91	84.3
1978	223	74.2	128	76.4
1979	121	88.8	89	86.7
1980	136	82.1	125	77.9
1981	125	84.7	136	76.6
1982	60	100.7	87	82.8
1983	45	100.5	102	77.8
1984	38	103.8	36	109.2
1985	29	147.1	37	109.0
1986	70	97.0	77	76.0
1987	97	93.5	75	89.5
1988	81	91.3	93	91.4
1989	35	108.7	61	98.8
1990	34	116.5	60	88.9
1991	61	89.1	62	89.9
1992	51	100.3	85	85.8
1993	48	102.4	58	104.6
1994	94	62.6	59	109.8
1995	118	64.1	108	80.0
1996	87	81.7	98	78.8
1997	62	108.5	134	79.5
1998	117	76.2	149	74.5
1999	122	76.6	151	72.3
2000	115	80.3	158	70.8
2001	76	101.6	123	78.2
2002	-	-	-	-

2003	97	83.3	101	84.1
2004	114	77.8	126	76.6
2005	102	79.2	127	69.5
2006	105	74.5	98	78.5
2007	76	93.4	104	70.4
2008	84	84.7	92	83.8
2009	94	78.7	98	77.1
2010	125	59.7	149	57.4
2011	83	90.7	90	76.7
2012	63	78.3	91	81.9
2013	69	87.8	84	81.0
2014	168	61.3	140	50.4
Averages	**103**	**86.0**	**100**	**81.8**
Maximum probings and minimum average nearest neighbour	**240**	**42.7**	**158**	**50.4**
Minimum probings and maximum average nearest neighbour	**29**	**147.1**	**36**	**109.8**

With the introduction of handheld GPS units, probing location coordinates are recorded. Prior to this, approximate locations were marked on maps. Snow depths at stakes, as well as the lengths of stakes above the snow surface, are recorded and used to verify snow probing results. Either one or two snow pits are dug to calculate snow depth-density relationships in order to convert snow depths to SWE values. However, for some early measurement years, many more snow density pits were dug (Pytte, 1964; Klemsdal, 1970). A 2014 snow pit is shown in Figure 2.1.1. Usually, 50cm long cylinders are used to extract a volume of snow in the vertical orientation, and the contents weighed. After the first 2 m, snow cores are taken to extract snow. The exact methodology can vary dependent on conditions and equipment used. For most years, a cumulative depth-density conversion is established to calculate the SWE values, however, for a few years a depth-averaged snow density value was used to calculate the SWE values.

Figure 2.1.2 Snow probe, inserted into the snow perpendicular to the snow surface, Hellstugubreen. Photograph credit: author's own.

Figure 2.1.1 Snow pit, dug at Hellstugubreen. Note the footprint clear area where the snow cylinder will be inserted. Photograph credit: author's own.

Prior to 2000, contouring using hand drawn isopleth lines and a planimeter was used to determine the extent of SWE value regions (NVE reports, 1965-1999). Post-2000, SWE values are average at 50 m elevation intervals, and multiplied by the elevation interval area to calculate volume balances. The sum of volume balances is divided by the total glacier area to calculate the specific mass balance. Escher-Vetter *et al*. (2009) find good agreement between the contour (pre-2000) and profile (post-2000) methodologies in calculating B_w, using the example of two comparable glaciers, Hintereisferner and Vernagtferner, in the Austrian Alps.

Examples of raw data maps are shown in Figure 2.1.3 and Figure 2.1.4 for Hellstugubreen and Gråsubreen respectively. Examples show original scanned maps with snow probing depths, some maps also show conversions to SWE values. Pre-2000 contour method maps and post-2000 digital profile maps are shown.

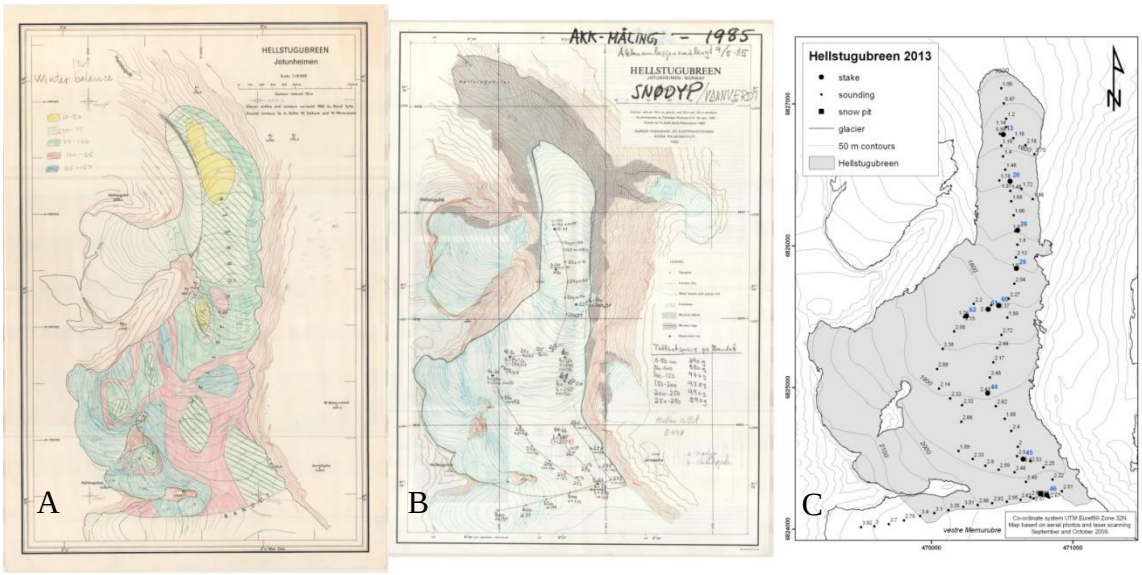

Figure 2.1.3 Hellstugubreen snow accumulation map examples, given in chronological order A) Contour method map from 1969, the year with the most probings, B) probing map with snow depths and SWE values from 1985, the year with the fewest probings, C) probing map with snow depths from 2013. Source: NVE.

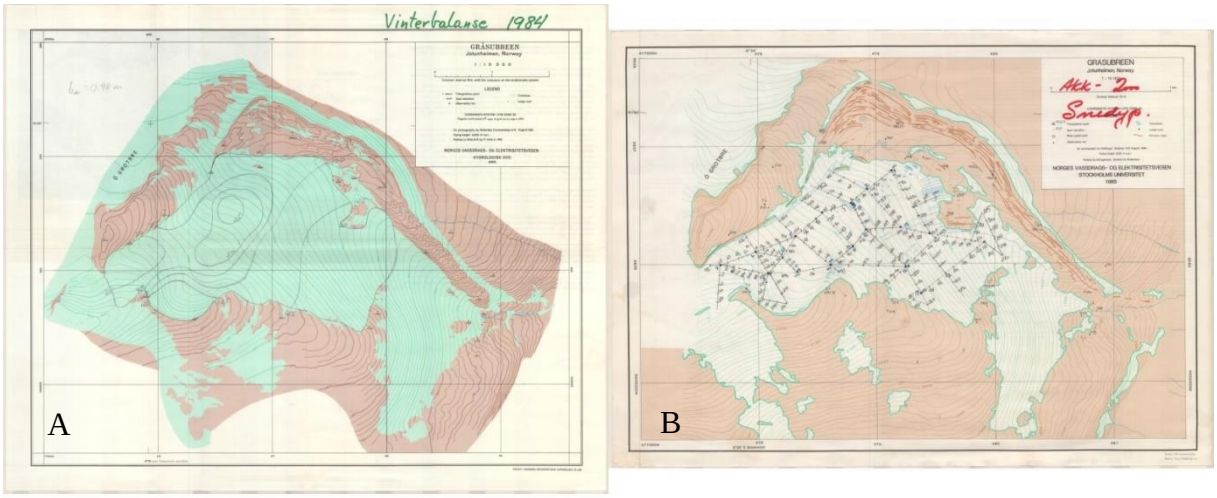

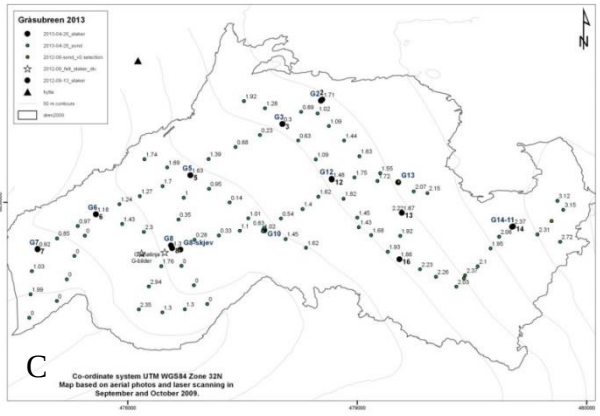

Figure 2.1.4 Gråsubreen snow accumulation map examples, given in chronological order. A) Contour method map from 1984, the year with the fewest probings, B) probing map with snow depths from 2000, the year with the most probings C) probing map with snow depths from 2013. Source: NVE.

2.2 Pre-processing: data assimilation, distribution and normalisation

Snow accumulation geographical information system (GIS) data were gratefully received from NVE. GIS manipulation in pre-processing, normalisation, kriging interpolation, creating stability maps and reliability maps, and survey design resampling were completed using ESRI ArcMap 10.1 ©. Statistical and graphical analyses were completed in Microsoft Excel 2010 © and Minitab 17.1.0 © statistical software.

Partial digitalisation of GIS data was completed and anomalous results from manual digitalisation were corrected or removed. Measurements taken off-glacier were excluded. In agreement with mass balance measurements, this thesis assumes that the glacier geometry was stable for the years subsequent to a new map being produced. No adjustments were made for incremental glacier geometry changes. Recent reanalysis work at Hellstugubreen shows that the small geometric changes found have limited influences on mass balance results (Andreassen, *pers. comm.*). For Hellstugubreen, b_w data were available for the period 1965-2014, excluding 1967 and 2002; for Gråsubreen, b_w data were available for the period 1968-2014, excluding 1969, 1970 and 2002.

Preliminary statistics on data distribution were carried out to understand data patterns and appropriate data manipulation techniques. This primarily involved testing normal distributions using the Anderson-Darling test for both individual data years, and for all years of data. Statistical normality is important to test, since it determines which further statistical tests are appropriate for the data. The Anderson-Darling test was chosen due to its acceptable power and its flexibility to data (Razali and Wah, 2011; Hawkins, 1981). The formal Anderson-Darling normality test was carried out in addition to histogram and probability plot analysis. The annual sample sizes, as shown in Table 2.1-1, are large enough to find conclusive results in formal normality tests (Razali and Wah, 2011), and consequently the Anderson-Darling test was deemed reliable.

The Anderson-Darling test found normal data distributions for 14 of 48 years at Hellstugubreen, and 17 of 44 years at Gråsubreen. This had significant implications for data normalisation (section 2.2.1) and interpolation data processing techniques (section 2.3).

The statistical data distribution of B_w values from the official NVE record was assessed. The data was split into quarters by B_w values, with corresponding years grouped as quarters 1, 2, 3 and 4, reflecting 0-25 %, 25-50 %, 50-75 % and 75-100 % of the range of winter balances. Owing to the distribution of data, the quantity of years within each 25 % B_w quarter grouping was variable. This categorisation was designed to further investigate how different overall winter balance may affect the spatial distribution of snow on glaciers. For example, specific patterns of snow distribution may be amplified or muted in data years in the bottom 25 % of all winter balances compared to data years in the top 25 %. This schema is also designed to assist fieldworkers, who can assess the winter balance in a future campaign relative to prior years using local knowledge and preliminary snow depth probings, afterwhich a specific quarter snow spatial distribution map can be used to gain the most precise and accurate survey design. Data in B_w quarters, or all data combined, are referred to throughout this thesis.

2.2.1 Normalisation

For inter-comparisons of different data years of snow spatial distributions, SWE data must be normalised or standardised. This allows data to be analysed between different years despite different mass balances.

Due to the majority of data being non-normally distributed, a feature scaling normalisation technique (Flach, 2012; Wang 2011) was applied to the SWE data, using equation (1).

$$S_n = \frac{d_i - min(d)}{max(d) - min(d)} \quad (1)$$

Where S_n is the normalised SWE value, d_i is the SWE value at the *i*th point, and *max* and *min* are the maximum and minimum SWE values in a data year, *d*. Following this normalisation, all values ranged between 0-1 and the distribution of original data was maintained.

This was preferred over the standard score, also referred to as z-score, standardisation technique employed by Winstral and Marks (2014) and Sturm and Wagner (2010), using equation (2).

$$S_s = \frac{d_i - \mu}{\sigma} \qquad (2)$$

Where S_s is the standardised SWE, d_i is the SWE value at the *i*th point, μ is the mean SWE for the data year, and σ is the SWE standard deviation for the data year. After equation (2), all values have a mean of 0, and a standard deviation of 1 (Wang, 2011). This standardisation is dependent on normally distributed data.

2.3 Kriging

Discrete point data covers different locations in any given year. Data interpolation and extrapolation are required in order to extend data to cover the whole glacier, and to find stable and reliable locations for future surveys.

Kriging was chosen as the most suitable interpolation and extrapolation technique. This statistical technique has a long history in glaciology, and is examined in detail by Hock and Jensen (1999). Kriging uses a semivariogram to assess the changing characteristic with distance between points. Kriging has the advantage over alternative interpolation techniques, such as inverse-distance weighting, that clustered points are weighed. Therefore interpolation between known points is dependent on the number of surrounding points, not

simply their location. Probabilistic kriging is true to known point data, and offsets any small scale measurement errors and discontinuities by adding a nugget effect (Wackernagel, 2003).

Co-kriging based on a secondary specific attribute, such as elevation, can positively influence the accuracy of interpolation. In this technique, a moving mean based on the secondary attribute is used to assist interpolation. Elevation is deemed a suitable secondary characteristic for assisting SWE kriging, however, preliminary analysis shows that there is a poor strength of glacier-wide relationship between elevation and b_w values for the combination of all normalised data years for both Hellstugubreen (r^2 = 0.2699) and Gråsubreen (r^2 = 0.0863), as shown in Figure 7.1.6 and Figure 7.1.12 in the appendix.

Kriging assumes a random underlying field of normal distribution with known covariance (Pilz and Spöck, 2007); however, using the Anderson-Darling normality test discussed in section 2.2, this assumption does not hold true for the majority of data years. Consequently, ordinary kriging may produce data with underestimated predicted errors. The variable distributions of data demands that different data transformations may be required for different data years. Bayesian kriging was preferred because it accounts for some of the uncertainty in model parameters. This technique does not assume the semivariogram model, and instead computes 100 semivariogram models based on Bayesian statistics. Bayesian kriging can also adapt to non-stationary data (Krivoruchko, 2012). It is thus more probable that an appropriate model is selected for the semivariogram, creating better interpolation results. Indeed Pilz and Spöck (2007; p. 621) comment that:

> *"It is the Bayesian approach, in our opinion, which is most appropriate for modelling the uncertainties with respect to the unknown model constituents [distributions and model parameters]."*

Bayesian kriging was used and resampled to 30x30 m cell sizes snapped in location between different data years. 30 m resolution was chosen due to the sampling spatial distribution, the data type, and the area interpolated and extrapolated over. The average nearest neighbour values of 86 m and 81.8 m for Hellstugubreen and Gråsubreen respectively, suggested that an interpolation resolution more than one third of the data spacing was inappropriate.

Nearest neighbour values are exceeded many times over where extrapolated data is extended to the glacier perimeter, thus limiting the accuracy of higher resolutions. Jansson (1999) finds that interpolation beyond the average nearest neighbour values does not increase accuracy of interpolated values. Further, the SWE values themselves may show highly localised variation due to uneven glacier surfaces, suggesting that higher resolution data may not necessarily increase accuracy. For digitalised data years, the spatial locations of probings have errors of ± 10 m in digitalisation; further, the manual marking on maps themselves prior to GPS increases potential spatial error with unknown error estimates. The exact probing locations have inherent uncertainty, and support the resampling and processing at 30x30 m resolution.

2.4 Stability

The stability of individual years was measured by several techniques. The root mean square error (RMSE) is a measure of the residuals away from an expected model. RMSEs of snow spatial distributions after kriging were computed on a cell-by-cell basis. The RMSEs were measured between a normalised data year and the combination of every data year after normalisation. RMSE uses the same units as the dependent variable, here normalised SWE.

The correlation between a data year and all other years was computed in a correlation matrix to identify data outliers, using the Microsoft Excel 2010 © data analysis ToolPak extension and Minitab 17.1.0 ©. Krigged normalised cell values were extracted and aligned for this calculation. The values presented were calculated using Pearson's correlation coefficients. This calculation is a measure of how well each 30x30 m cell in a given year correlates to that of another year. The correlation *matrix* was superior to using a baseline value as a 'regular' year, since all values were compared to all other years to identify regularity or irregularity.

Stability maps were produced by considering a group of multiple years (B_w quarters or all years of data), and calculating the maximum range of values of normalised SWE in a given 30x30 m cell. The range was calculated as a percentage of total maximum normalised value

range, 1. The stability is then a measure of the range of normalised SWE values at a given location. The stability values were grouped in 20 % variability zones to produce stability maps, and areas calculated for these zones.

Stability maps were also enhanced by using optimum allocation stratified sampling, also known as Neyman allocation stratified sampling. This method suggests the best sample size as a proportion of the overall sample, based on the variability of samples in an area, and cost of sampling that area (Foreman, 1991; Neyman, 1934). This technique for stratified sampling is highly appropriate for variable stability data, and accounts for the need for accurate data at a minimal expense. Optimum allocation stratified sampling is based on equation (3) (Foreman, 1991).

$$S = p \cdot \frac{\left(\frac{N_h \cdot S_h}{\sqrt{C_h}}\right)}{\left(\sum \frac{N_i \cdot S_i}{\sqrt{C_i}}\right)} \qquad (3)$$

Where S is the sample size of a given stability zone area, p is the total required sample (set to 100 to obtain percentage requirements of the overall sample), N_h is the population of a variability zone area, S_h is the variance of a variability zone area, and C_h is the cost of sampling a variability zone area.

Equation (3) is adapted for survey design here, such that N_h is the sum area of a variability zone, S_h is the mean variability percentage of a total variability zone, and C_h is the area fraction of a variability zone of the total glacier area. The sample size percentage values are then multiplied by areas of smaller individual non-contiguous variability zones.

2.5 Reliability

In order to test the reliability and representativeness of b_w measurements, three different types of survey sampling regimes were created. The first was designed to find the single index site location on a glacier that is most representative of the overall B_w. The second survey type finds locations within each 50 m elevation interval that were most representative of the mean winter balance in that elevation interval, and then calculated B_w. The third survey used centreline only probings to calculate B_w, as explained in section 2.5.1. The first two survey designs were completed on all years of data, and quartered data years, effectively creating ten sampling survey designs. Table 2.5-1 shows the abbreviations used to refer to the first two types of survey sample designs.

Table 2.5-1 Matrix of reliability survey designs created.

	One location	**One location per elevation interval**
All years of data	$B_w one_{all}$	$B_w ele_{all}$
B_w quartered data years	$B_w one_q$	$B_w ele_q$

Reliability was evaluated by constructing maps where b_w probing results fell within ± 10 % of the official record for a given area (either the entire glacier, or a 50 m elevation interval). Kriging maps of SWE values were used, and binary searches were completed for all constituent map years in Table 2.5-1, with data extracted from the NVE glaciological reports (NVE Glaciological Investigations in Norway reports, 1965-2010). These binary map rasters were then summed and cells with the highest number of data year layers were considered the most representative.

These reliable cells were used a sampling point locations in new survey designs. The maximum cell value was not necessarily reflective of the total number of data years used in its calculation, since there may be data years that do not fit with the overall snow spatial distribution. The selection of representative cells was guided by multiple criteria to reduce subjectivity. This included finding the maximum value; if multiple cells had the same

maximum value, those in the largest cluster were chosen, since it was probable that the region was more stable. Areas that were on the peripheries of the glacier were given less preference, since they were likely to experience a greater degree of glacier geometry changes. Where glacial retreat has caused 50 m elevation intervals to cease overlapping through time, the 2009 50 m elevation contours were used. This was because the survey sample design is intended to be used in the future, and as such, the most updated glacier geometries were used, despite the possibility that some values may have been extracted from the adjacent elevation interval.

From the survey points, SWE values were extracted and B_w reconstructed. This process was completed to construct four datasets. The values were compared to the official record to examine the RMSE and average percentage errors.

2.5.1 Centreline reliability

The reliability of using probing data collected only on the centreline of the glacier was computed. The probing data for the centreline transect was used with area-elevation intervals to calculate the B_w, and compared to the official B_w record. Data were not extrapolated to areas where probings were not taken. Here, the centreline should not be confused with the flowline. Centreline only probings are extracted from annual data years along the centremost probing transect on a glacier. This transect is used annually, however, it is not a strictly defined transect, and features small variations. At Hellstugubreen, the centreline only probings follow a central transect which finishes at the border with Vestre Memurubrean. At Gråsubreen, the centreline only probings follow a central transect along the glacier.

2.5.2 Randomized samples

The number of probings needed from a random sample to calculate the official B_w was computed, using the Sample Size for Estimation tool in Minitab 17.1.0 © statistical software. This process used the total number of probings and the standard deviation of results in a given year to compute the number of probing necessary to calculate winter balance to within 50, 75, 90 and 95 % accuracies of the mean SWE value. Results were within a 95 % certainty threshold. The mean SWE probing was used as reference metric rather than the absolute B_w for a data year.

2.6 Wind frequency distributions

Weather station data was taken from four nearby Norwegian Meteorological Institute WSs: 15360 Elveseter, 15310 Bøverdal-Sletten, 55290 Sognefjellhytta, and 15270 Juvvasshøe, all shown in Figure 2.6.1. Data were downloaded from the eKlima webportal (eKlima, 2015). WS information is summarised in Table 2.6-1.

Table 2.6-1 WS information.

Station number	Station name	Elevation (m a.s.l.)	Data available from	Data available to	Northing (°)	Easting (°)	Distance to Hellstugubreen†	Distance to Gråsubreen†
15360	Elveseter	674	1965	1969	61.70	8.28	16.2	16.3
15310	Bøverdal-Sletten	594	1972	1979	61.72	8,33	16.7	14.9
55290	Sognefjellhytta	1413	1978	2006*	61.56	8.00	22.4	32.1
15270	Juvvasshøe	1894	2009	2014	61.68	8.37	11.8	11.3

†*as the crow flies *data not available 1991-2005*

Data were used to analyse wind frequency distributions, as a potential influence on snow spatial distributions. Data for specific data years that did not conform to wider snow spatial

distributions were been analysed relative to regular wind field patterns. Multiple weather stations have been used due to the incomplete records for the full time period from individual WSs. Elveseter has wind data from 1965-1969; Bøverdal-Sletten from 1972-1979; Sognefjellhytta from 1978-2006 (with the exception of 1991-2005); and Juvvasshøe from 2009-2014. Data are thus unavailable for the years 1970, 1971, 1991-2005, 2007 and 2008. The WSs recorded wind speeds and directions at 10 m above the ground surface. Elveseter and Bøverdal-Sletten recorded data at 07:00, 13:00 and 19:00; Sognefjellhytta and Juvvasshøe recorded data at hourly intervals (all times UTC+1).

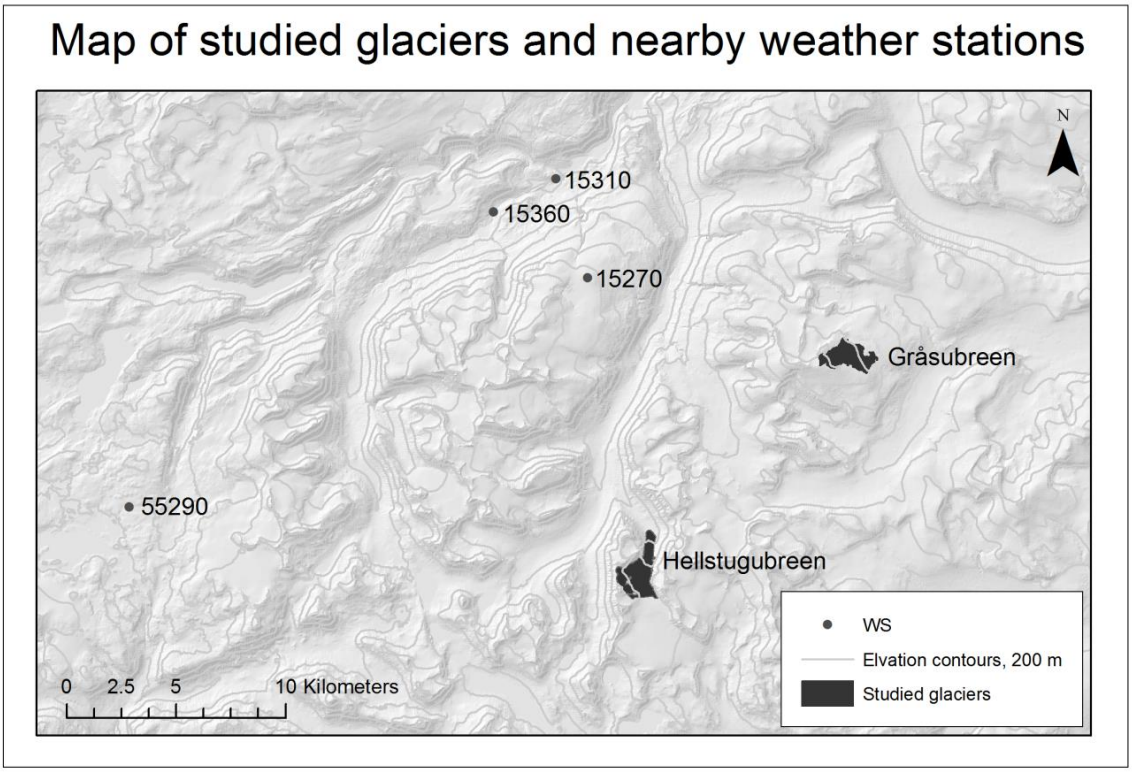

Figure 2.6.1 Map of WS locations and studied glaciers. WS data is used for wind frequency analysis.

3. Results

3.1 Hellstugubreen

3.1.1 Data distribution

Data statistical distributions show 14 of 48 data years are normally distributed at Hellstugubreen. Histograms of data distributions are shown in the appendix, Figure 7.1.1. Associated probability plots are shown in the appendix in Figure 7.1.2. A range of statistical distributions can be observed, including but not limited to normal distributions, skewed distributions, and bimodal distributions, however, no statistical distribution fits all of the data to a significant level. Results from the Anderson-Darling normality test are shown, alongside B_w and the number of b_w probings taken, in the appendix in Table 7.1-1.

Data years that are normal bear negligible relationships to either overall B_w, or the number of probings taken, as shown in Figure 3.1.1 and Figure 3.1.2. Variability of statistical data distribution is therefore independent of B_w or the number of probings taken in a given year.

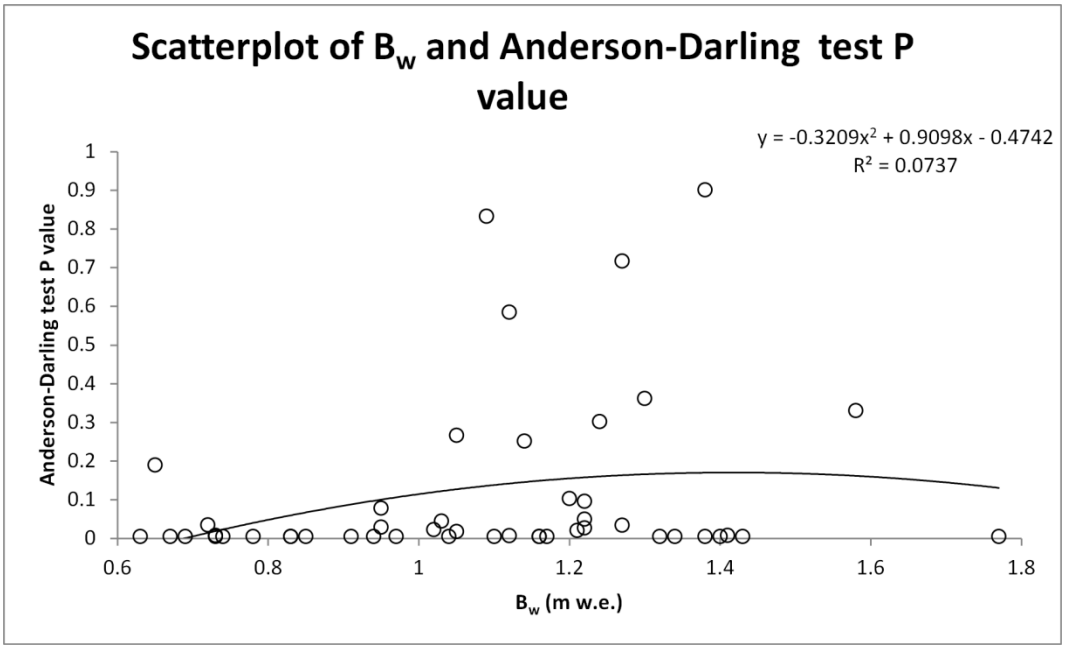

Figure 3.1.1 Scatterplot of B_w and Anderson-Darling normality test P values. A polynomial trendline is fitted to the data.

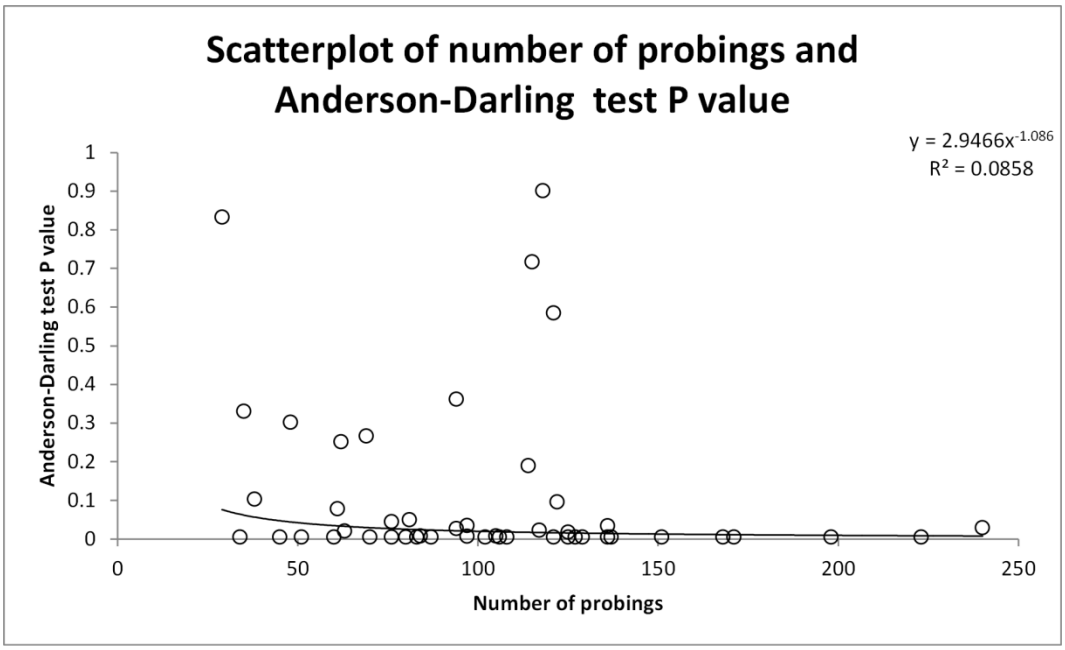

Figure 3.1.2 Scatterplot of the number of probings taken and the Anderson-Darling normality test P values. A power trendline is fitted to the data.

Probing data merged together post-normalisation are of a non-normal statistical distribution. The P value of <0.005 for the Anderson-Darling normality test for merged data shows that the inclusion of all data does not produce a normal distribution. Data are graphically shown in the appendix in Figure 7.1.3 and Figure 7.1.4 (all merged data has as sum 4929 b_w points). The distribution of official winter balances is shown in the appendix in Figure 7.1.5, showing positive skew. The categorisation of B_w years into quarters is shown in Table 3.1-1, and is referred to throughout the thesis. Notably, different number of years are found in each quarter, with only two years in B_w quarter 4.

Table 3.1-1 B_w quarter data categorisation, Hellstugubreen.

Quarter 1	Quarter 2	Quarter 3	Quarter 4
1970	1966	1965	1989
1972	1969	1968	1990
1977	1971	1975	
1980	1973	1979	
1982	1974	1983	
1986	1976	1988	
1996	1978	1993	
2001	1981	1994	
2003	1984	1995	
2004	1985	1999	
2006	1987	2000	
2010	1991	2005	
2011	1992	2008	
	1997	2009	
	1998	2012	
	2007		
	2013		
	2014		

3.1.2 Snow probing spatial distribution and normalised SWE values

Snow probing spatial distributions show excellent coverage for the central part of the glacier, with limited probing data in the cirques to the south-west, as shown in Figure 3.1.3. Indeed,

the cirque areas are only covered in the years: 1966, 1968, 1970-1979, and 2014. Coverage is emphasised during the earlier years of glacier monitoring. However, these years demonstrate a good range of B_w values.

Notably, a generalised trend shows increasing normalised SWE values upglacier, however as shown in Figure 7.1.6 in the appendix, the general relationship between elevation and SWE value is weak. The relationship is stronger at low elevations; however, the glacier-wide relationship is poor. The central area of the glacier shows the greatest range of normalised SWE values, and is likely to be responsible for the poor fit of elevation and SWE values. The clustering of SWE values in the 0-0.2 normalised range at the snout, and at the 0.8-1 range directly beneath the cirques demonstrates reasonable stability of snow distribution patterns in these areas. The central area of the glacier is more variable.

For quartered normalised SWE maps shown in Figure 3.1.4, the snout pattern retains stability at 0-0.2 normalised SWE values. Higher normalised SWE values are found beneath the cirques; clustering is more pronounced for B_w quarters 2 and 3. Comparatively, other quarters show a less distinct pattern. Quarter 4 has very limited coverage, a remnant of the difficulty in collecting data in the most snow-laden years.

The central region of the glacier shows considerable variation between the B_w quarters. Quarter 3 shows a cluster of high SWE values in the central region where quarter 1 shows low values and quarters 2 and 4 show mid ranging values respectively.

When considering the organisation of spatial patterns of normalised SWE between quarters (i.e. how clustered or random different SWE values appear between quarters), quarter 3 shows the most distinguishable clustering of results. All years demonstrate some degree of clustering of normalised SWE values, which is better evaluated in stability results, section 3.1.3.

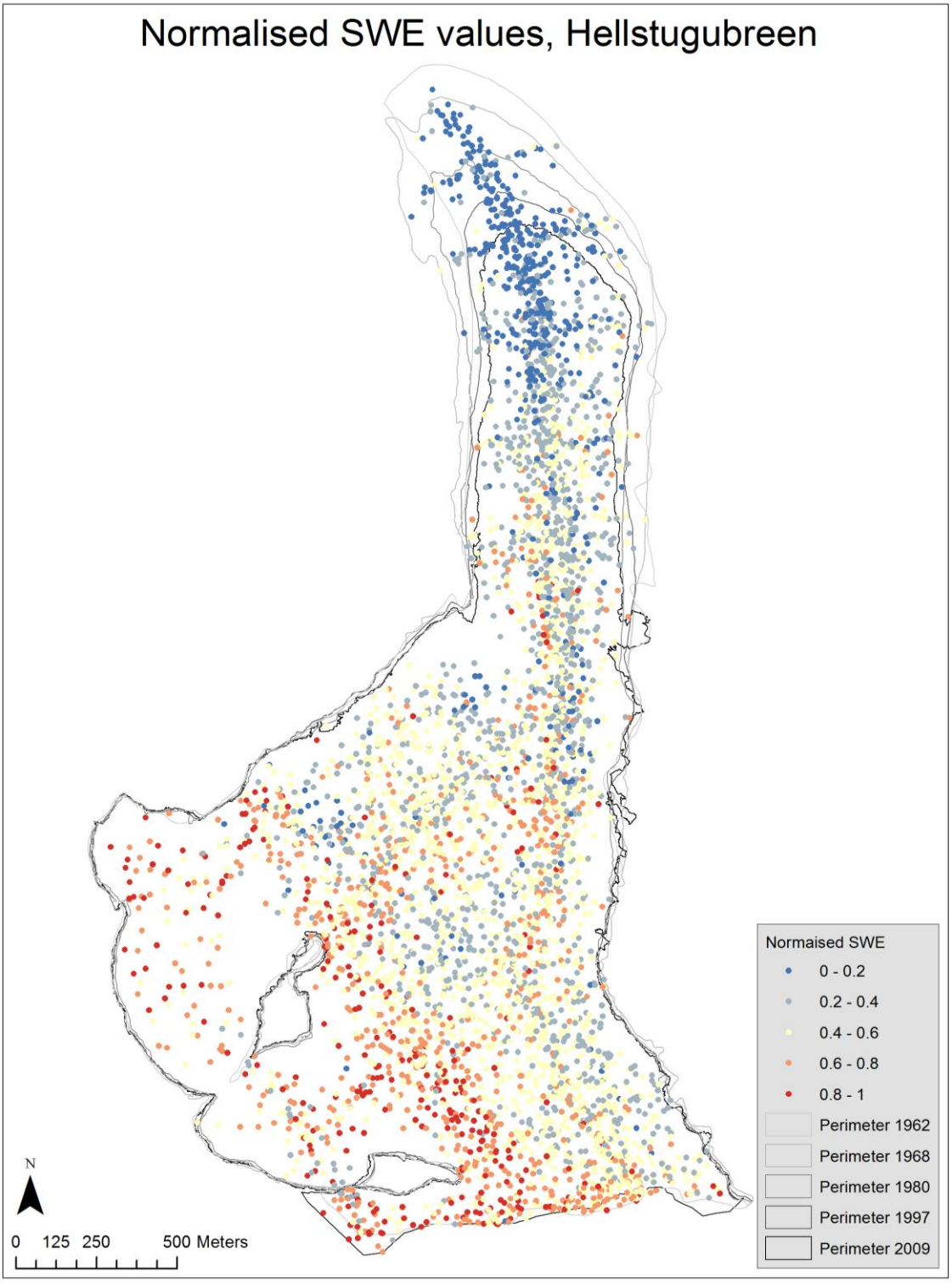

Figure 3.1.3 Map of probing locations for all years, shown with normalised SWE values.

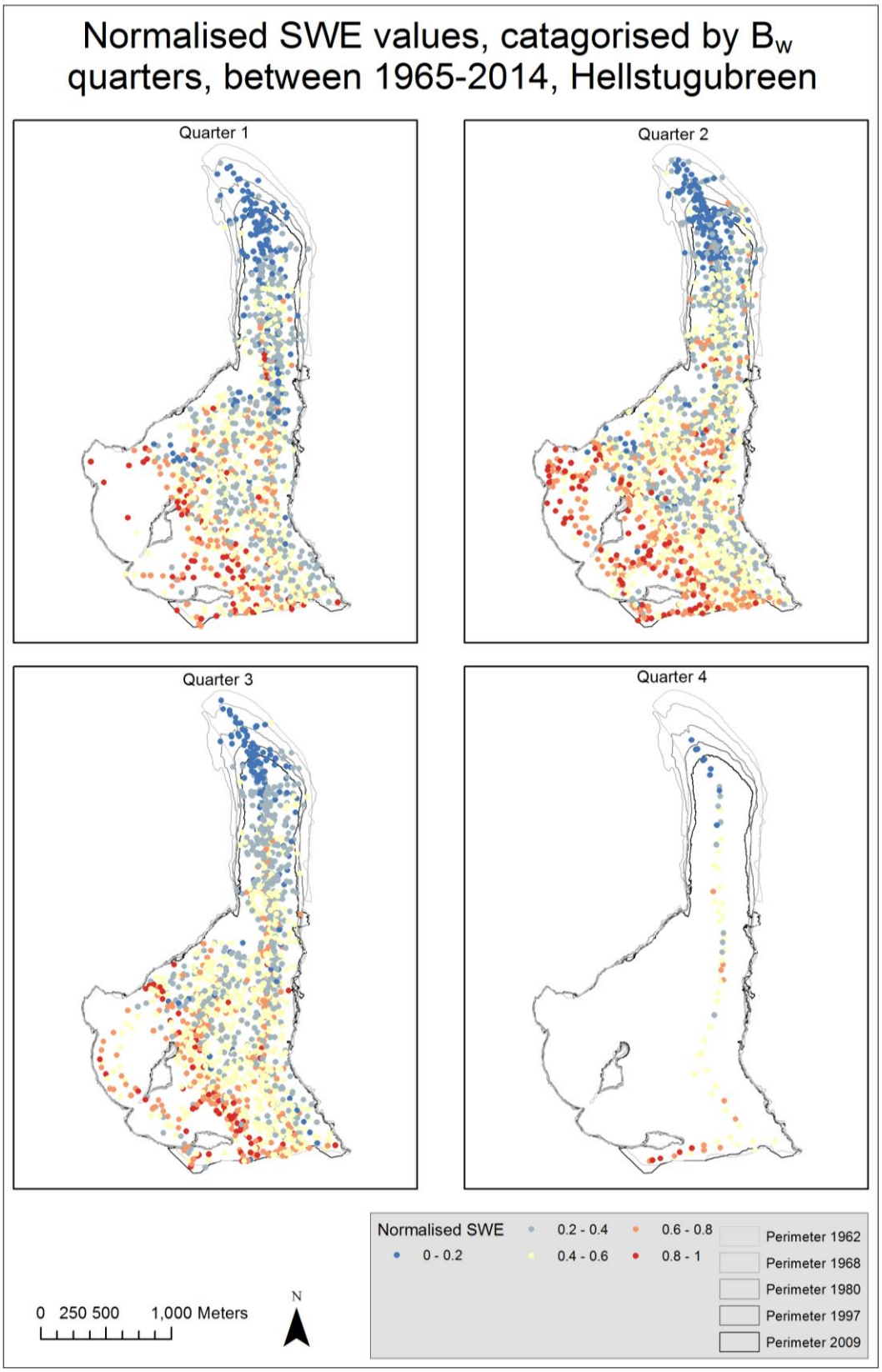

Figure 3.1.4 Map of probing locations, categorised by B_w quarters, and shown with normalised SWE values.

3.1.3 Stability

i. Inter-annual snow spatial distribution variation

The RMSEs of normalised SWE between individual cells of each data year and the combination of all years of data is shown in Figure 3.1.5. The dependent variable is normalised SWE, thus the same normalised units, ranging from 0-1, are used for the RMSE values.

RMSE values range between 0.08 to 0.25, indicating that at Hellstugubreen all years show a strong likeness to a model combination of all data. RMSE values are plotted with B_w values in Figure 3.1.6. There is a limited relationship, suggesting that the residuals between different SWE years spatial distribution patterns are not dependent on B_w values. This does not mean that a specific spatial distribution in seen at difference B_w levels, but that the size of residuals are similar across the range of B_w values.

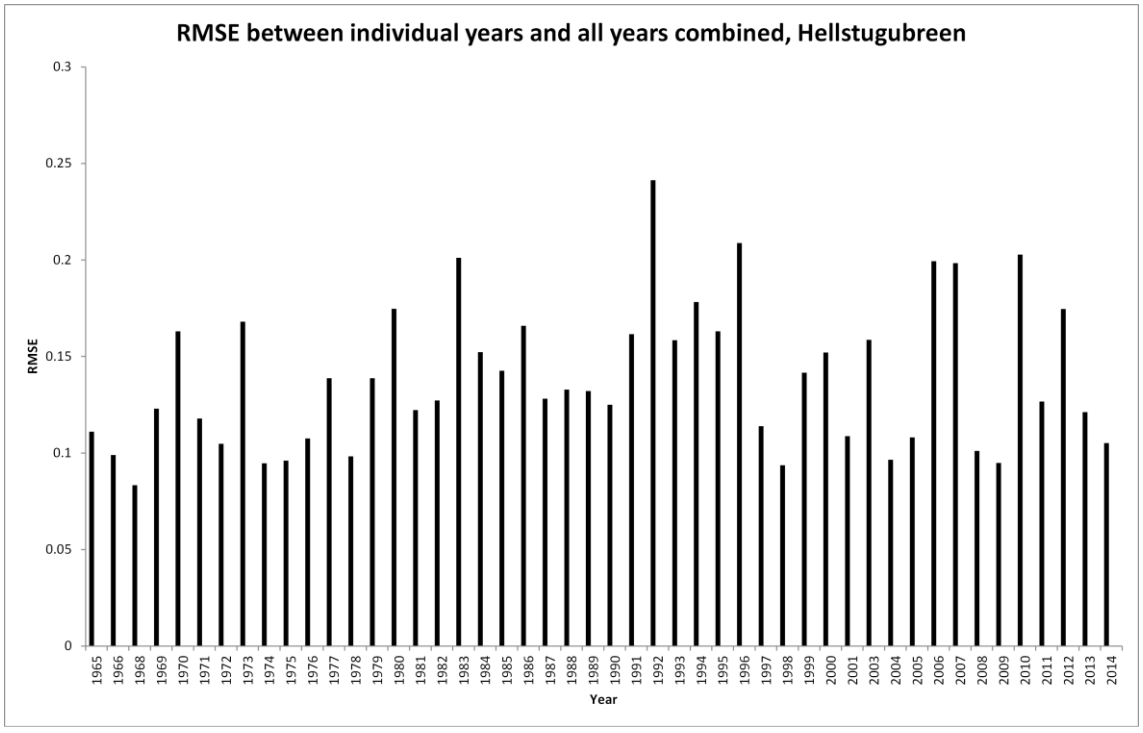

Figure 3.1.5 RMSE between each year and all years combined. Normalised SWE values are used in this calculation.

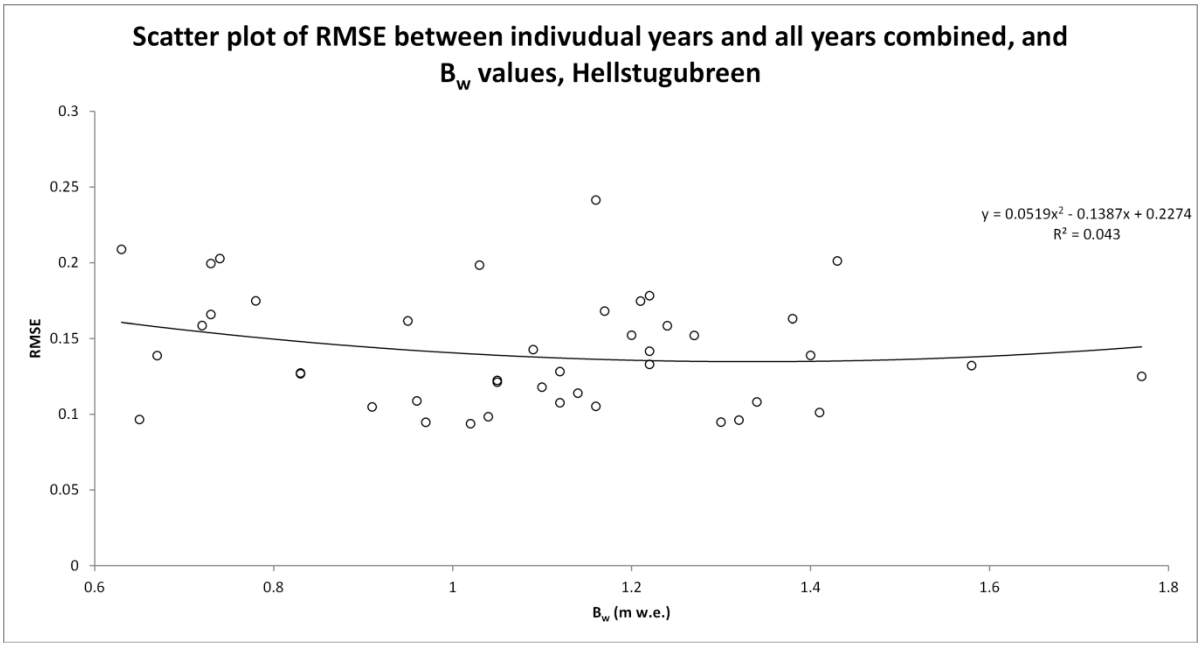

Figure 3.1.6 Scatterplot of RMSE and B_w values.

An inter-correlation matrix of boxplots between a data year and all other individual data years is shown in Figure 3.1.7. The boxplots shows the correlation values between different data years. They consist of the box representing the interquartile range (IQR), meaning range between the first and third quartiles; the central mark denoting the median; and whiskers extending to the maximum and minimum correlation values. Where a maximum or minimum is one and half times greater than the IQR, an asterisk is used to denote this as an outlier.

The correlation value is a measure of the linear relationship between overlapping 30x30 m cells, such that a linear trend between the values of all cells in two compared years can be determined. Each year is compared to all other years to produce the matrix and boxplots shown in Figure 3.1.7. All years have a positive correlation to all other years, with the median below 0.5 on for only two years: 1984 and 1992. The majority of years feature a tight IQR of between 0.10 (1968) and 0.25 (1980); suggesting most correlation values, and therefore spatial patterns, fall in a small range for a given year. However, IQRs, whiskers and outliers show that most years are negatively skewed; with a broader range of values falling below the median value. This shows that whilst good correlation is found in most cases, the cases with poor correlation fall further from the median than those with good

correlations. The high number of negative outliers also denotes that there are serval instances of poor correlations between data years.

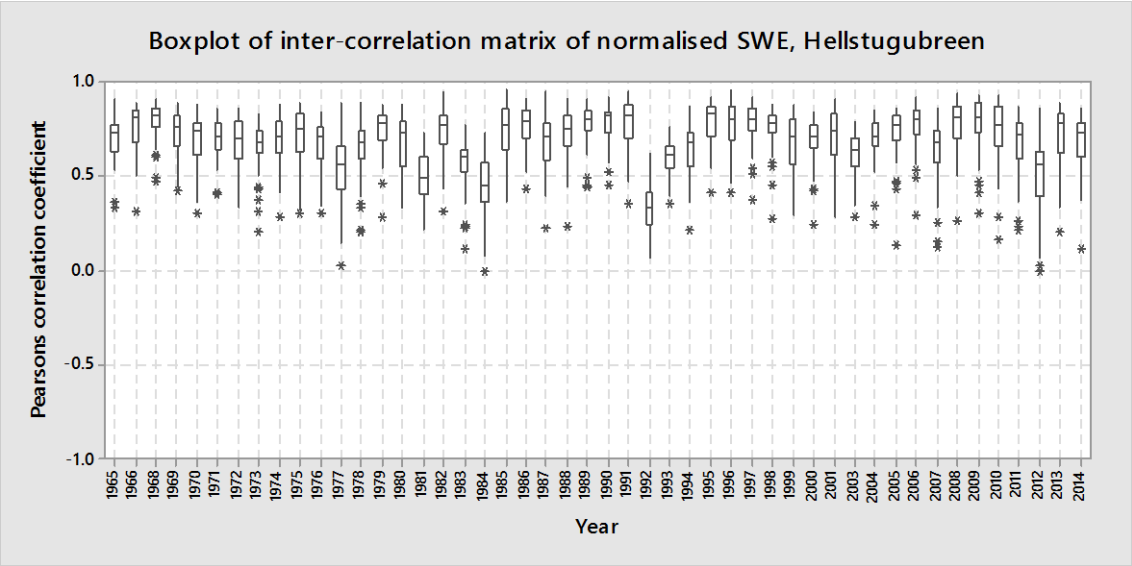

Figure 3.1.7 Boxplot of inter-correlation matrix between an individual data year and all other data years. Normalised SWE values are used in this calculation.

ii. Probing stability

Maps of probing stability, and suggested probing sample percentages computed using optimum allocation are shown in Figure 3.1.8 through Figure 3.1.12 for all years of data, and B_w quarters 1 through 4 respectively. With the exclusion of quarter 4, there is a predominance of stability in the snout area of the glacier and low stability in the cirques, though the extent of this pattern is variable. Quarter 4 shows the highest degree of stability, possibly owing to the limited years in the quarter.

The map for all years of data shows the least stable data, with the highest proportion of stability within the 60-80 % and 80-100 % variability zones (8 % of optimally allocated probings are required in the 80-100 % variability zone). For the quarters 1-4 the optimum allocation probing requirements in the variability zone 80-100 % are 2, 0, 0, and 0 %. Conversely, the most stable map overall is for quarter 4, with the largest proportion of optimally allocated probings in the 0-20 % variability zone (56 % of all optimally allocated probings). Indeed, for all data and quarters 1, 2 and 3, the percentage of optimally allocated

probings in the 0-20 % variability zone are 0, 4, 0 and 1 %. The area of greatest stability for quarter 1 is along the eastern edge; for quarters 2 and 3, the most stable area is slightly north of the centre of the glacier, covering the width of the glacier.

The large central-upper area of the glacier is well represented in generally stable conditions. The variability ranges 20-40 and 40-60 % dominate in this area, with the exception of quarter 4, which is largely represented by the 0-20 % variability zone in this region of the glacier. This area is important to consider, since it amounts to some of the largest area-elevation zones between 1800-1950 m a.s.l.

The stratified sampling optimum allocation percentage probing requirements are heavily dominated by large variability zones. Indeed, two large contiguous zones make up 77 % of all suggested probings in the map for all years of data. The small regions of lower or higher stability are by return often of small sample size suggestions, effectively limited by the size of these areas.

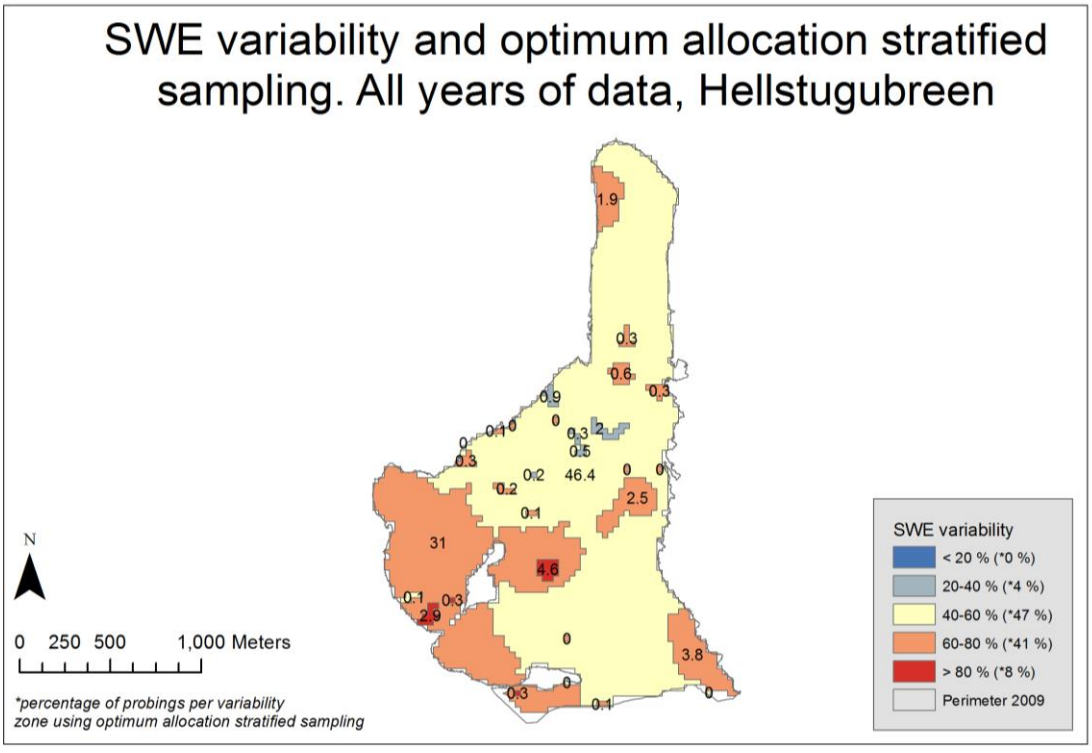

Figure 3.1.8 Probing stability map and optimum allocation stratified sampling percentages, for all years of data.

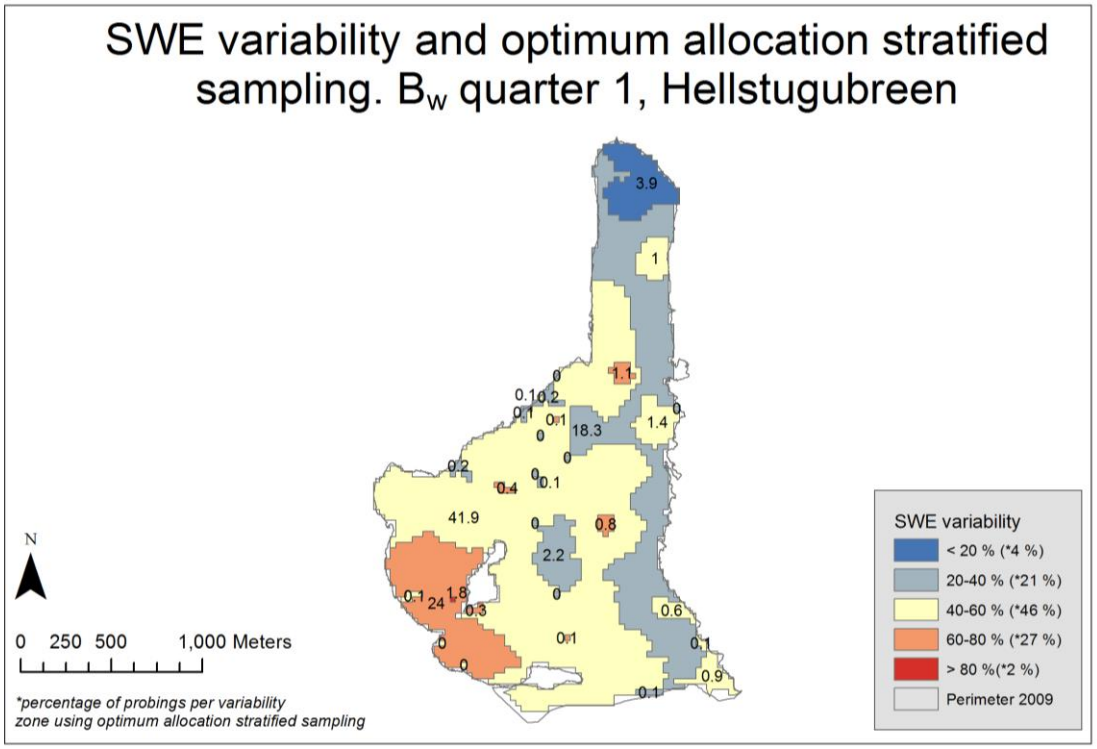

Figure 3.1.9 Probing stability map and optimum allocation stratified sampling percentages, for B_w quarter 1.

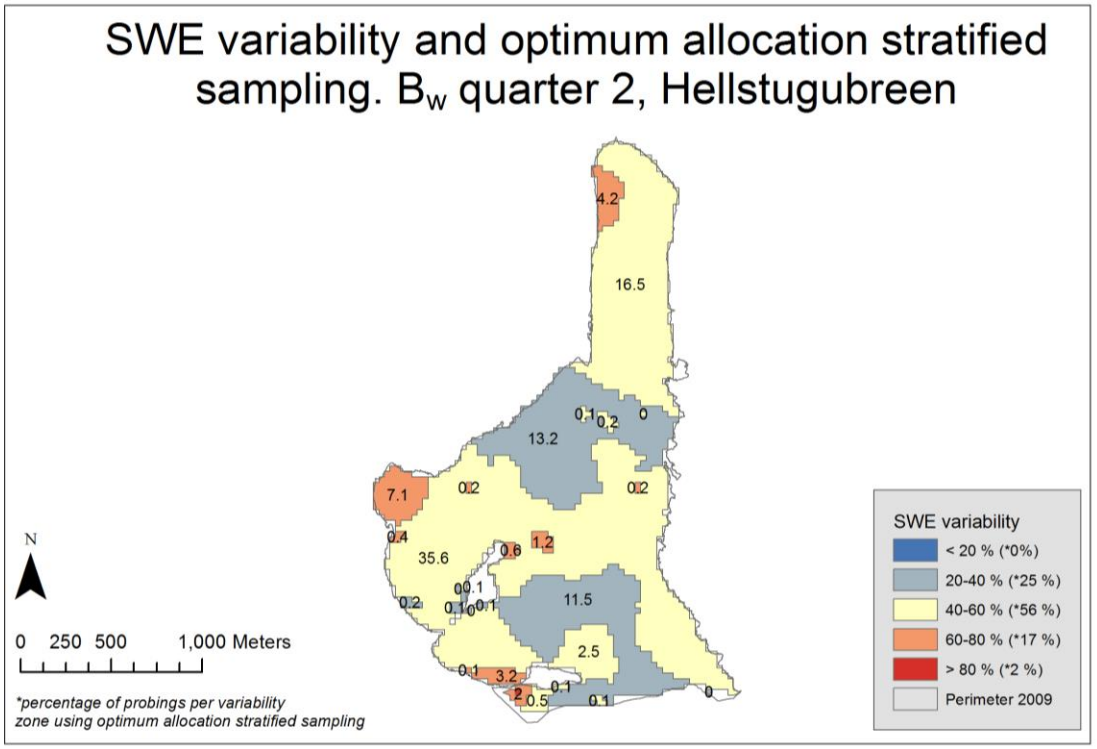

Figure 3.1.10 Probing stability map and optimum allocation stratified sampling percentages, for B_w quarter 2.

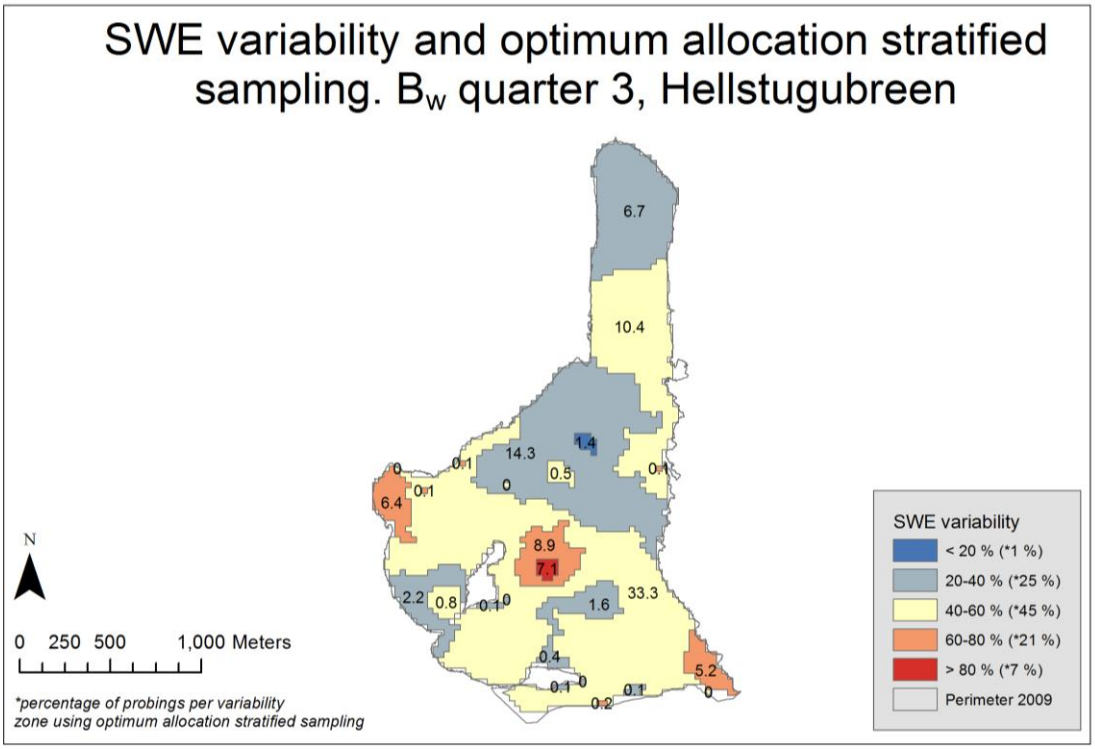

Figure 3.1.11 Probing stability map and optimum allocation stratified sampling percentages, for B_w quarter 3.

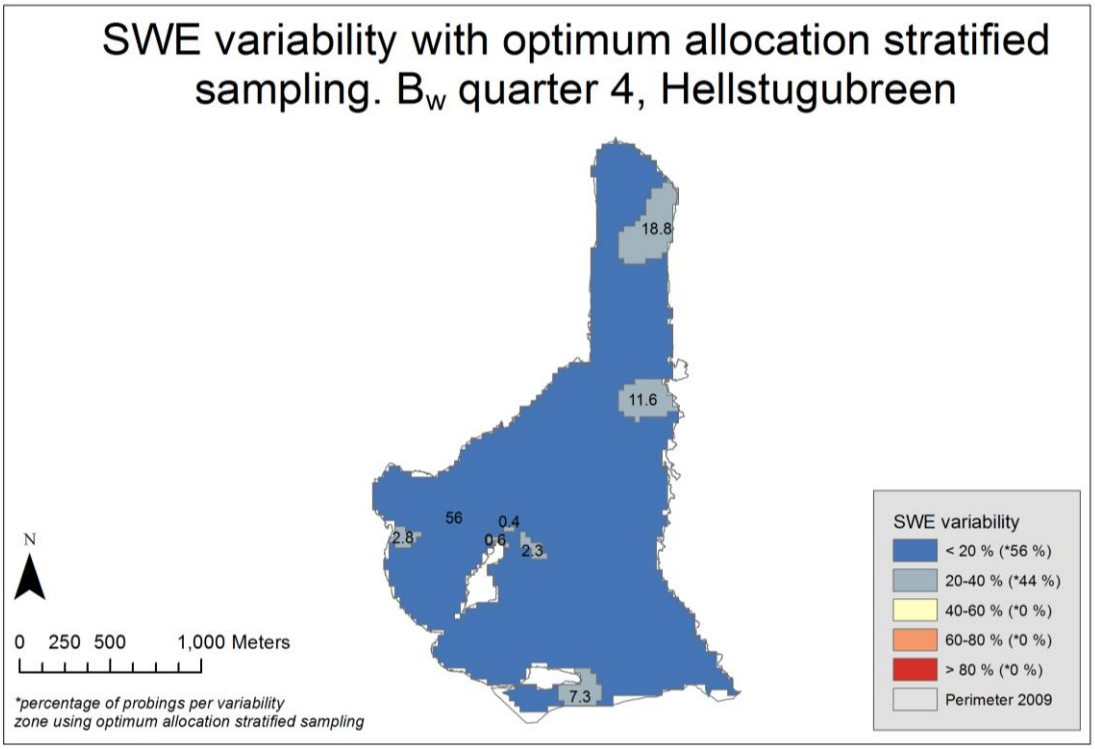

Figure 3.1.12 Probing stability map and optimum allocation stratified sampling percentages, for B_w quarter 4.

The areas of different variability zones for the above five maps are shown in Figure 3.1.13. Note that the data is colour coordinated to compliment the above stability maps. Data for all years shows the greatest skew towards low stability. When data years are split by B_w quarters, they demonstrably show advantageously stable probing areas.

Notably, the vast majority of areas fall in the 20-40 and 40-60 % variability zones, with varying degrees of agreement. The degree of stability by area appears to increase with the B_w quarters. Notably, of the quarters, quarter 1 has the largest area in the 60-80 % variability zone, where quarter 4 has the largest area in the 0-20 % variability zone. Without exception, the high variability zone 80-100 % makes a small to negligible contribution to the total area of the glacier.

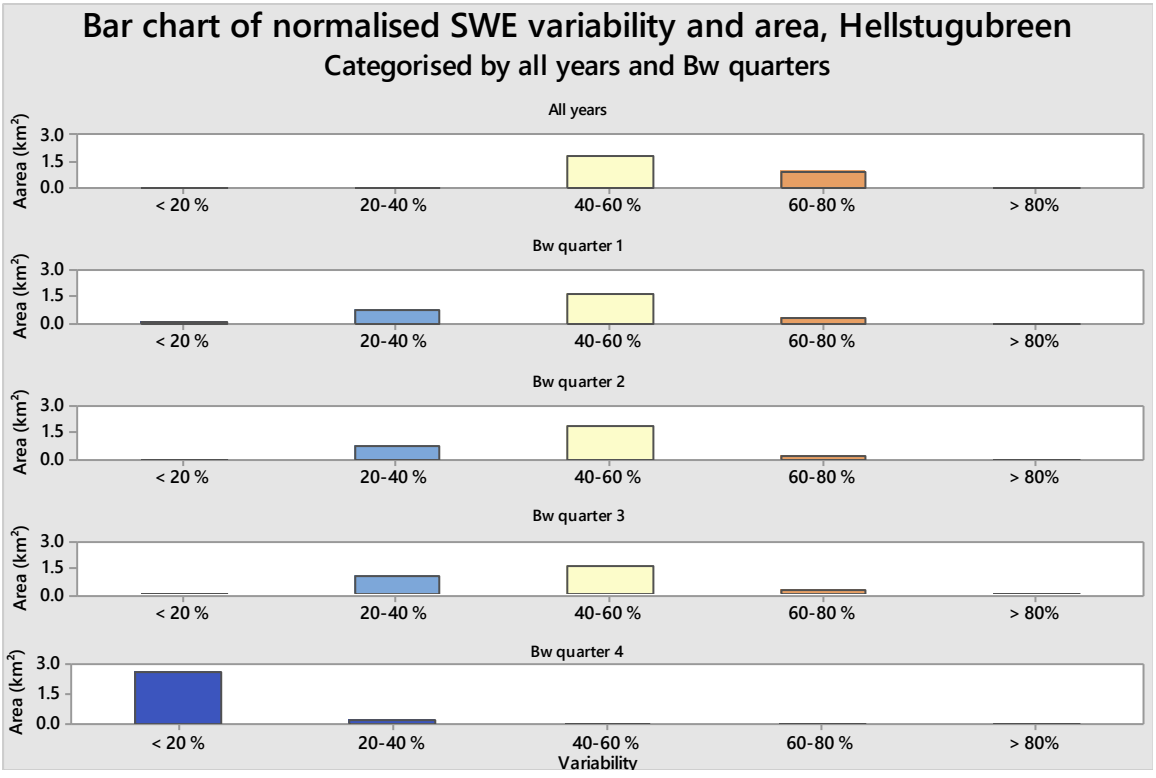

Figure 3.1.13 Areas of of different variability zones for all years of data, and data categorised by B_w quarters.

3.1.4 Reliability

Reliability maps are constructed for one representative probing location for the entire glacier in Figure 3.1.14 ($B_w one_{all}$ and $B_w one_q$), and separately for representative probing locations in each 50 m elevation interval in Figure 3.1.15 ($B_w ele_{all}$ and $B_w ele_q$).

For the $B_w one_{all}$ and $B_w one_q$ maps, there is good consistency between the maps, highlighting the central area of the glacier. The area to the east of the glacier centre in particular is highly reliable for representing the overall B_w. Conversely, the snout and cirques are the most unreliable places.

When considering $B_w ele_{all}$ and $B_w ele_q$, there are increased differences between all years of data, and the quartered data. The region to the east of the glacier appears to have less pronounced reliability for elevation interval banded locations than when considering just one representative index location; however, the pattern of fewer reliable locations in the snout and cirque is repeated.

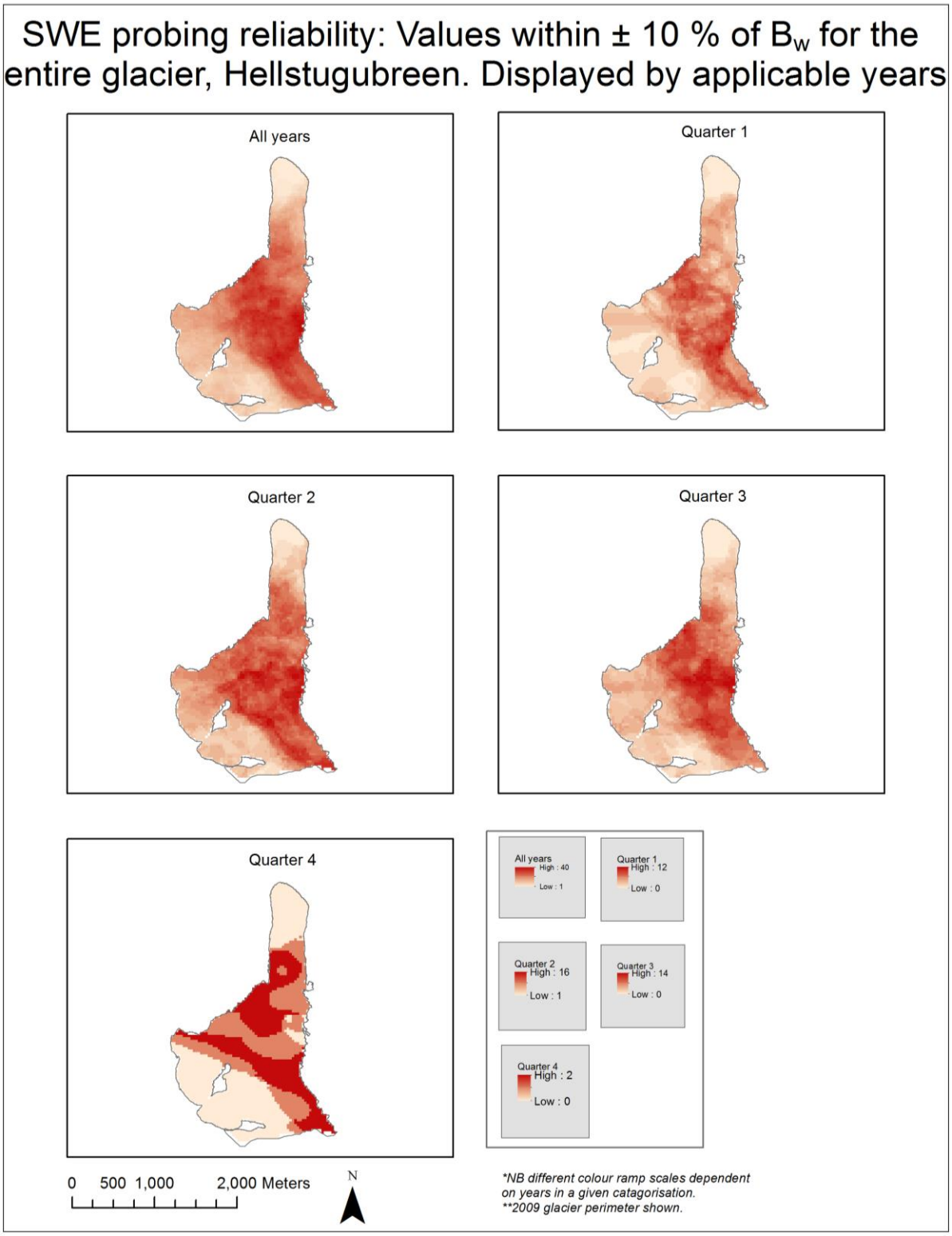

Figure 3.1.14 Reliability maps for one representative probing for the entire glacier, categorised by all years of data and by B_w quarters.

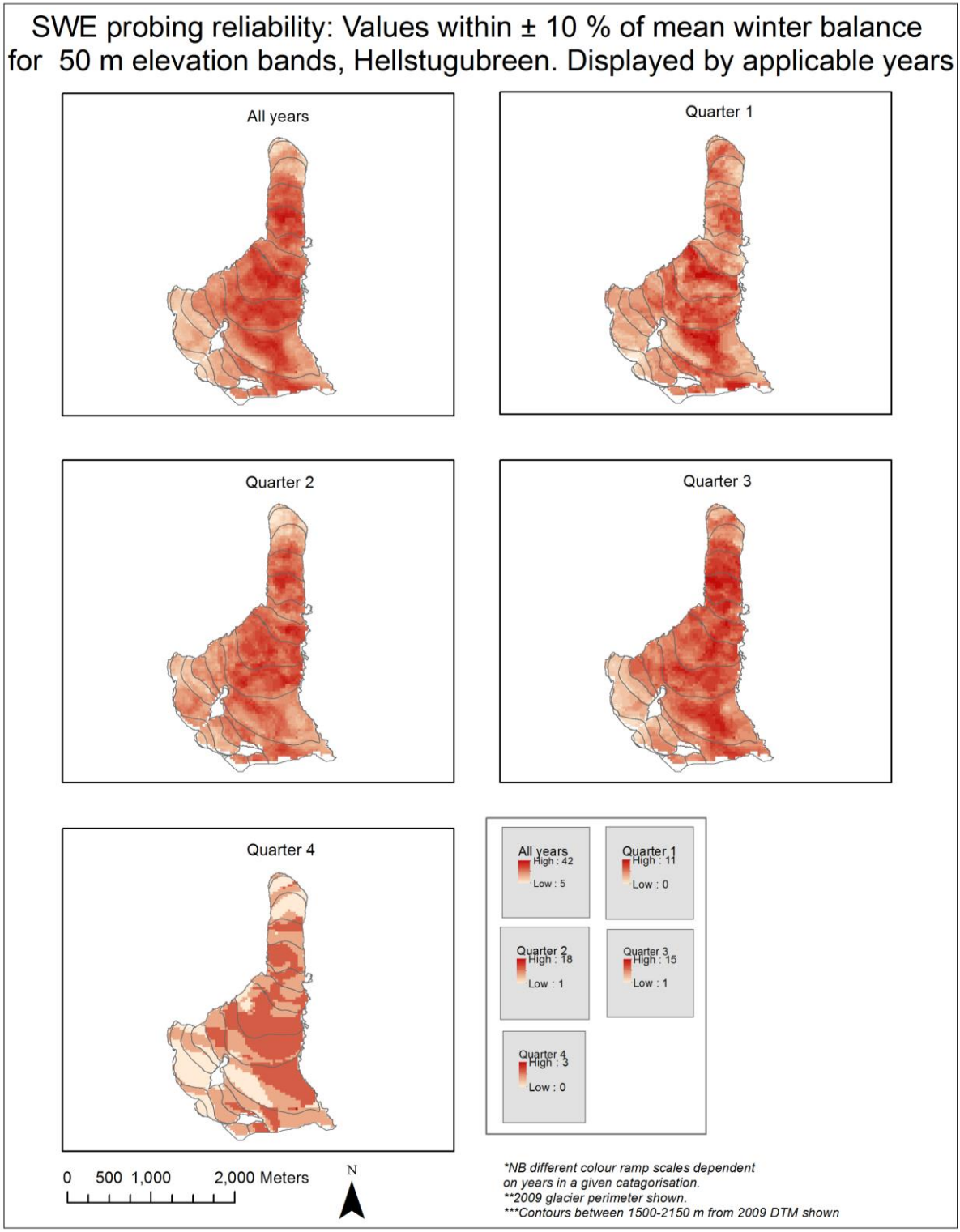

Figure 3.1.15 Reliability maps for one representative probing at 50 m elevation intervals, categorised by all years of data and by B_w quarters.

The reliability maps are constructed by identifying representative cells locations where multiple years of data fall within ± 10 % of a chosen SWE value. The number of years accounts for stability, in addition to reliability. Not all representative cell locations give SWE values within ± 10 % of a specified value. Here, the percentage of data year layers that provide cells that are within ± 10 % of a chosen SWE value at a representative cell for $B_w one_{all}$ and $B_w one_q$ are shown in Figure 3.1.16; and respectively for $B_w ele_{all}$ and $B_w ele_q$ in Figure 3.1.17.

For $B_w one_{all}$ and $B_w one_q$ (where the probing locations directly reflect the glacier-wide B_w) all locations use over 80 % of the available years of data. The reliability map for $B_w one_{all}$ uses the lowest percentage, at 83 %, whilst $B_w one_q$ maps all use 89 % or more of available categorised data years.

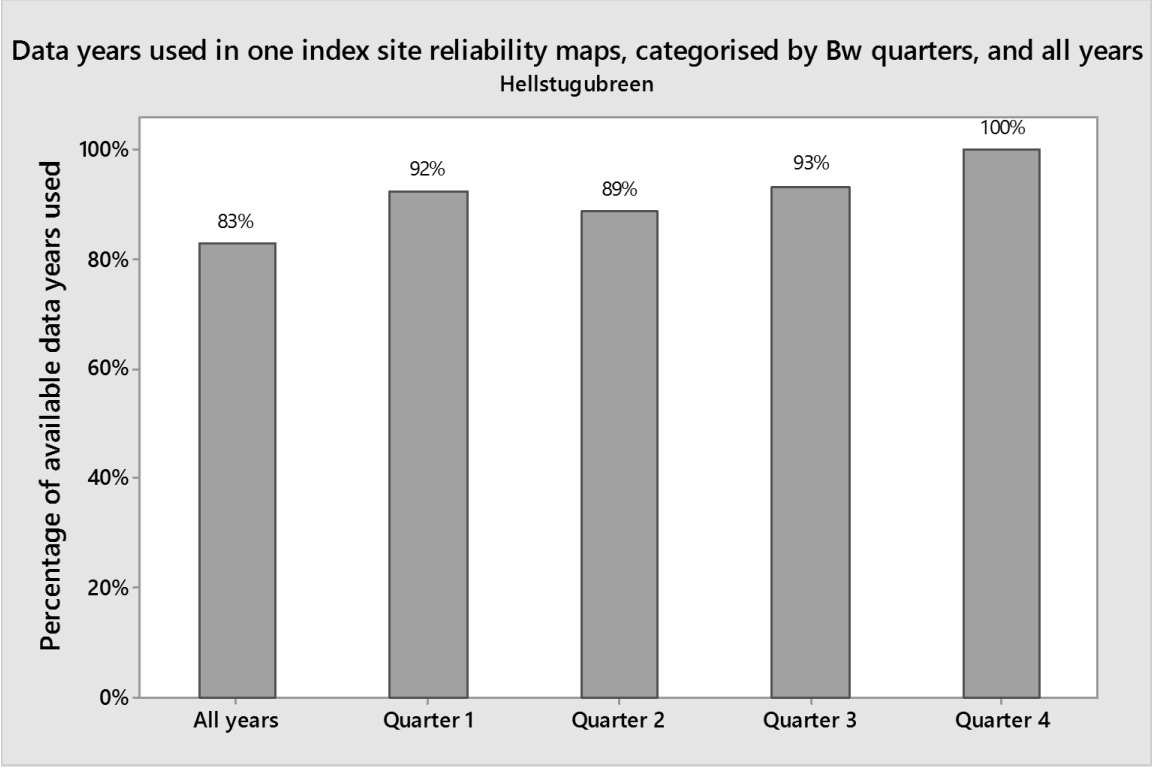

Figure 3.1.16 Chart of percentage of year layers at one representative probing reliability location for the entire glacier, relative to all available years. Data categorised by all years of data, and B_w quarters.

For B_wele_{all} and B_wele_q, the percentage of years of data used varies significantly. However, a generalised pattern is valid for all categorisations of data, suggesting that at low and high elevation intervals, fewer data years possess representative SWE values. By contrast, mid-range elevations show the highest proportion or reliable data years. Quarter 4 has the highest percentage of reliable data years, in agreement with the stability section 3.1.3. B_wele_{all} and quarter 1 show the lowest percentages of data years used at representative probing locations.

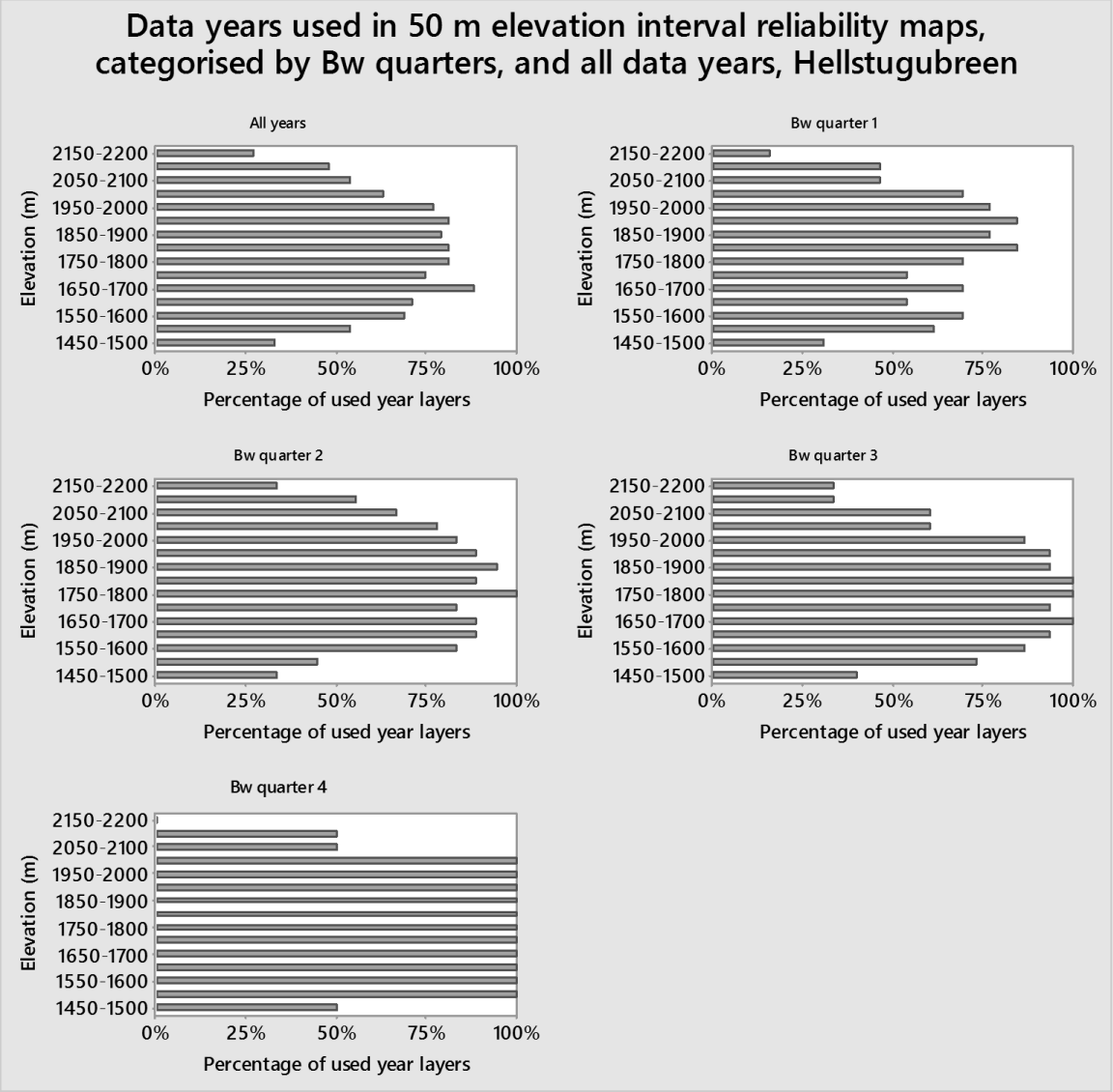

Figure 3.1.17 Chart of percentage of year layers at representative probing locations at 50 m elevation intervals, relative to all available years. Note, elevation distributions are taken from the 2009 contour map.

3.1.5 Survey design

The representative probing locations are used to extract data SWE data, which are then compared to the official B_w record. The locations for the most representative b_w probing based on the reliability maps are shown in Figure 3.1.18 and Figure 3.1.19 for one index site locations for the entire glacier, and for a representative probing location per 50 m elevation interval respectively. Where probings are taken in every 50 m elevation interval at Hellstugubreen, high elevation probing locations are inaccessible for future fieldworkers. These locations are used in order to extract data for B_w resampling and reconstructions, necessitating probing locations despite poor practical usability.

At lower B_w quarters, where precipitation is lower, the reliable probing locations are further upglacier. As shown in Figure 3.1.20, there is good agreement for the majority of years between the official B_w record, and the reconstructed B_w based on resampling and extracted values from selected probing locations.

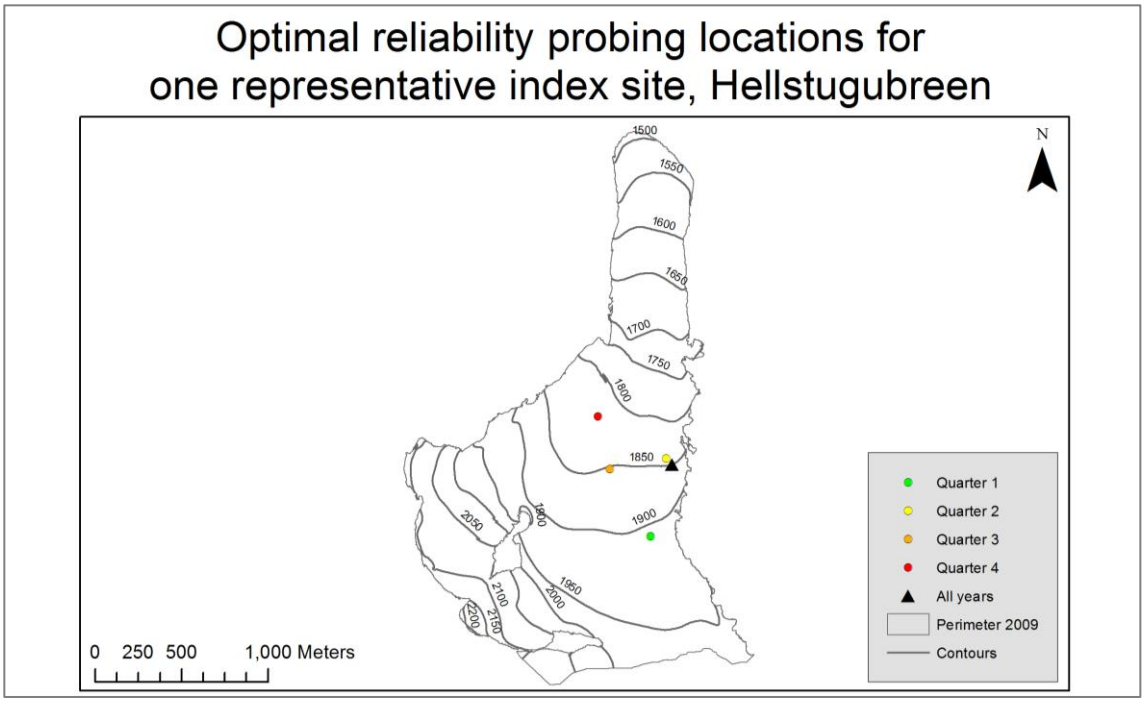

Figure 3.1.18 Survey design b_w probing locations for one index site for B_w calculation. Shown for all data years, and B_w quarters, Hellstugubreen.

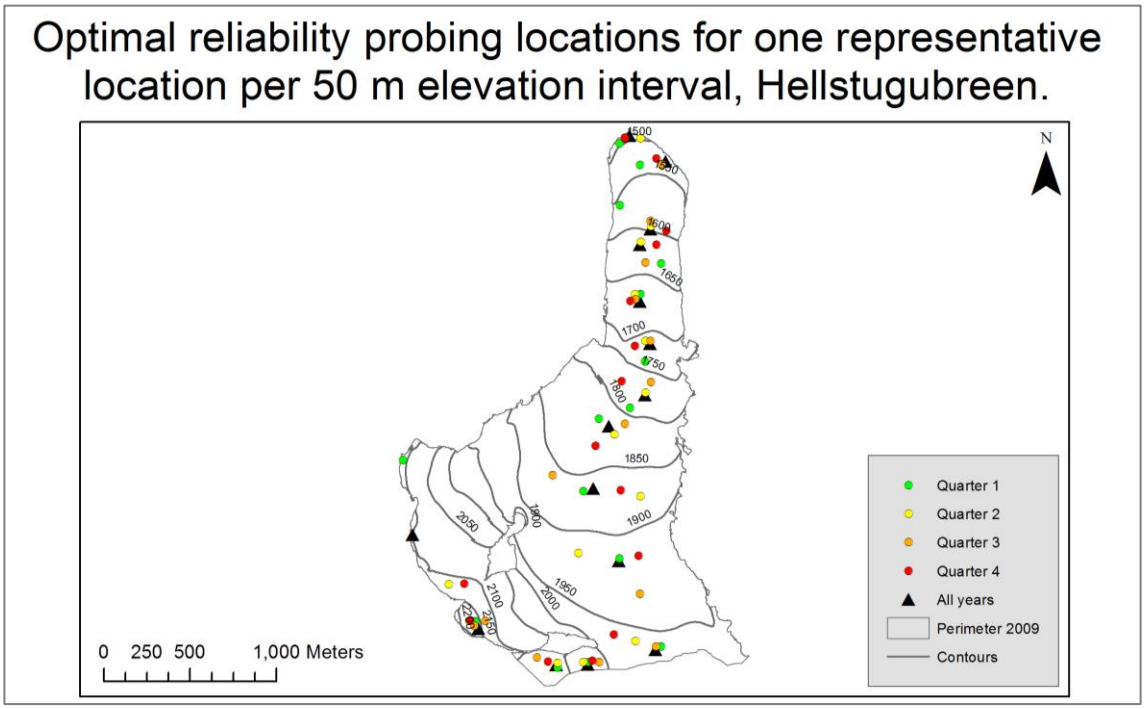

Figure 3.1.19 Survey design b_w probing locations for one b_w probing per 50 m elevation interval. Shown for all data years and B_w quarters, Hellstugubreen.

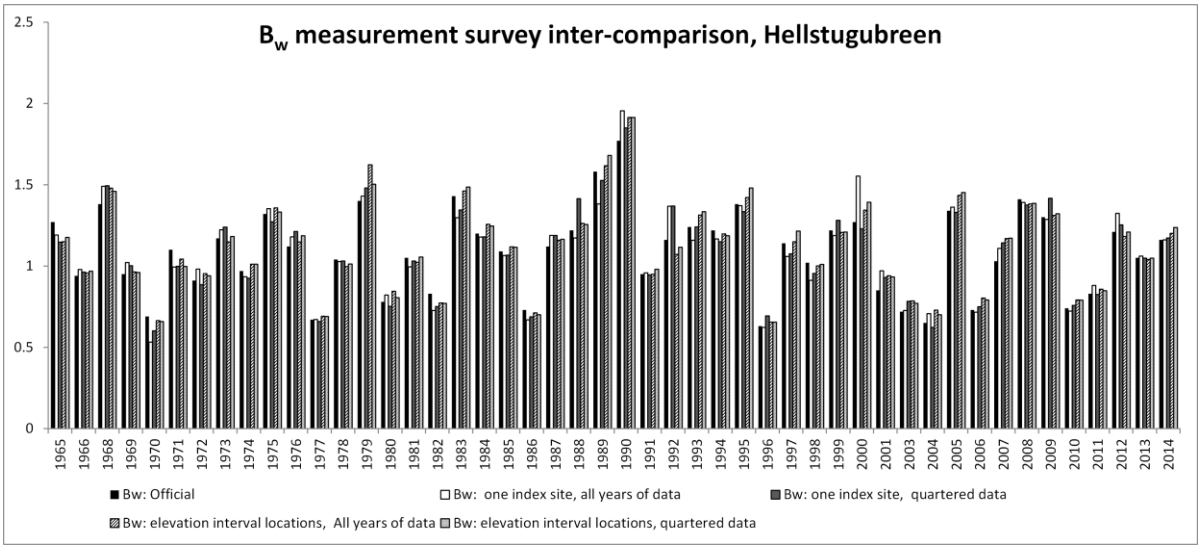

Figure 3.1.20 B_w values from the official B_w record and extracted probing locations, Hellstugubreen.

The differences between the official B_w record and the reconstructed B_w values based on representative probing site resampling are shown in Table 3.1-2. RMSE values are in m w.e., the dependent variable, and show no value greater than 9 cm error. The greatest RMSE is for $B_w one_{all}$. The lowest RMSE value, 0.06 m w.e., is for $B_w ele_q$. The mean percentage error is lowest for $B_w ele_q$ and $B_w ele_q$, at 4.8 %. The mean percentage error is greatest, at 6.1 % for $B_w one_{all}$, so too is the maximum percentage error, at 22.8 %, demonstrating the potential for considerable errors by using just one index site probing location based on all years of data. The lowest maximum percentage error, 13.7 %, is found when B_w is calculated using $B_w ele_q$.

Table 3.1-2 Errors and residuals between the official B_w record and calculated B_w values from survey designs, Hellstugubreen.

	RMSE (m w.e.)	Mean percentage error	Maximum percentage error	Minimum percentage error
All years of data: one location ($B_w one_{all}$)	0.09	6.1	22.8	0.0
B_w quartered data: one location ($B_w one_q$)	0.07	5.3	18.0	0.0
All years of data: elevation interval locations ($B_w ele_{all}$)	0.07	4.8	15.9	0.0
B_w quartered data: elevation interval locations ($B_w ele_q$)	0.06	4.8	13.7	0.1

The mean B_w values for the 48 year datasets are constructed for the variable survey designs, as shown in Table 3.1-3. Compared to the official B_w record, all survey designs produce higher B_w values, to a higher degree for elevation interval banded probing locations, and to the highest degree when data is also compiled from quartered B_w data years.

Table 3.1-3 Mean B_w values for the 48 years dataset using different survey designs.

	Mean B_w
B_w official	**1.08**
All years of data: one location ($B_w one_{all}$)	1.09
B_w quartered data: one location ($B_w one_q$)	1.09
All years of data: elevation interval locations ($B_w ele_{all}$)	1.11
B_w quartered data: elevation interval locations ($B_w ele_q$)	1.12

Differences between the official B_w record, and calculations using probings taken along the glacier centreline only are shown in Table 3.1-4. As previously noted, centreline only probings are based on the most central probing transect in a data year. The RMSE at 0.11 m is higher than any survey design in Table 3.1-2. So too is the mean percentage error at 8.9 %.

Table 3.1-4 Errors and residuals between the official B_w record and calculated B_w values from centreline only probings, Hellstugubreen

	RMSE (m w.e.)	Mean percentage error	Maximum percentage error	Minimum percentage error
Centreline	0.11	8.9	20.6	0.1

The mean B_w values for the official record and the values from centreline probing are shown in Table 3.1-5. Using only the centreline probings considerably underestimates the official B_w record. Indeed, of the 48 years, 42 years produce values lower than the official record.

Table 3.1-5 Mean B_w values for the official 48 year dataset and using centreline only probings, Hellstugubreen.

	Mean B_w
B_w official	**1.08**
Centreline	1.00

The number of probings required to calculate the mean SWE at different accuracy levels from random sampling is shown in Figure 3.1.21. The calculation is based on the standard deviation of data, and suggests that where SWE values fall in a broad data range, the number of random samples required to calculate the mean SWE value is high. As shown in Figure 3.1.22, many of the random sample sizes needed for 95 % accuracy are, in fact, significantly higher than the actual sample sizes taken. Indeed, the years 1986, 1989 and 1990 suggest over 300 % of the actual sample size is needed to accurately calculate the mean SWE value. Only 13 of the 48 years, require fewer than 100 % of the actual sample size to accuracy construct the mean SWE from random samples.

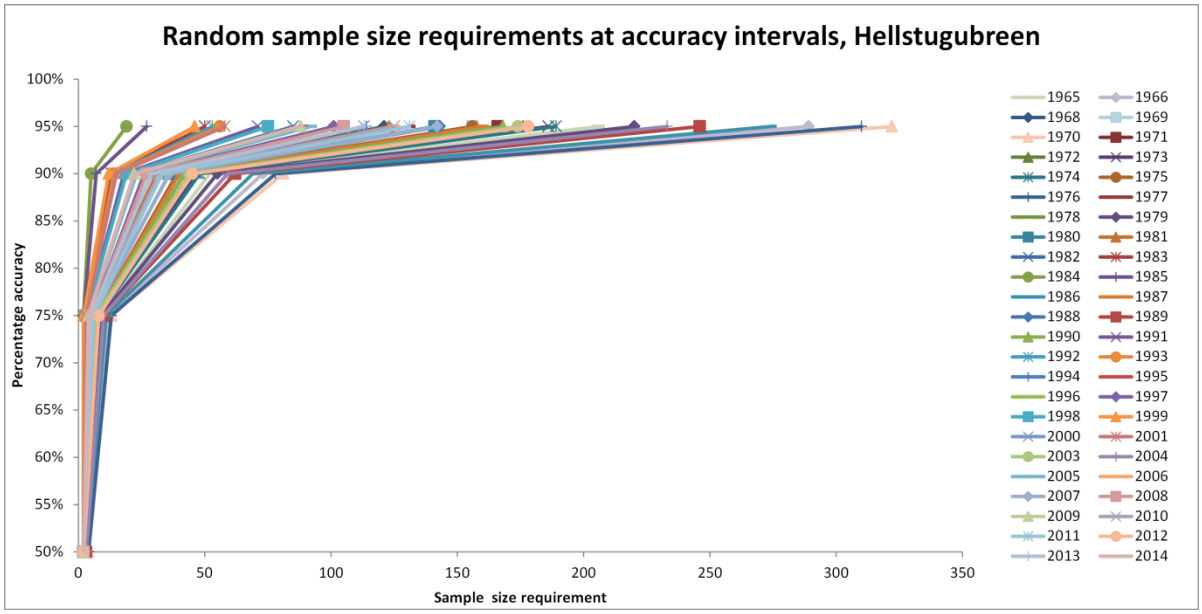

Figure 3.1.21 Survey sample size requirements from a random sample, for accuracy intervals.

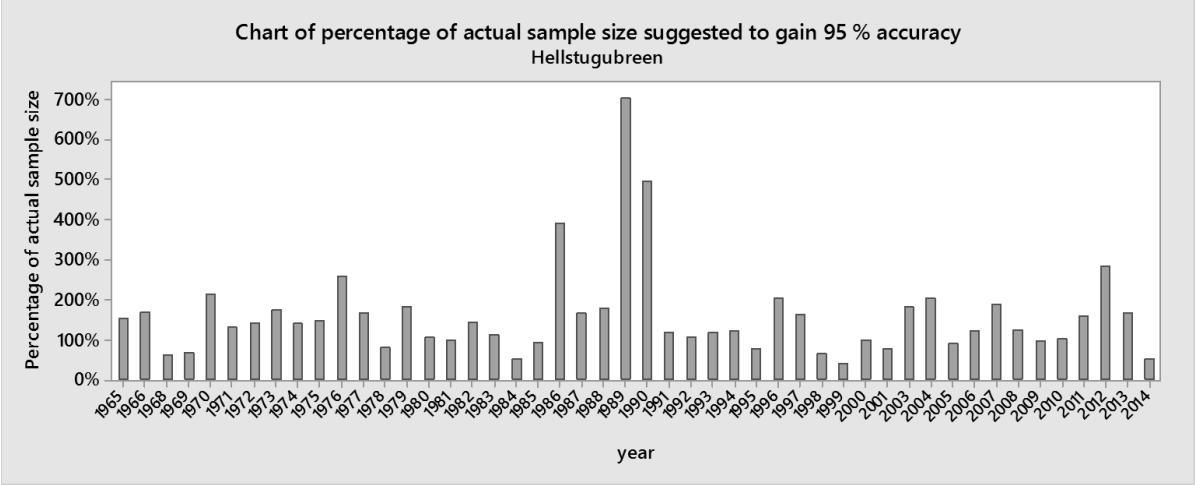

Figure 3.1.22 Chart of the percenatge of actual sample sizes suggested to gain 95 % accuracy of the mean SWE.

3.2 Gråsubreen

3.2.1 Data distribution

At Gråsubreen, 17 of 44 data years are normally distributed. Histograms of data distributions are shown in the appendix in Figure 7.1.7. Associated probability plots are shown in Figure 7.1.8. Note that the x and y scales are constant for all data years. No statistical distribution type was found to be significant for all of the individual data years. In agreement with the Anderson-Darling normality test, the majority of data years are non-normally distributed. Results from the Anderson-Darling normality tests are shown, alongside B_w and the number of b_w probings taken, in the appendix in Table 7.1-2.

The strength of normality has little relationship to the overall B_w, or the number of probings taken, as demonstrated by Figure 3.2.1 and Figure 3.2.2. Statistical distributions of SWE are not determined by the B_w, or the number of snow probings taken.

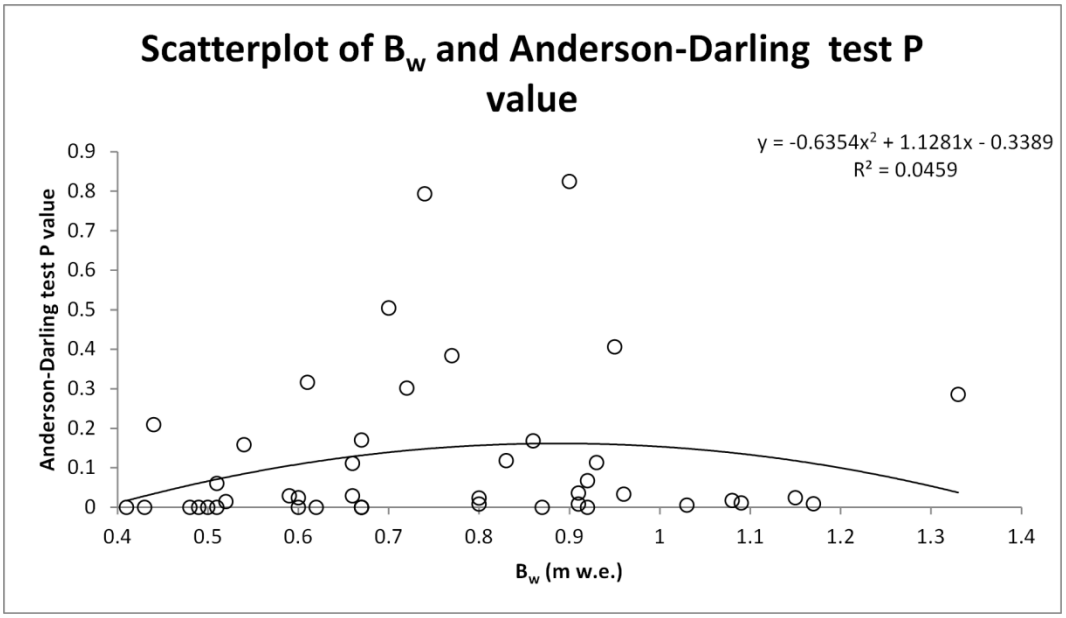

Figure 3.2.1 Scatterpot of B_w and Anderson-Darling normality test P values. A polynomial trendline is fitted to the data.

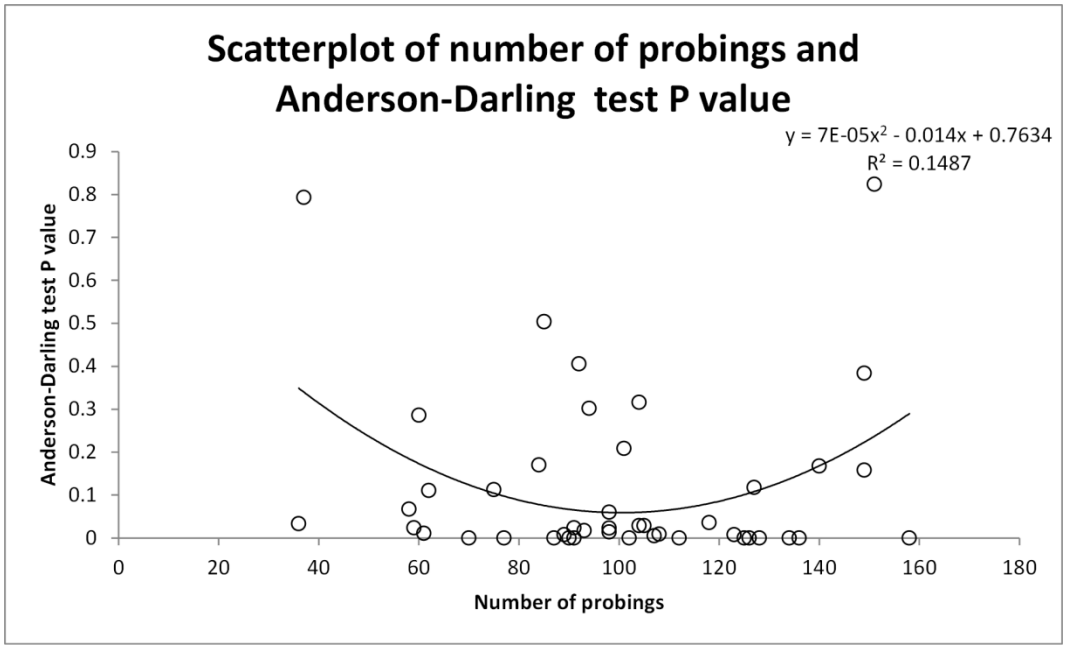

Figure 3.2.2 Scatterplot of the number of probings taken and the Anderson-Darling normality test P value. A polynomial trendline is fitted to the data.

Similar to Hellstugubreen, merged normalised probing data are also non-normally distributed. Again the Anderson-Darling normality test P value is <0.005. The distribution of data is shown in the probability plot in the appendix in Figure 7.1.9 and the histogram Figure 7.1.10.

The statistical distribution of winter balances is shown in the appendix in Figure 7.1.11. The data years are categorised by B_w quarters, and are shown in Table 3.2-1. These data year groups are referred to throughout the thesis. Notably, different numbers of years are found in each quarter, with only three years in B_w quarter 4.

Table 3.2-1 B_w quarter data categorisation, Gråsbreen.

Quarter 1	Quarter 2	Quarter 3	Quarter 4
1971	1972	1968	1990
1974	1973	1975	1994
1976	1978	1979	1995
1977	1985	1983	
1980	1991	1984	
1981	1992	1987	
1982	1997	1988	
1986	1998	1989	
1996	2000	1993	
2003	2001	1999	
2004	2005	2008	
2006	2009		
2007	2011		
2010	2013		
2012	2014		

3.2.2 Snow probing spatial distribution and normalised SWE values

The spatial coverage of snow probing data is very good. Figure 3.2.3 shows the spatial distribution of all years of compiled normalised SWE data. An inverse pattern of SWE with elevation is shown, with higher values near the snout of the glacier, and lower values in the mid-high elevation areas.

Notably, a cluster of probings in the 0-0.2 normalised SWE range is shown in the central region of the glacier. This is balanced by higher normalised SWE values in the 0.8-1 range towards the lower region of the glacier. The peripheral regions on the north, east and southern edges of the glacier show a high degree of variability in normalised SWE values. In particular, high variability in normalised SWE values is exhibited along the south-western edge of the glacier.

Different B_w quarters of data show a generalised similar spatial distribution of normalised SWE values, as shown in Figure 3.2.4. However, differences in the distributions can be

noted. In particular the size and extent of the large clustering of low normalised SWE values in the centre of the glacier varies. The region is largest for B_w quarter 1, and extends on a south-west to north-east axis to a greater extent than all other B_w quarters. For quarter 1, there is also the greatest continuity of this region to the south-east, whereas other B_w quarters exhibit more discontinuity.

The clustering of high normalised SWE values in the 0.8-1 value range at the snout of the glacier is most prominent for B_w quarter 3, where other years show less defined clustering. All B_w quarters show poor clustering in the south-western edge of the glacier, where normalised SWE values appear to vary greatly in close proximity.

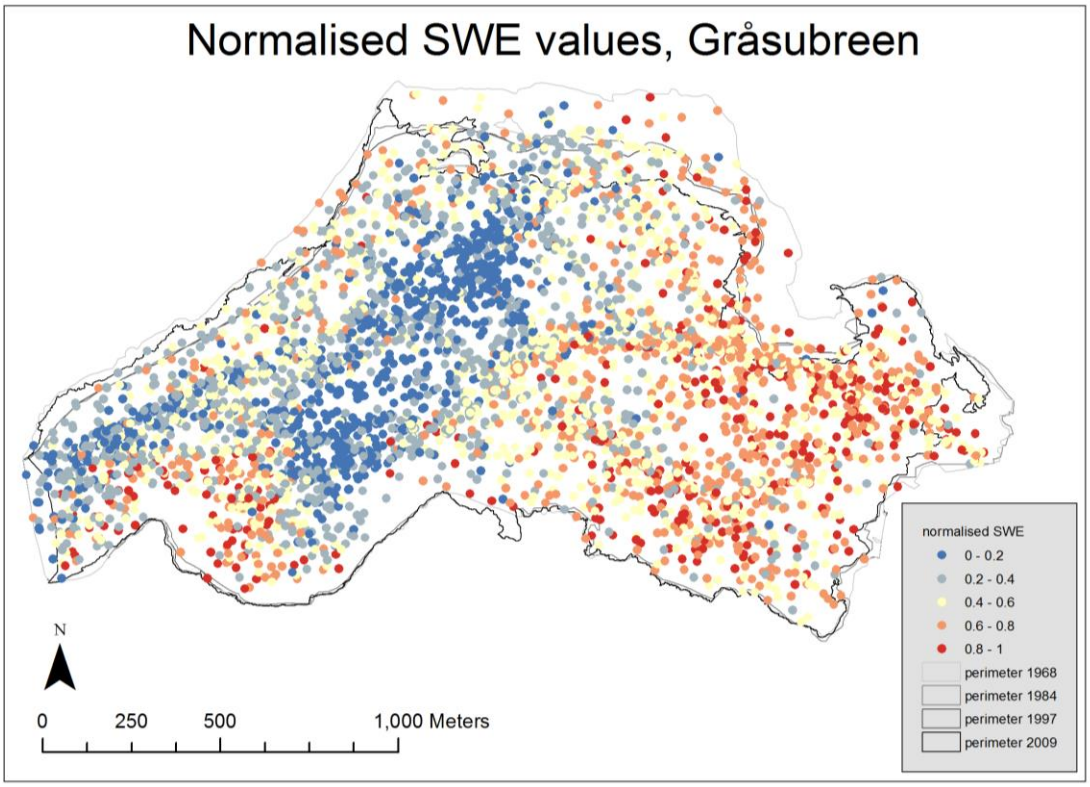

Figure 3.2.3 Map of probing locations for all years, shown with normalised SWE values.

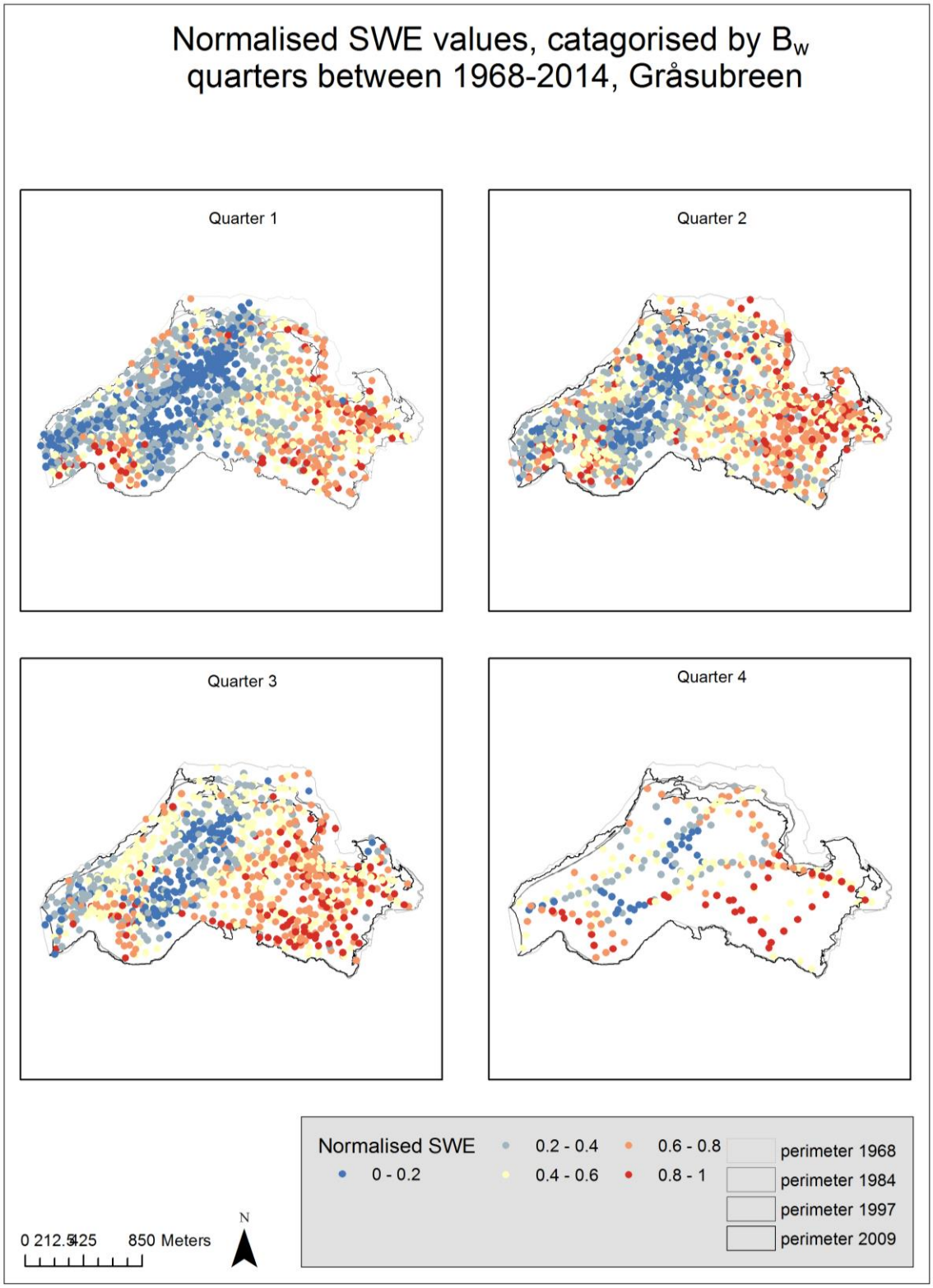

Figure 3.2.4 Maps of probing locations, categorised by B_w quarters, and shown with normalised SWE values.

3.2.3 Stability

i. Inter-annual snow spatial distribution variation

RMSE values of one data year against all years of data combined are shown in Figure 3.2.5. Here, RMSE is calculated on a cell-by-cell basis. RMSE values range from 0.07-0.41. Note that normalised SWE is the dependent variable, and therefore the RMSE scale ranges from 0-1. The relatively broad range of values shows a high level of differences in the spatial distribution of SWE data at Gråsubreen: some years are similar to the pattern with all years combined, where others show defined differences.

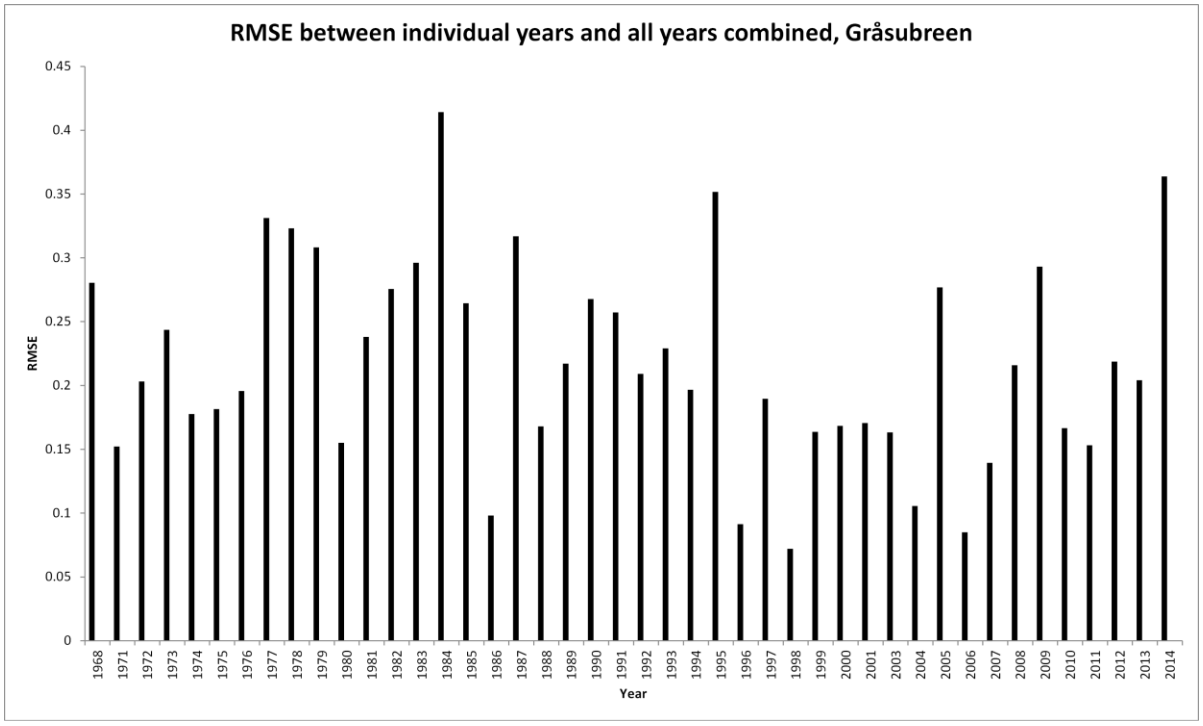

Figure 3.2.5 RMSE between each year and all years combined. Normalised SWE values are used in this calculation.

RMSE values are plotted with B_w values in Figure 3.2.6. There is a very weak positive relationship between B_w values and RMSE values, showing that residuals between different data years spatial distributions relative to all data are not strongly influenced by the overall B_w.

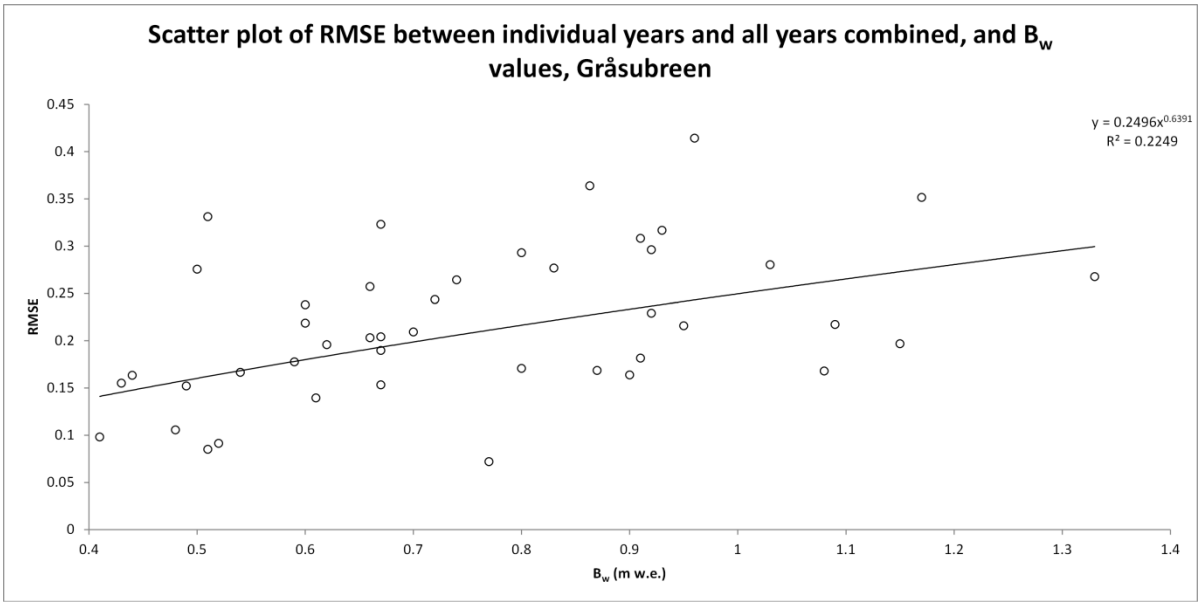

Figure 3.2.6 Scatterplot of RMSE and B_w values.

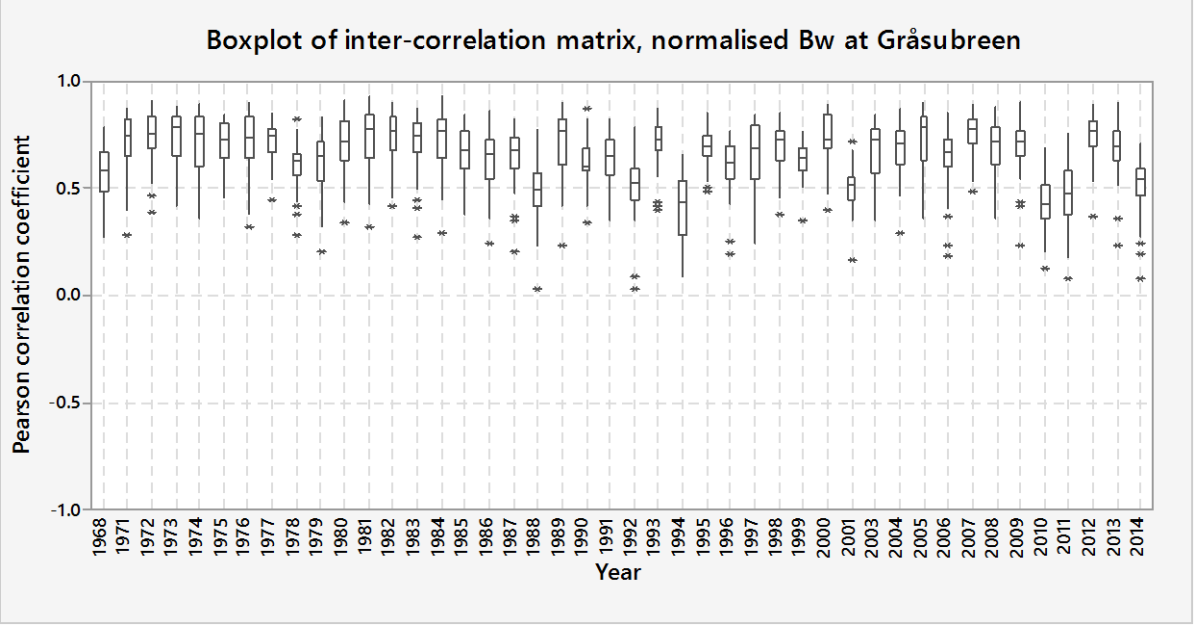

Figure 3.2.7 Boxplot matrix of inter-correlations between an individual year and all other years. Normalised SWE values are used in this calculation.

An inter-correlation matrix between a year and all other years is shown in Figure 3.2.7. Similar to Hellstugubreen, all years have a positive correlation to all other years, with the median below 0.5 for only four years: 1988, 1995, 2010 and 2011. The IQR varies between 0.10 (1978) and 0.25 (1997); suggesting that most spatial pattern correlations fall in a small range for a given year. However, IQRs, whiskers and outliers show that most years are negatively skewed; with a broader range of values falling below the median value. Whilst a good correlation is found in most cases, the cases with poor correlation fall further from the median than those with good correlations. The high number of negative outliers (shown by asterisks), also denotes that there are years with poor correlations to other years.

ii. Probing stability

Maps of probing stabilities and percentages of required probings under an optimum allocation stratified sampling survey regime are shown in Figure 3.2.8 through Figure 3.2.12 for all years of data, and B_w quarters 1 through 4 respectively. A generalised spatial pattern shows greatest stability in the central area of known thin snowpack, and reduced stability at the peripheral edges of the glacier.

The most stable map is B_w quarter 4, especially along the southern perimeter edge of the glacier. Note this quarter has only three constituent data years, the fewest of all B_w quarters. The same stable southern edge, is however, less stable than other surrounding areas for quarters 1 and 2. The map of all years of data is the least stable, with greatest normalised SWE variability in the western high elevation areas, and at the northward curve at the glacier snout.

The stability map for all data years shows the greatest degree of variability, and therefore lowest stability. Optimised allocation stratified sampling percentage probing requirements are greatest in the high variability zones for all years of data. Indeed, 53 % fall in the 60-80 % variability zone, and 22 % in the 80-100 % variability zone. Comparatively for quarters 1-4, 9, 8, 12 and 0 % of probings should be taken in the 80-100 % variability zones under the sampling survey regime. For all stability maps featuring the highest variability zone, these are located at or towards the peripheries of the glacier.

The stability maps for quarter 4 shows the greatest degree of stability. The optimum allocation stratified sampling probing requirements for the 0-20 % variability zone is 8 %, where for all years of data and quarters 1 through 3, the requirements are 0, 3, 0 and 0 % respectively, demonstrating the limited contribution of this stability zone in other maps. The 0-20 % variability zone is only present in quarters 1 and 4, and is located in the central snow-poor area in quarter 1, and along the southern perimeter edge in quarter 4.

The map for all years of data has the highest percentage of optimised allocation stratified sampling probing requirements in variability zone 60-80 %; for quarters 1-3 variability zone 40-60 % has the highest percentage; for quarter 4, variability zone 20-40 % has the highest percentage of probing requirements.

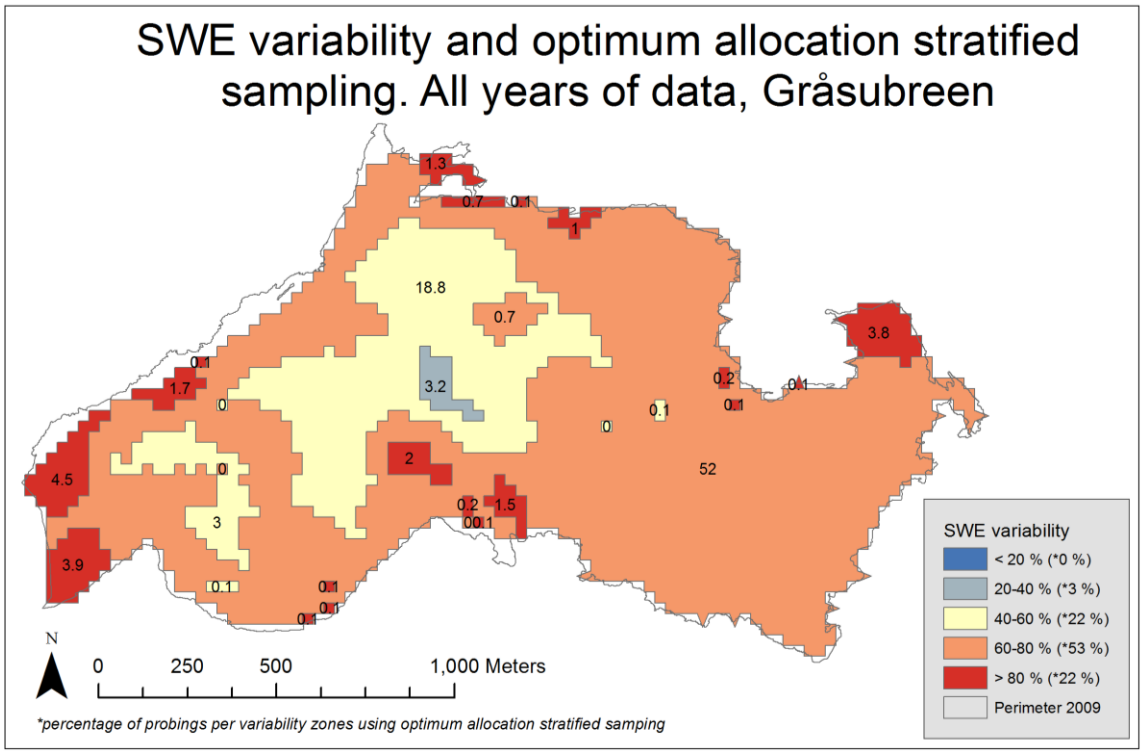

Figure 3.2.8 Probing stability map and optimum allocation stratified sampling percentages, for all years of data.

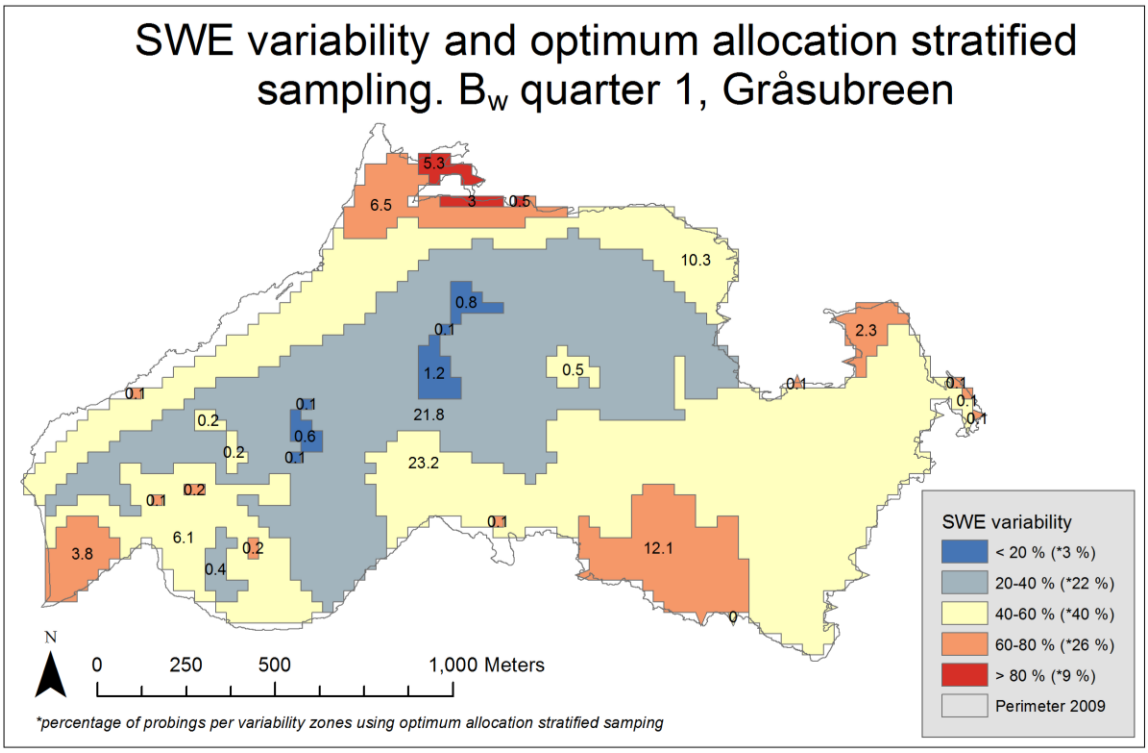

Figure 3.2.9 Probing stability map and optimum allocation stratified sampling percentages, for B_w quarter 1.

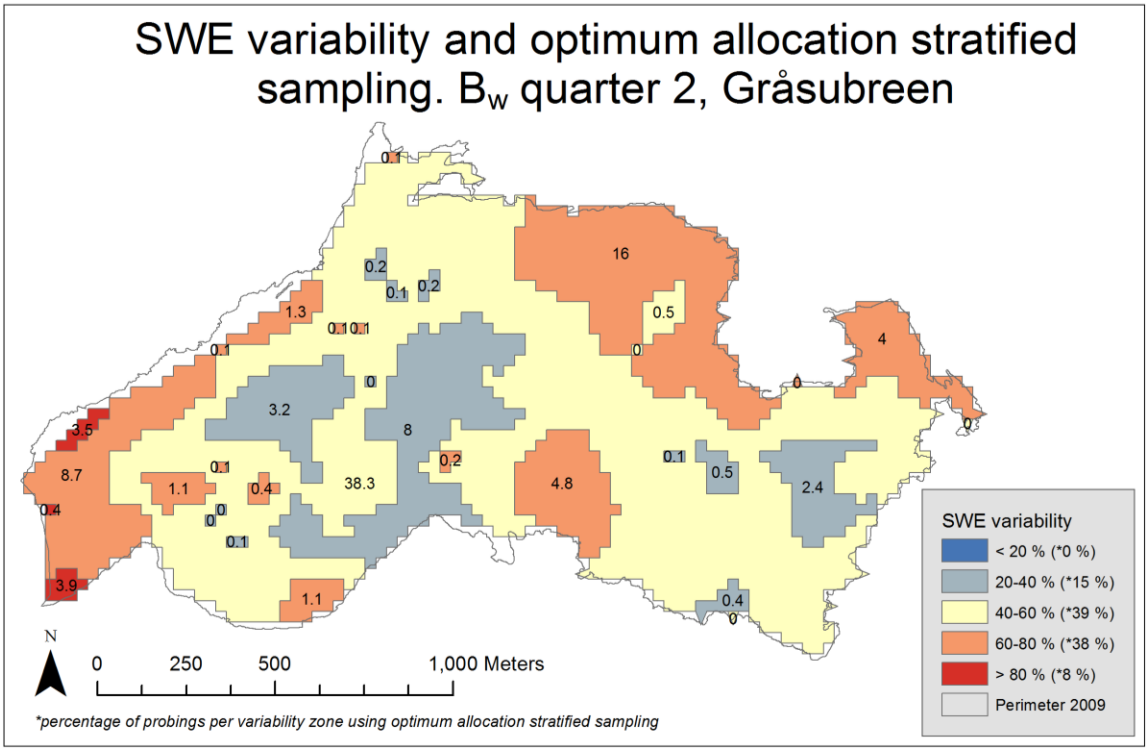

Figure 3.2.10 Probing stability map and optimum allocation stratified sampling percentages, for B_w quarter 2.

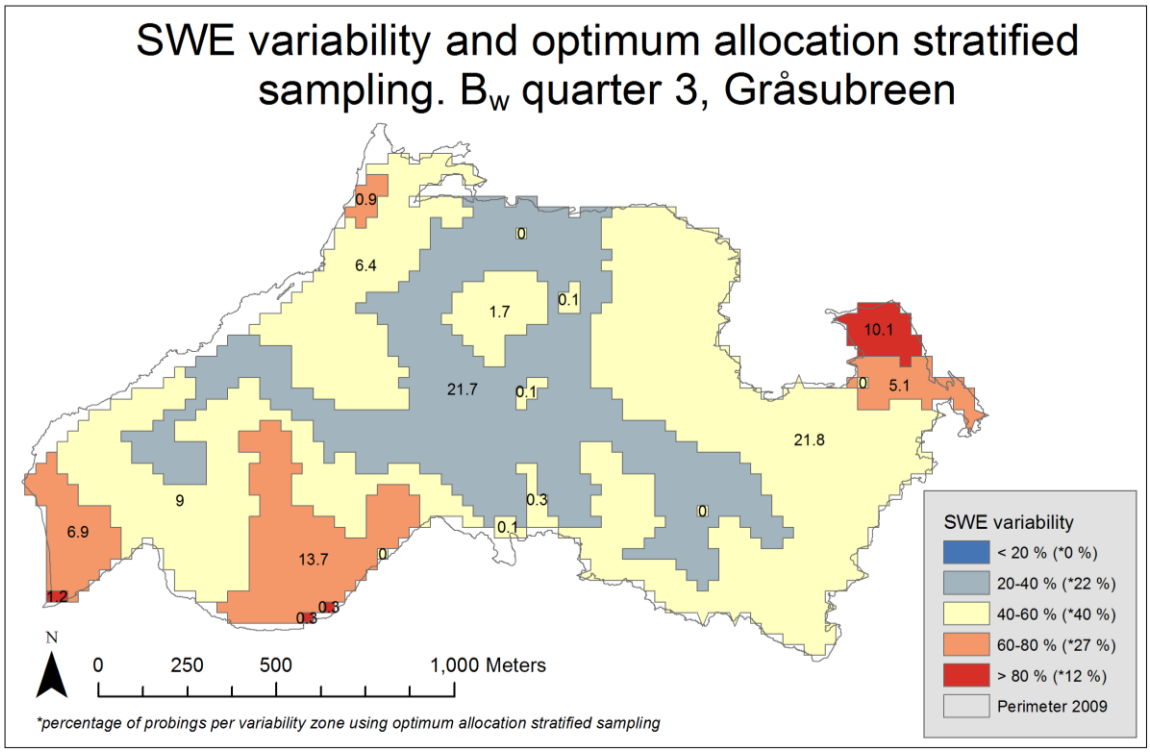

Figure 3.2.11 Probing stability map and optimum allocation stratified sampling percentages, for B_w quarter 3.

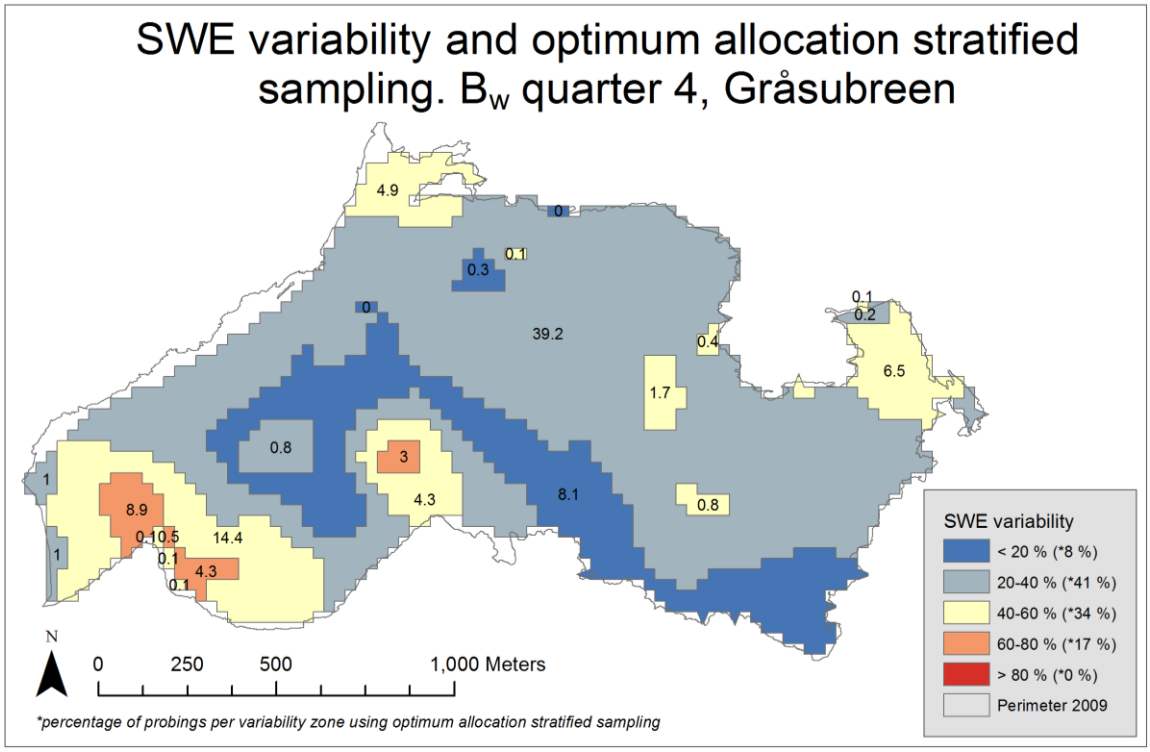

Figure 3.2.12 Probing stability map and optimum allocation stratified sampling percentages, for B_w quarter 4.

The areas of different variability zones for the five above maps are shown in Figure 3.2.13. The distribution of data is skewed towards high variability for all years of data, showing reduced variability for quartered data.

The all years of data map has the largest area in the 60-80 % variability zone; quarters 1-3 have the largest area in the 40-60 % variability zone; quarter 4 has the largest area in the 20-40 % variability zone. These proportions are in agreement with the optimised allocation stratified sampling regime described above. Quarter 4 shows the greatest area defined stability as shown by the highest proportion of area in the <20 % and 20-40 % variability zones, followed by the similar quarters 1 and 3, with quarter 2 the least stable B_w quarter by area. The 80-100 % variability zone area is negligible for all quartered data, and is only notable for all years of data.

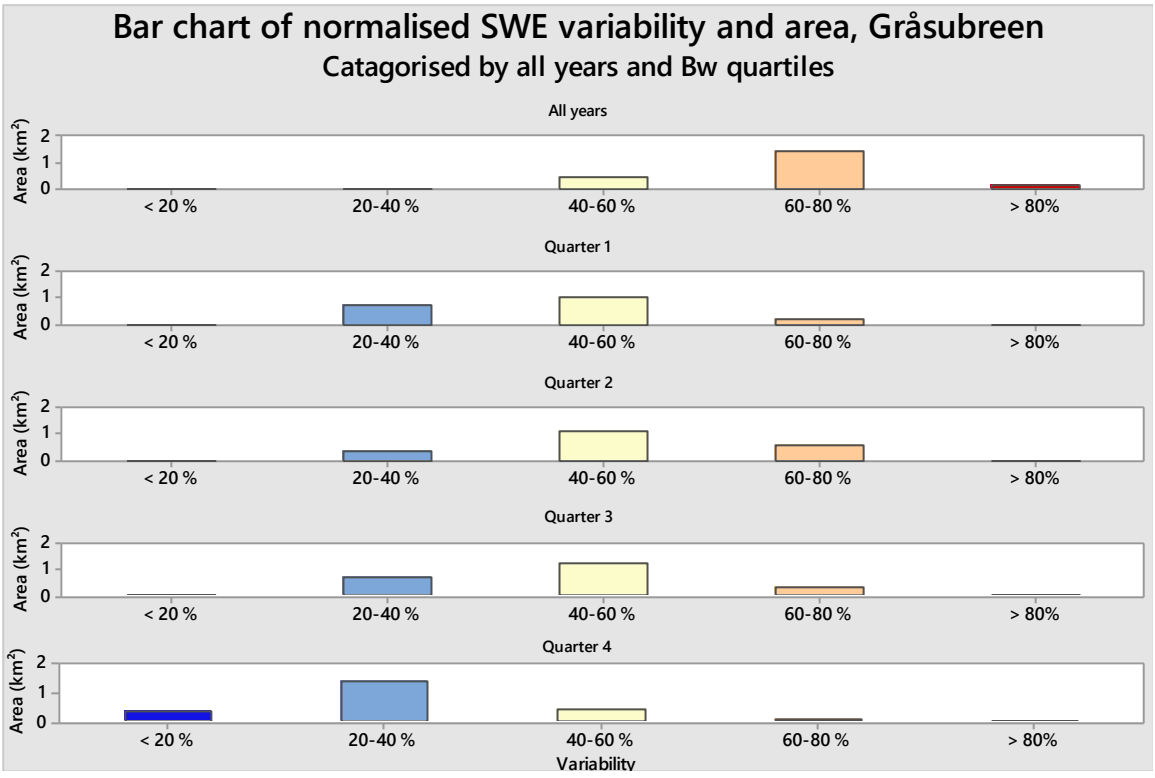

Figure 3.2.13 Areas of different variability zones for all years of data, and B_w quarters.

3.2.4 Reliability

Reliability maps for one probing location for Gråsubreen are shown in Figure 3.2.14 ($B_w one_{all}$ and $B_w one_q$), and for 50 m elevation interval probing locations in Figure 3.2.15 ($B_w ele_{all}$ and $B_w ele_q$). For $B_w one_{all}$ and $B_w one_q$, there is general consistency of representative probing locations across the centre of the glacier. The representative zone stretches across the glacier for $B_w one_{all}$, however, the zone is thinner for $B_w one_q$ quarter 4. The central thin snowpack area and the snout of the glacier are particularly unrepresentative probing locations.

When probing locations are taken in every 50 m elevation interval ($B_w ele_{all}$ and $B_w ele_q$), the elevation intervals with the greatest level of representativeness are downglacier. The central elevation interval found most representative for $B_w one_{all}$ and $B_w one_q$ retains a high, though diminished, level of representativeness as an elevation interval banded probing location. The central thin snowpack area is similarly unrepresentative for $B_w ele_{all}$ and $B_w ele_q$, as it is for $B_w one_{all}$ and $B_w one_q$.

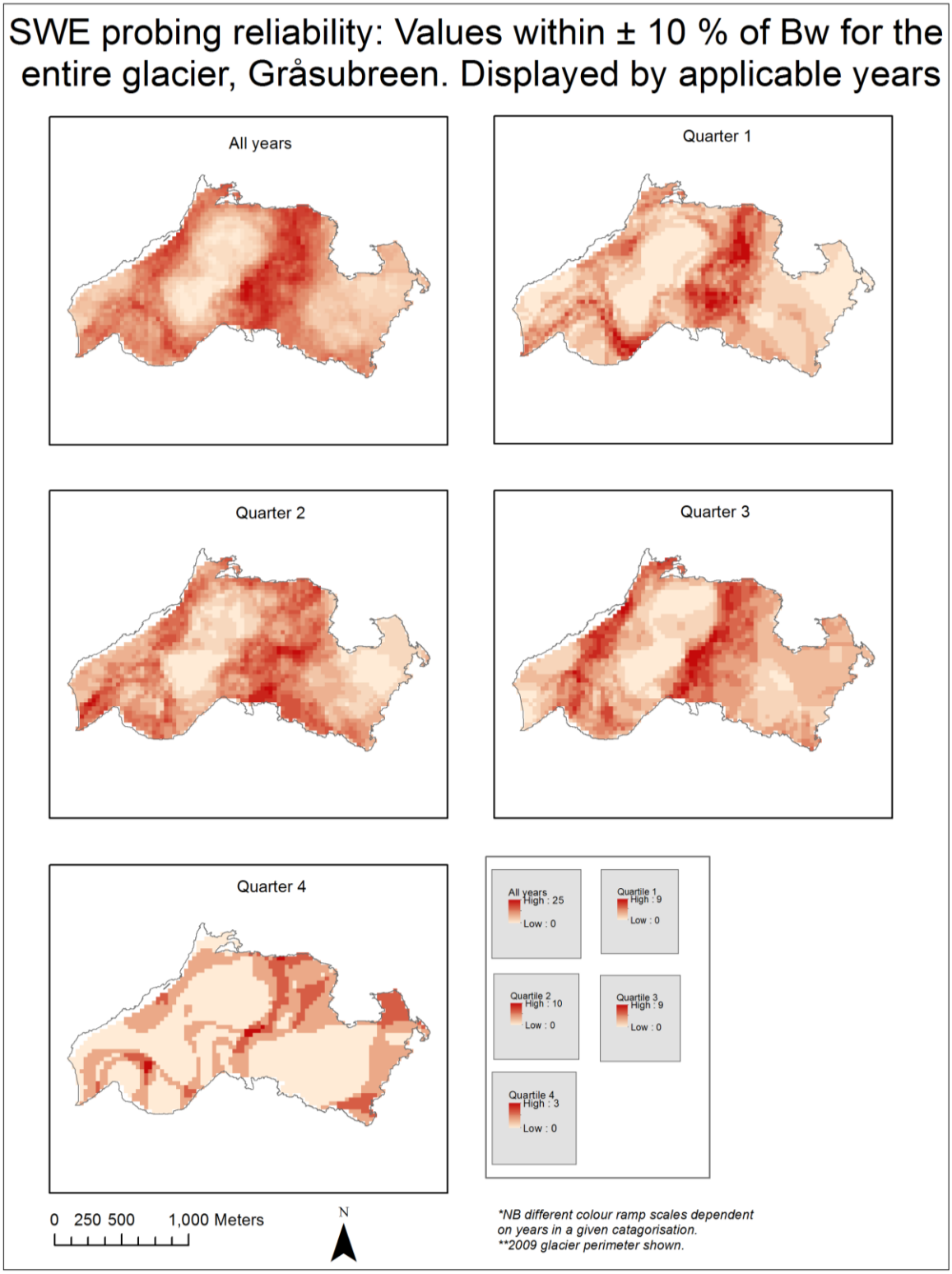

Figure 3.2.14 Reliability maps for one representative probing for the entire glacier, categorised by all years and by B_w quarters.

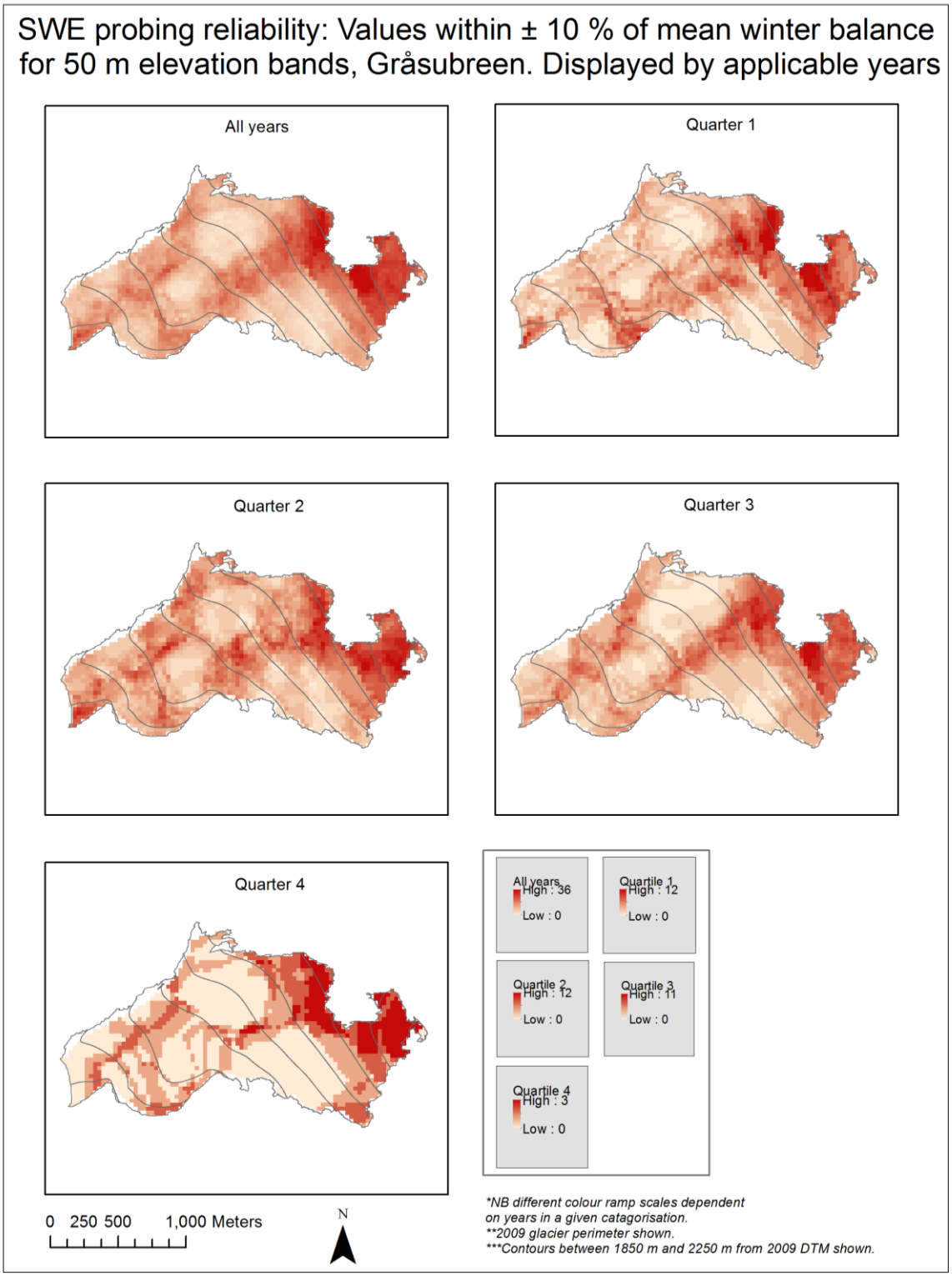

Figure 3.2.15 Reliability maps for one representative probing at 50 m elevation intervals, categorised by all years of data and B_w quarters.

The percentage of available data years used in reliability map chosen representative probing locations for $B_w one_{all}$ and $B_w one_q$ are shown in Figure 3.2.14, for $B_w ele_{all}$ and $B_w ele_q$ they are shown in Figure 3.2.15.

For $B_w one_{all}$ and $B_w one_q$, the lowest percentage of year layers used is 59 % for $B_w one_{all}$. This then increases through the $B_w one_q$ quarters from 60 % to 100%. This pattern is near coherent with the decrease in the number of available data year layers in total (44 for all years, 15, 15, 11 and 3 for quarters 1-4. Note that quarters 1 and 2 have the same number of available data years, but different percentages of data year layers used).

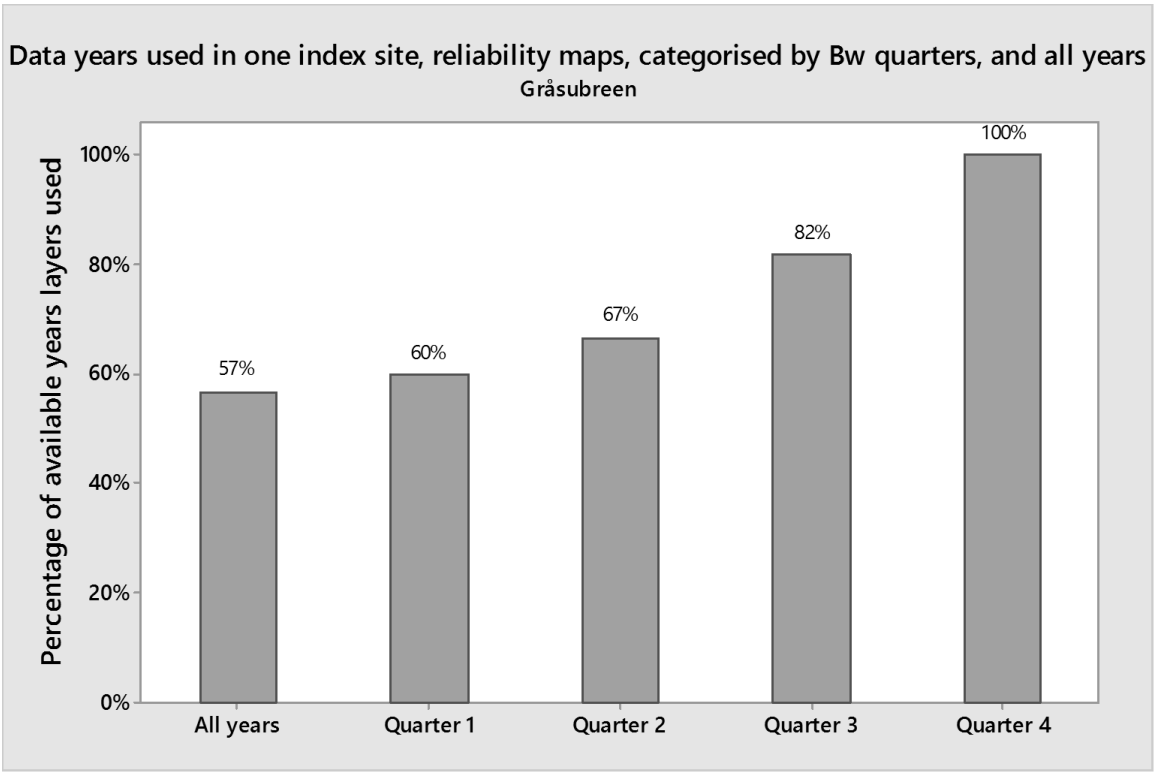

Figure 3.2.16 Chart of percentage of year layers at one representative probing reliability location for the entire glacier, relative to all available years. Data categorised by all years of data, and B_w quarters.

The percentage of layers used in elevation interval banded representative probing locations show significant variation. For $B_w ele_{all}$, there is an increase in the percentage of layers used as elevation increases. This pattern is not shown in $B_w ele_q$; moreover, a generalised counter-

effect is visible, with a higher percentage of data year layers used at lower elevation intervals. Though for $B_w ele_q$ quarter 1 and 3, the lowest elevation (1830-1900 m) interval has a lower percentage of years used than the next two elevation intervals (1900-1950 and 1950-2000 m). $B_w ele_{all}$ and $B_w ele_q$ quarter 1 show the overall lowest percentage of data year layers used in the construction of elevation interval banded reliability maps.

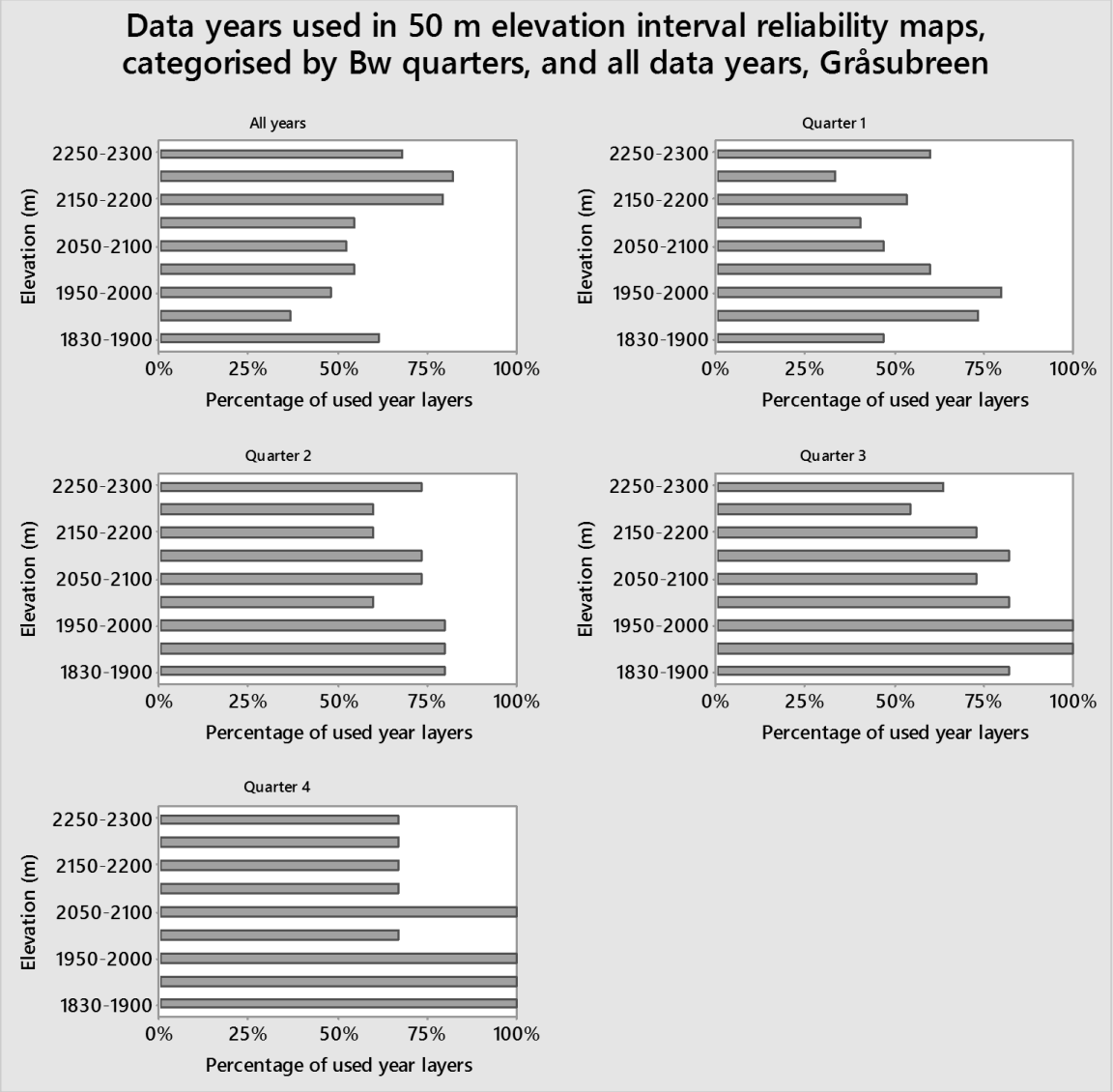

Figure 3.2.17 Chart of percentage of year layers at representative probing locations at 50 m elevation intervals, relative to all available years. Note, elevation distributions are taken from the 2009 contour map.

3.2.5 Survey design

The representative probing locations are used to extract SWE data and reconstruct B_w for the four reliability map designs, as outlined in Table 2.5-1. The sites of the most representative b_w probing locations based on the reliability maps are shown in Figure 3.2.18 and Figure 3.2.19 for one index site locations for the entire glacier, and for a representative probing location per 50 m elevation interval respectively. The extracted B_w results, displayed adjacent to the official B_w record, are shown in Figure 3.2.20. There is a general good degree of agreement between the methods, however, significant differences from the official B_w record can be seen in 1991 for $B_w one_q$. In 2007, all four survey design techniques exceed the official B_w record by a significant margin.

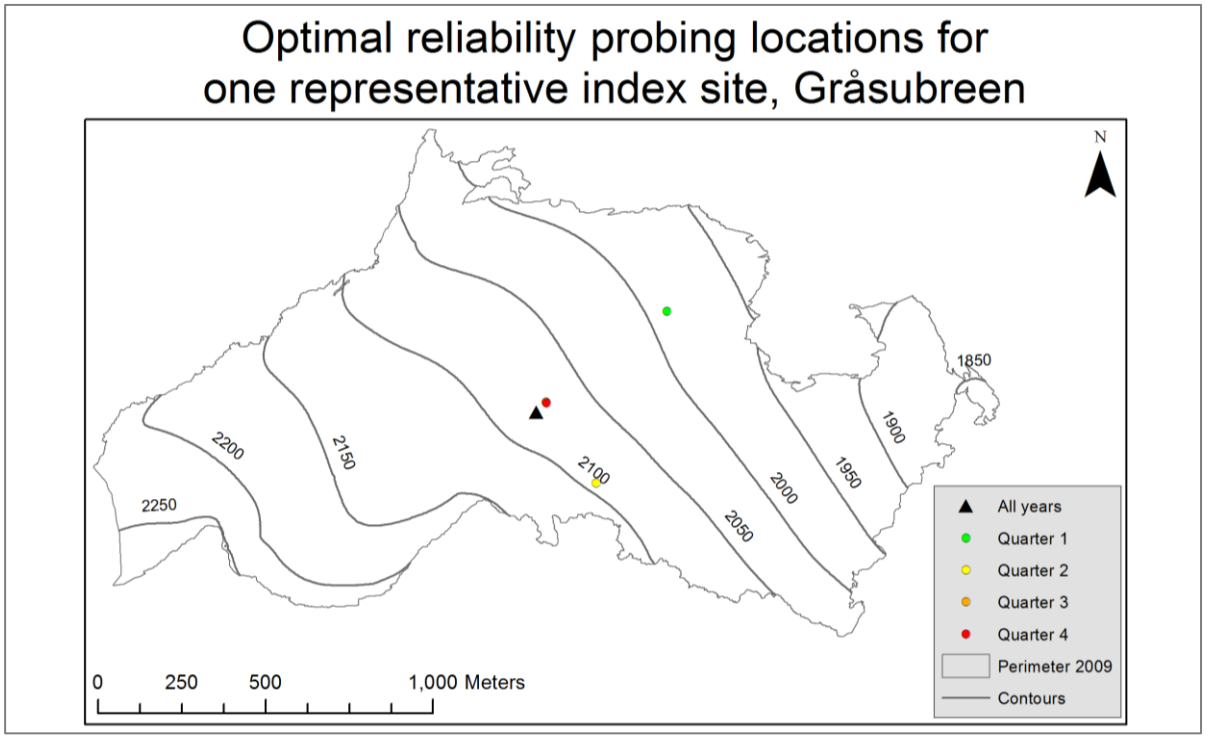

Figure 3.2.18 Survey design b_w probing locations for one index site for B_w calculation. Shown for all data years, and B_w quarters, Gråsubreen. Note that the locations for quarters 3 and 4 overlap, obscuring quarter 3.

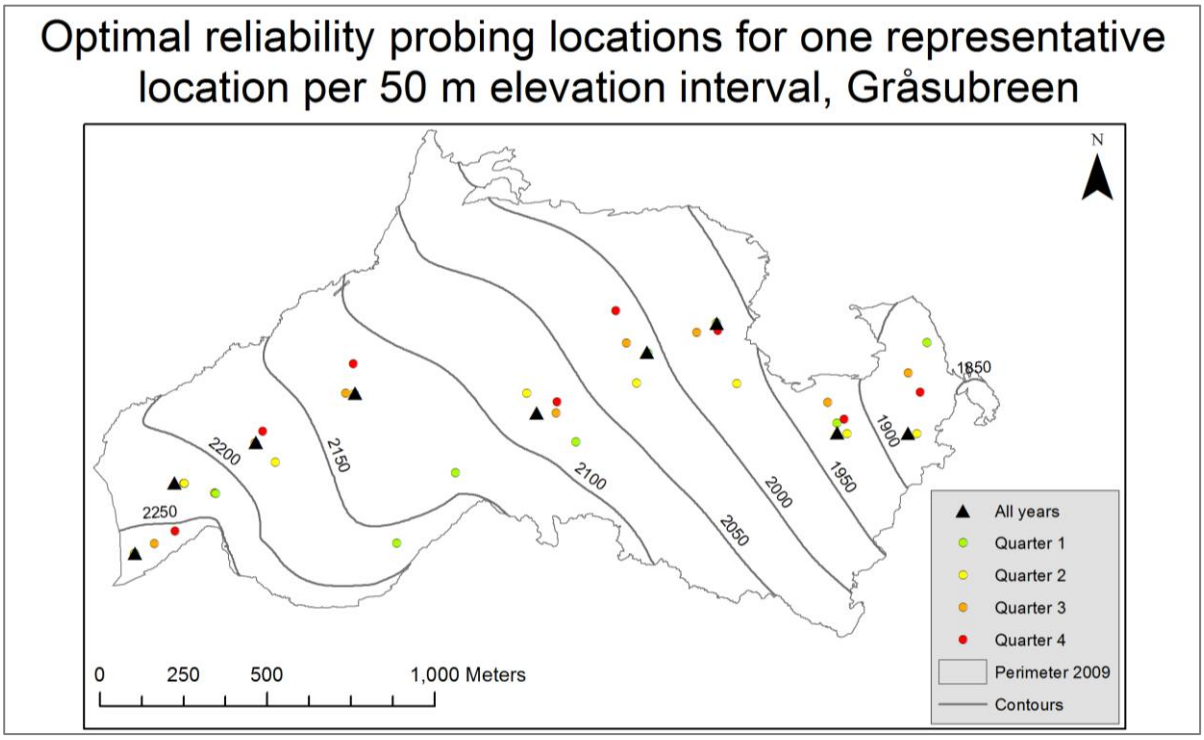

Figure 3.2.19 Survey design b_w probing locations for one b_w probing per 50 m elevation interval, shown for all data years, and B_w quarters, Gråsubreen.

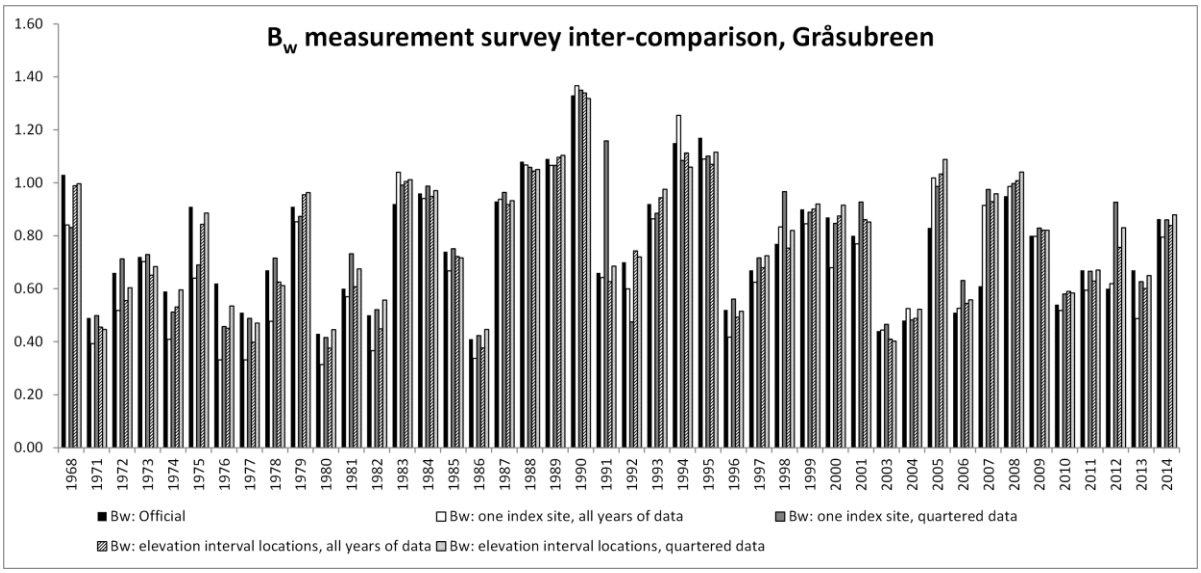

Figure 3.2.20 B_w values from official B_w record and extracted probing locations, Gråsubreen.

The differences between the survey designs and the official record are given in Table 3.2-2. Significantly, both the RMSE and the mean percentage error are lower when B_w is calculated from 50 m elevation interval probings ($B_w ele_{all}$ and $B_w ele_q$), than for one probing location for $B_w one_{all}$ and $B_w one_q$. The RMSE using $B_w one_{all}$ and $B_w one_q$ is above 0.12; using $B_w ele_{all}$ and $B_w ele_q$, the RMSE is below 0.09 in all cases. The mean percentage error is greater than 12.1 % when using $B_w one_{all}$ and $B_w one_q$; using $B_w ele_{all}$ and $B_w ele_q$ the mean percentage error is below 8.3 %. The RMSE is highest for $B_w one_q$, at 0.14, and lowest at 0.08 using $B_w ele_{all}$.

High maximum percentage errors are seen for all survey designs, ranging from 49.9 % to 75.6 %. For the grouping, $B_w one_{all}$, $B_w ele_{all}$ and $B_w ele_q$, the high error is caused by the 2007 data year. For the grouping $B_w one_q$, the highest error is due to the 1991 survey design.

Table 3.2-2 Errors and residuals between the official B_w record and calculated B_w values from survey designs, Gråsubreen.

	RMSE (m w.e.)	Mean percentage error	Maximum percentage error	Minimum percentage error
All years of data: one location ($B_w one_{all}$)	0.12	13.6	49.9	0.3
B_w quartered data: one location($B_w one_q$)	0.14	12.1	75.6	0.4
All years of data: elevation interval locations ($B_w ele_{all}$)	0.08	8.3	52.4	0.1
B_w quartered data: elevation interval locations ($B_w ele_q$)	0.09	8.1	57.2	0.1

The mean B_w values for the 44 years, based on the official record and on survey designs, are shown in Table 3.2-3. Using all years of data 23, the mean B_w is underestimated relative to the official record; conversely, using B_w quartered data, the mean B_w is overestimated. The smallest mean error value is given by using reliability maps based on $B_w ele_{all}$.

Table 3.2-3 Mean B_w values for the 44 years dataset using different survey designs.

	Mean B_w
B_w official	**0.75**
All years of data: one location	0.71
B_w quartered data: one location	0.78
All years of data: elevation interval locations	0.75
B_w quartered data: elevation interval locations	0.78

Using the glacier centreline only probings produces different residual and error results relative to the official B_w record, as shown in Table 3.2-4. Both the RMSE at 0.11, and the mean percentage error at 11.9 %, lie below those produced by using one probing location for the entire glacier, but above those produced by using one probing per 50 m elevation interval.

Table 3.2-4 Errors and residuals between the official B_w record and calculated B_w values from centreline only probings, Gråsubreen.

	RMSE (m w.e.)	**Mean percentage error**	**Maximum percentage error**	**Minimum percentage error**
Centreline	0.11	11.9	55.4	0.01

The mean B_w values from the official record, and using just the centreline, are shown in Table 3.2-5. Using only centreline probings underestimates the B_w relative to the official record. Of the 44 years of data, 26 produced B_w values lower than the official record when using only the centreline probings.

Table 3.2-5 Mean B_w values for the official 44 year dataset and using centreline only probings, Gråsubreen.

	Mean B_w
B_w official	**0.75**
Centreline	0.74

The number of randomized b_w probings required for different accuracy intervals, based on the mean value and standard deviation, are shown in Figure 3.2.21. Significant increases in sample sizes are required between the 90 and 95 % accuracy intervals.

Owing to the high spread of data, and the high standard deviation relative to the mean, many required sample sizes for 95 % accuracy are higher than the actual sample size taken. This is shown in Figure 3.2.22. Indeed, greater than 500 % of the sample size is required for the years 1971, 1976, 1980, 1982, 1984, 1986, 1989, 1996 and 2012; over 1000 % of the actual sample size is required for the years 1976 and 1984, demonstrating the spread of SWE values recorded in those years. Of the 44 data years, only three, 1988, 2001 and 2010, require fewer than the actual sample size to gain 95 % accuracy.

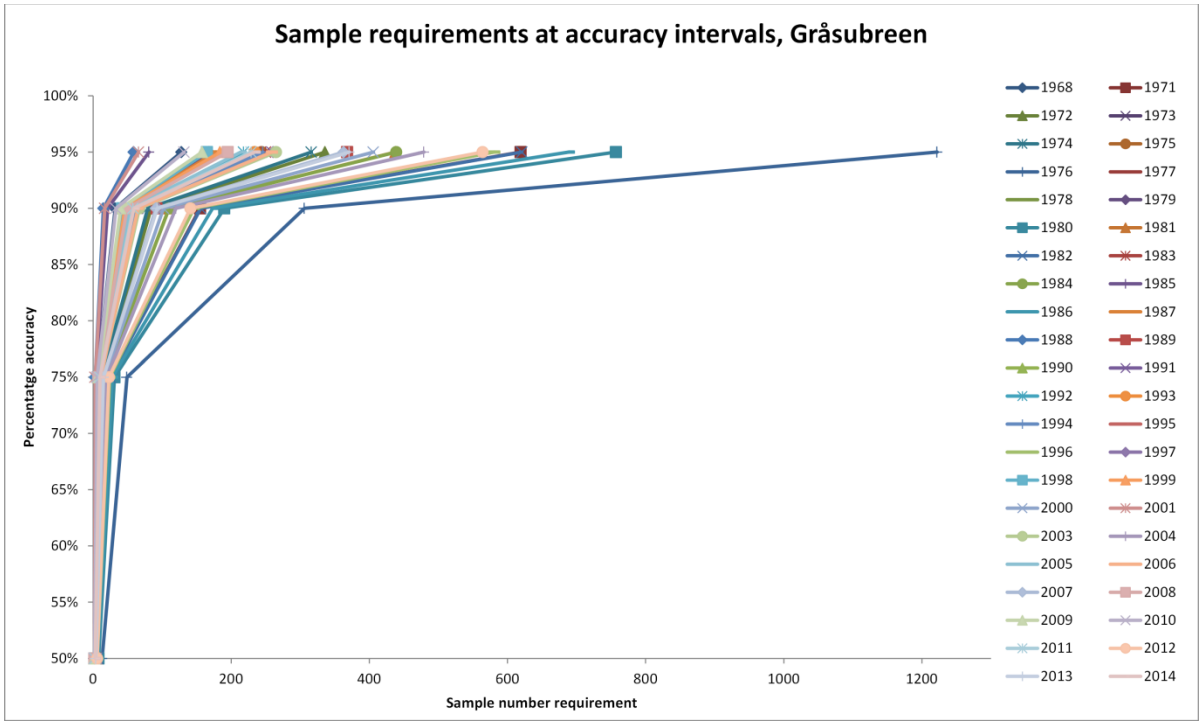

Figure 3.2.21 Survey sample size requirements from a random sample, for accuracy intervals, Gråsubreen.

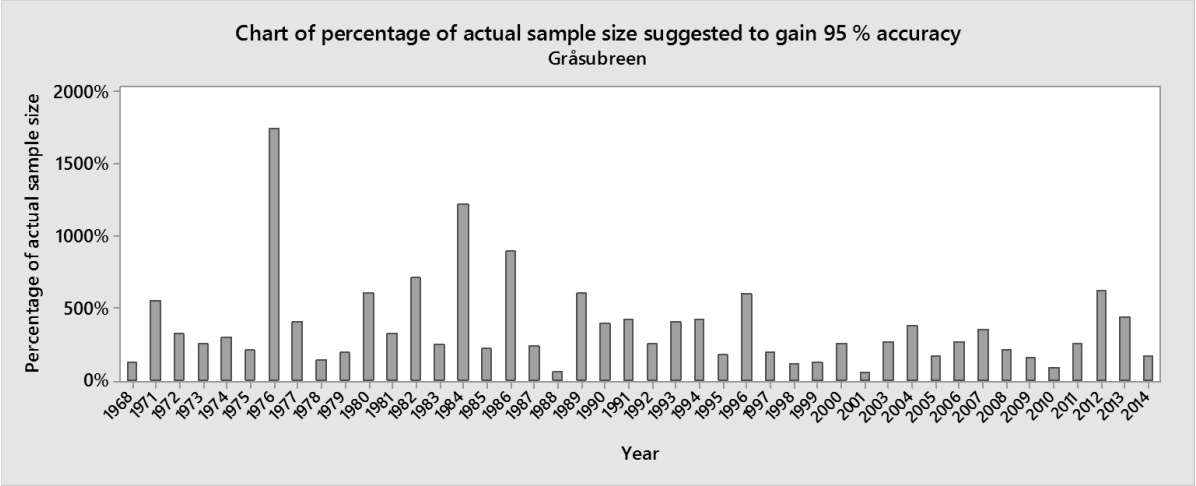

Figure 3.2.22 Chart of the percentage of actual sample sizes suggested to gain 95 % accuracy of the mean SWE.

3.3 Wind frequency distributions

Wind frequency distributions, shown as wind roses in Figure 3.3.1, give details of dominant wind conditions in the latter accumulation months of all individual data years. Note that different WSs have different data series lengths and timings, as noted in section 2.6. For all WS locations, winds from the south-west dominate. However, detailed analysis of different WSs show variable wind patterns, as similarly found in WS wind data inter-comparisons by Giesen *et al*. (2009). At Elveseter, generally weak south-westerlies are the most frequent, with significant winds also found from the geographically opposite north-east. At Bøverdal-Sletten, westerlies are the most frequent. These are generally weak winds ranging mostly from 0.1-10 ms^{-1}, with 47 % of all data described as calm. At Sognefjellhytta, a broader range of directions are observed, though still dominated by south-westerlies, with some south-south-easterlies. At Juvvasshøe, the strongest winds are found reaching over 20 ms^{-1}, with a broad directional spread, again covering westerlies, south-westerlies, with some south-south-easterlies.

Figure 3.3.1 Wind rose frequency distributions at nearby WSs. Note variable time series lengths, and WS locations, shown in Table 2.6-1 and Figure 2.6.1.

4. Discussion

4.1 Statistical data distributions

The statistical distributions of snow data are revealing about the nature of snow patterns on Hellstugubreen and Gråsubreen. They can also assist in understanding the role of inter-annual variations in snow spatial distributions.

4.1.1 Normality

For SWE values at both Hellstugubreen and Gråsubreen, the majority of years do not show a normal data distribution. Similarly, data compiled for all years to form a global dataset are not a normally distributed. Data does not conform well to alternative statistical distributions to a significant level. Neither B_w nor the number of probings are explanatory variables for this pattern. Normally distributed data years exhibit no differential pattern in probing spatial coverage. For Hellstugubreen, normal data is shown in years both covering and not covering the cirque areas. At both glaciers, there is no clear threshold or other defining characteristic between data years that are or are not normally distributed.

From these analyses, it must be considered that either 1) a multivariate assortment of interacting factors control the normality of data distributions, or 2) the normality of data is dependent on the specific probing locations that vary annually, and the small glacier areas and spatial heterogeneity of the glacier geometry causes some years of data to be normally distributed, and others not. It appears that the latter explanation is more credible based on the irregularity of both the glacier geometries, and the survey sampling locations from year to year. The heterogeneity of snow distributions is in agreement with Hodgkind *et al*. (2006) who found that only 40-62 % of snow distribution variability on glaciers could be explained

by elevation changes; similarly, Lehning *et al*. (2011) found only 20 % of snow distribution in mountain environments could be explained by elevation, meaning many other factors affect snow spatial distributions. The variability of data distributions is in agreement with the diverse and complex controls on snow distribution, as suggested by the above studies.

The conclusion that data is inherently variable, and poignantly does not conform well to a range of alternative statistical distributions, is important since it demonstrates the high spatial heterogeneity of the snow distribution across the glacier surface, as also found by Machguth *et al*. (2006) in a comparable alpine glacier setting. This further contributes to the overall motivation of the thesis by demonstrating that snow distributions are highly variable, and require attention when considering effective snow sampling surveys. This does not prejudice the potential for either strong time stability, or representative probing locations.

The inconsistent statistical distributions give reason for the interpolation and normalisation techniques used in this thesis. It also explains why the coefficient of variability (CV) in either snow depths or SWE is not used as a measure of snow stability. This method is computed by the ratio of the sample standard deviation to the mean, which for reliable results requires a normally distributed dataset. Whilst this technique is used by Winstral and Marks (2014) and Sturm and Wagner (2010), it is absent from this investigation. Further research may pursue the potential for gamma distributions to fit the data, as found by Skaugen (2007) and Alfnes *et al*. (2004), with possible time variant functions through the course of an accumulation season.

4.1.2 Quartering

The data years are categorised by either all years of data, or splitting data into quarters based on B_w values. This is designed to assist in inter-comparisons between precipitation levels for stability and reliability patterns. Quarters were chosen over quartiles, since the range of data in quartiles was too large; it is also most practical for fieldworkers to compare the years with the highest 25 % of B_w to those of other quarters. Similarly, data can be added to in future

years without adjusting the categorisation (provided that new data are not B_w outliers); category adjustment would be required if using B_w quartiles.

Both glaciers have a similar pattern of positive skew, with fewer data years in the higher B_w quarters. The years in the quartered groups are different between the two glaciers. It is possible that differences in snowfall occurred due to the distance between Hellstugubreen and Gråsubreen further east in a more continental setting. However, it is also possible that localised differential snow patterns at the glacier regions have a role in the different constituent years of B_w quarters. For example, windfields on the more exposed Gråsubreen may be responsible for the different years of high B_w relative to Hellstugubreen. These conclusions highlight the space specific variations of snow accumulation on different glaciers, which by extrapolation can also be expected regarding snow spatial distributions.

4.2 Stability

4.2.1 Interannual snow spatial distributions

The RMSEs of normalised SWE values computed on a cell-by-cell basis are significantly higher at Gråsubreen than at Hellstugubreen, ranging between 0.07-0.41 and 0.08-0.24 respectively. Further, Gråsubreen exhibits more data years with high RMSE values than Hellstugubreen, and is therefore considered less time stable than Hellstugubreen.

The Pearson's correlation coefficient, computed on a cell-by-cell basis in a data matrix, ranges from 0-0.96 with a mean of 0.69 at Hellstugubreen; it ranges from 0.03-0.93 with a mean of 0.65 at Gråsubreen. These values are of a far wider range than Winstral and Marks (2014) found in a US mountain catchment, which ranged from 0.7-0.97 with a mean of 0.84. Comparatively, the Norwegian glacier show greater heterogeneity between snow distribution patterns in different years. The negative skew of the Norwegian glacier correlation coefficients suggest that a small number of poorly correlating snow distribution years

adversely affect stability results. The negative outliers and the skewed data are in agreement with Sturm and Wager's (2010) and Jansson and Pettersson's (2007) conclusions that whilst a generalised time stability is apparent, a minimal number of poorly correlated data years may not fit the overall trend. Indeed, Jansson and Pettersson (2007) found a number of b_w points of data with a negative or zero correlation to glacier-wide averages, thus supporting the results found at Hellstugubreen and Gråsubreen. The long data series of 55 years used by Jansson and Pettersson (2007) at Storglaciären shows more likeness to the dataset used here than the 21 year dataset used by Winstral and Marks (2014), both by virtue of dataset size and on-glacier location. It is therefore accepted that the negative data skew and number of poor correlations are not erroneous, and instead highlight the potential for multiple irregular years of snow distribution lying outside a time stable pattern.

RMSEs and Pearson's correlation coefficients highlight different characteristics in the datasets. Their inter-comparison can, however, highlight co-variable characteristics of time stability. The top five and bottom five years of RMSE and Pearson's correlations are shown in Table 4.2-1. A covariation between low RMSE and high correlation is seen only at Hellstugubreen, for the years 1968 and 2009. The opposite, high RMSE and low correlation is seen only at Hellstugubreen, for 1992. There are no years of high (low) RMSE and high (low) correlations, showing that there is no strong disagreement between the tests, despite limited agreement. RMSE and correlations only produce comparable results for a few years, demonstrating the independence of the tests, and also the differences in using a matrix, which provides greater year on year specificity. At Hellstugubreen, the year 1992 appears to be highly irregular, and has a spatial snow distribution significantly different to other years. This year is in the second B_w quarter, showing high potential snow distribution variability at mid-range B_w. However, the years 1968 and 2009 (which show strong likeness both to every other year (correlation) and to a model of all years combined (RMSE)), are both in the third B_w quarter, therefore also showing good stability potential in mid-range B_w.

No data years show this pattern at Gråsubreen, meaning that there is likely a greater variability between individual data years, creating a more complicated pattern when all data years are combined in the RMSE calculation.

Table 4.2-1 Inter-comparisons of RMSE and correlation coefficients, using the top and bottom five years of each characteristic, at Hellstugubreen and Gråsubreen. Grey highlighting shows synchronisity between low (high) RMSE and high (low) correlations.

Hellstugbreen		Gråsubreen	
Low RMSE	**High correlation**	**Low RMSE**	**High correlation**
1968	1995	1998	1973
1998	1991	2006	2005
2009	1990	1996	2007
1974	1968	1986	1981
1975	2009	2004	1989
High RMSE	**Low correlation**	**High RMSE**	**Low correlation**
1992	1992	1984	2010
1996	1984	2014	1994
2010	1981	1995	2011
1983	2012	1977	1988
2006	1977	1978	2001

4.2.2 Stability maps

Stability maps show significant changes in variability zones, both in area and location, between B_w quarters, for both glaciers. At Hellstugubreen, B_w quarter 1 shows good time stability on the eastern edge. This may be a result of westerly winds, and may be more prominent at low snow levels, since alternative snow spatial distribution patterns have not yet had enough snow to fully form. This suggests that a banking of snow along the eastern edge of Hellstugubreen is a primary factor in snow stability, and may take place before alternative time stable snow spatial distribution patterns are able to form. With higher snow volumes, greater time stability is then seen at the centre of the glacier.

At Gråsubreen, the pattern of most stable snow spatial distributions in the central snow thin zone is most prominent in B_w quarter 1. This suggests that this is a prominent stable formation that can be found even in low snow years. With increased snow at higher B_w quarters, this pattern remains, yet becomes less distinctive as alternative areas of the glacier feature time stability when more snow is available to redistribute.

Time stability does, however, show some common results. At both glaciers, the categorisation of data years into B_w quarters assists in increasing the time stability of maps. This is not simply an artefact of fewer constituent years, since the variability zones themselves change in location. Further commonalities show reduced stability in the cirques of Hellstugubreen, and in the margins of Gråsubreen. These low stability areas can be explained by the extrapolation of probings adjacent to these areas, extending uncertainty towards peripheral areas, and greater variability between different data years. Further, few probings are taken in the cirque regions at Hellstugubreen, therefore amplifying uncertainty in extrapolation and increasing poor stability in these areas. It is also important to consider that these peripheral areas are likely to accumulate snow drifting to varying degrees, thus creating an enhanced variability dependent on meteorological effects.

4.2.3 Stability by area

The areas of different variability zones are evaluated. Notably, for both glaciers, the total area in the highest uncertainty group, > 80 %, reduces when data are categorised by B_w quarters. This vitally demonstrates the primary advantage that by categorising data, time stability is increased. The degree of increased stability for the different B_w quarters varies between the glaciers.

At Hellstugubreen, increasing B_w quarters create increasingly time stable maps. This is in agreement with both Sturm and Wagner (2010) and Jansson and Pettersson (2007) who state that with low snow years, spatial distribution patterns are less readily formed, and cause greater variability in time stable patterns. With increasing snow levels, repeat snow distribution patterns can be formed to a greater extent.

At Gråsubreen, increasing B_w does not increase stability by area directly. B_w quarters 1 and 4 are the most stable by area, followed by quarter 3, then quarter 2. This alternative pattern partly reflects increasing stability with B_w for quarters 2, 3 and 4, however the largely stable quarter 1 does not fit this general trend. An explanation may be that the exposed glacier surface at Gråsubreen allows the glacier surface to be well reflected in low snow years, thus

stable snow distribution patterns can form under limited snow conditions. The largest stable area at B_w quarter 1 is the central snow-poor area. This region may be able to reflect strong stability at low B_w due to the thin snowpack here, which can form with minimal snow levels. Indeed, for 6 separate years (1971, 1976, 1977, 1980, 1982, and 1986), there were snow probings in the central area with a complete absence of snow. The similar locations of the snow starved b_w probing points shows the strong stability of the snow-poor central region at Gråsubreen. With increasing snowfall the surface is less well reflected until there is enough snow to form regular stable patterns, as seen at higher B_w data years. This explanation is in agreement with the continental glacier setting, and reduced precipitation levels relative to Hellstugubreen further west.

For both glaciers, the highest B_w years form the most stable snow distribution patterns. Sturm and Wagner (2010) counter that at the highest snow levels, stability may be reduced because of topographical controls becoming snowed over, and having limited influence on the snow spatial distribution patterns. This is not the case for Hellstugubreen or Gråsubreen, suggesting that the threshold at which topographical controls on snow distribution are limited has not been met, or is of little impact. Topographical controls on snow spatial distribution appear to retain their prominence.

4.2.4 Optimum allocation stratified sampling

The optimum allocation stratified sampling technique suggests sample size requirements, given the variability of a population, and the cost of sampling it (Foreman, 1991; Neyman, 1934). This sampling scheme follows the suggestion by Pelto (2000), that areas with the greatest variability should be probed more densely than areas with low variability. Compared to proportional allocation, the variability of the sample is included in addition to the relative size of an area. Kronholm and Birkeland (2007) find that stratified randomized sampling produces a good representative sample for snow depth measurements. Similarly, Elder *et al.* (1999) find superior results when using stratified sampling survey designs compared to random sampling, for SWE data collection.

The sample proportions as percentages at Hellstugubreen and Gråsubreen emphasise the sizes of the stability areas, practically limiting the proportion of samples suggested in small stability areas, often to below 1 %. It should therefore be considered that these areas are of limited overall impact on the overall B_w results. The areas of lowest time stability at the peripheries of Gråsubreen feature generally low sample proportion sizes, reflecting the small sizes of the areas despite their high variability. The inverse is true of the central area of low variability at Gråsubreen; here, the large area has a small resultant sample proportion relative to the area, due to the low variability. These features accomplish the desired effect of best probing allocation relative to the stability and cost of data collection.

4.3 Reliability and survey designs

4.3.1 Reliability maps

Reliability maps are constructed based on layering data years of binary searches for values within ± 10 % of a winter balance value. By choosing re-sampling locations where the greatest number of data year layers are found, time stability is accounted for in the reliability maps. The ± 10 % searches produced some instances where not every data year in a categorisation was fulfilled. In order to find locations where all data years are represented, the accuracy threshold must be at least ± 30 % of the winter balance searched for, creating a wide window of error. It was decided that a ± 10 % window was suitable to fulfil a suitable accuracy level for the majority of data years.

Of the data year layers used in searches for one representative B_w index site at Hellstugubreen, 80 % of all years are used for $B_w one_{all}$, and over 89 % for all $B_w one_q$ quarters. At Gråsubreen, the figures are far lower, with 57 % for $B_w one_{all}$, and increases with $B_w one_q$ quarters. The significant difference shows the greater stability of the Hellstugubreen

probing locations through time, relative to Gråsubreen. This evidences the poorer level of agreement in stable probing locations at Gråsubreen than Hellstugubreen.

At both glaciers, there is a general increase in the percentage of data year layers used in reliability probing locations with increasing B_w quarters. At Hellstugubreen, this is more nuanced, with a decrease at B_w quarter 2. This is contrary to the above discussion on stability areas for B_w quarters at Hellstugubreen; however, the differences are very minimal, accounting to a limited disagreement in stability measures. At Gråsubreen, the pattern of greatest stability by area in B_w quarters 1 and 4 is not replicated in the representative probing layers analysis. The percentage of layers used is, however, very low, suggesting that they may not fully reflect the total glacier area, as covered by stability maps. Only point locations are used here, in comparison to the stability maps which cover the whole glacier area. Stability maps are therefore a useful robust verification method to assess the stability results found in reliability maps.

When the percentage of layers used in reliability maps is explored for quartered data, there is a general pattern of more layers being used in the central areas of the glaciers than at snouts and headwalls. The pattern is less clear at Gråsubreen than at Hellstugubreen. This adds weight to the potential for generally greater variability at Gråsubreen, as noted by the greater cell-by-cell RMSE values, and the less stable representative probing locations.

4.3.2 Mass balance resampling and reconstructions

Using the reliability maps and chosen most representative b_w probing locations, B_w is reconstructed for different survey designs. Comparison to the official B_w appears to presume that the official record is ‘correct’. This is, however, a misinterpretation and each B_w construction or reconstruction is an amalgamation of various discrete points of data used to evaluate continuous data. The official record uses the most b_w probing points and has the widest spatial coverage. However, it is still averaged in area-elevation intervals to calculate winter balances, since exhaustive point data collection is not possible. All B_w calculations must interpolate point b_w data, and in this sense all B_w records are valid, and are likely to be

accurate to a degree, since real data is used. Moreover, it is a question of scales of accuracy, rather than a zero-sum approach to whether a B_w is correct relative to the official record. Comparisons are used to the official record, in order to highlight the degree of (dis)agreement in B_w reconstructions against a set benchmark.

Reconstructions of B_w are important as they highlight how representative a reduced probing network would be. This section discusses the reconstructions of B_w for the survey designs, excluding centreline only probing surveys which are covered in section 4.3.3. Jansson (1999) found that a reduced network of probings at 400 m intervals, rather than at 100 m intervals, would reconstruct B_w values to within 7 % of the official record. The ability to reduce survey sizes is also noted and supported by López-Moreno *et al*. (2011), based on the strong spatial autocorrelation of snow depths in alpine environments. Jansson and Pettersson (2007) comment that a reduced network may produce results to within ± 0.1 m w.e., and substantiate the sufficient accuracy of doing so by citing Funk *et al.'s* (1997) contribution that error ranges in density pit measurement could produce final B_w results within ± 0.6 m w.e. As such, the degree of accuracy in probing measurements is negligible relative to the potential errors introduced by density pit measurements.

This investigation finds a range of RMSEs between the official B_w record and survey B_w reconstructions in general agreement with Jansson and Pettersson (2007), with values ranging between 0.07-0.09 m w.e. at Hellstugubreen, dependent on the data categorisation method. Using all years of data produces the highest RMSE. At Gråsubreen, the RMSE ranges from 0.08-0.14 m w.e., again in agreement with Jansson and Pettersson (2007). Mean percentage errors largely agree with Jansson's (1999) 7 % estimation. At Hellstugubreen the mean error ranges between 4.8-6.1 %. Mean errors are slightly higher at Gråsubreen, ranging between 8.1-13.6 %. At both glaciers, using all years of data produces the largest errors. The greater mean errors at Gråsubreen demonstrate poorer data reliability when using the most representative survey probing locations. This may be an artefact of poor time stability, and changing snow distributions, meaning the probing locations are less reliable. This analysis is in agreement with the lower percentage of data year layers used in constructions of reliability maps at Gråsubreen than at Hellstugubreen.

Maximum percentage errors highlight the main drawback of using these reduced probing networks. The highest errors at Hellstugubreen range from 13.7-22.8 % dependent on data

categorisation, and between 49.9-75.6 % at Gråsubreen. These maximum errors would cause significant problems if only the reduced probing surveys were used in the erroneous years.

Interestingly, a few specific years are responsible for multiple outlying maximum errors and are repeated across data categorisations. At Hellstugubreen, nine different years are responsible for the top four most erroneous years across the four B_w reconstructions (16 possible combinations); At Gråsubreen eight years are responsible the top four erroneous years respectively. If the top four most erroneous years are excluded, the maximum error falls to 9.6-12.6 % at Hellstugubreen, and between 12.5-29.6 % at Gråsubreen. This demonstrates that irregular snow distributions of a few years have the ability to substantially skew the error range of reconstructed B_w data. At Hellstugubreen, the years of highest error percentages are 1970, 2000, 2007 and 1992. At Gråsubreen the years 2007 (accounting for the maximum error at 3 of the four B_w reconstructions), 1991, 2012, and 1976 are the most erroneous B_w reconstruction years. Notably, the only data year with poor reconstruction values at both glaciers is 2007. At Hellstugubreen, 2007 has a particularly high RMSE value, and has several correlation outliers, suggesting that it is poorly related to the snow distribution of other data years. However, at Gråsubreen the RMSE and correlation values for 2007 are unremarkable.

No connection is found between high error years and overall B_w at Hellstugubreen. At Gråsubreen, all high error years are in B_w quarters 1 and 2, suggesting that these lower precipitation years are of poor stability. This is, however, not in keeping with the time stabilities derived from the stability maps for B_w quarter 1. As outlined earlier, a potential cause for this discrepancy is that by using a limited probing survey, errors are magnified at a reduced set of locations. Comparatively, stability maps cover the whole glacier, and are likely to give a more representative image of the snow spatial distribution time stability.

High B_w reconstruction error years 2007, 1996, 1992 and 1970 at Hellstugubreen also have high RMSE values cell-by-cell normalised SWE. At Gråsubreen, the same can be said for only 2005 and 1977. This limited synchronicity shows that whilst a general agreement may be found on the spatial snow distribution of data years, as exemplified by moderate cell-by-cell RMSE values, using specific probing locations may magnify spatial snow distribution irregularities, since only specific cells are considered.

Generally, using B_w quarters are preferable over using all years of data; using probing locations at 50 m elevation intervals are preferable to using one probing location for the entire glacier. These conclusions suggest that snow spatial distribution patterns can be better understood, and vary with, overall B_w, and that sampling at multiple representative locations improves B_w calculations.

4.3.3 Centreline probings

Centreline only probings are used to reconstruct B_w for all individual data years. Using only the centreline is common when sampling conditions are especially testing, for example in 1989 and 1990 on Hellstugubreen. This may, however, create unreliable results by excluding other regions of the glacier.

At Hellstugubreen, the B_w relative to the official record was underestimated for 42 of the 48 data years when using centreline only probings. At Gråsubreen the proportion is lower but still a majority, with 26 of 44 data years underestimating B_w. At Hellstugubreen the RMSE and mean percentage error relative to the official record were higher than the alternative four survey designs considered above. At Gråsubreen the RMSE and mean percentage error fell between surveys using one probing for the whole glacier, and using one probing per 50 m elevation zone, regardless of data categorisation.

The greater error margins at Hellstugubreen may be partially explained by the valley formation of the glacier, relative to the more exposed Gråsubreen. The centreline region of Hellstugubreen exhibits significant convex formation in the ablation zone, which makes up the majority of the retreating glacier, as further evidenced by the high accumulation area ratios (AAR) in recent years (NVE Glaciological Investigations in Norway, 2000-2010). This form may expose the centreline region to enhanced thinning relative to the margins, causing systematic underestimation of the overall winter balance by probing only along this transect, as shown in Figure 4.3.1. Note that the gulley peripheral edge zones accumulate the greatest volume of snow, whereas the exposed convex centreline loses snow by snow-drifting. Effectively, this may cause a systemic underestimation of B_w if only the centreline probings are used in calculations, particularly at valley glaciers.

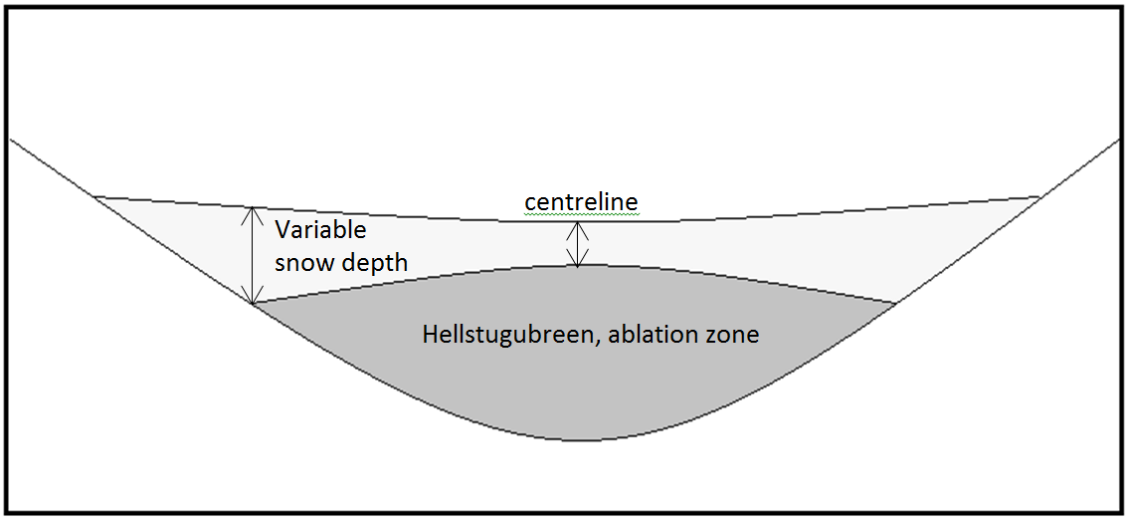

Figure 4.3.1 Y axis schematic cross-section of a valley glacier. Note the variable snow depths, owing to snow redistribution patterns.

These significant errors demonstrate the importance of attempting largescale glacier coverage where possible. Where only the centreline can be probed, caution should be taken with the results. Using the specified probing locations per 50 m elevation zone may produce favourable results, however, this introduces the potential for irregular snow spatial distribution years to adversely affect results.

4.3.4 Randomised sampling

Calculations for the randomized sample size requirements use the relationship between the mean value, and the standard deviation. As noted earlier, this investigation acknowledges that this test requires an expected normal data distribution, which many data years do not exhibit, and therefore the randomized sample size requirements should be seen as indicative only.

The high suggested sample sizes for 95 % accuracy, the vast majority of which exceed the actual sample sizes, demonstrate the broad range of SWE values found on the glaciers. In

agreement with Machguth *et al*. (2006), this is indicative of the broad heterogeneity of both the SWE values themselves, and their spatial distribution. This conclusion further adds weight to that of spatially heterogeneous snow distributions shown above.

4.4 Wind frequency distributions

Variable wind speed and direction distributions at different WS locations show that wind patterns can be highly localised, as found by Giesen *et al*. (2009) in their surface energy balance study on two glaciers in southern Norway. For example, the prevailing weak south-west to north-east wind axis at Elveseter reflects the geographical low elevation valley position of the site. Conversely, the high elevation, highly exposed Juvvasshøe WS site features a far higher range of wind directions and strengths, reflecting its location. Similar wind distributions to Juvvasshøe can be noted at Sognefjellhytta, but to a lower extent. These considerations add caution to causal links between wind frequencies and controls on snow spatial distributions.

Wind roses for years that feature irregular snow spatial distributions patterns are further commented on below. These years are compiled from the above discussion on high RMSE data years relative to all data years combined (appendix Figure 7.2.1 and Figure 7.2.2 for Hellstugubreen and Gråsubreen); low correlation data years relative to all other year combinations (appendix Figure 7.2.3 and Figure 7.2.4 for Hellstugubreen and Gråsubreen); and high error years in B_w reconstructions (appendix Figure 7.2.5 for Gråsubreen only).

Generally, wind frequency distributions at Elveseter, Bøverdal-Sletten, and Sognefjellhytta show good agreement in years of regular and irregular snow spatial distribution. At Juvvasshøe, the wind frequency distributions for regular and irregular snow spatial distribution are notably different. This trend is better defined at Gråsubreen than at Hellstugubreen, and most notably for low correlation and high B_w reconstruction error years. For these irregular snow spatial distribution years, differences are seen in reduced southerly winds, and increased westerlies. The strength is, however, variable with for example stronger

winds in 2012 and weaker winds in 2010, limiting any conclusions on wind strength affecting snow spatial distributions.

There are limited differentiating trends in wind frequency distributions at Elveseter, Bøverdal-Sletten, and Sognefjellhytta separating irregular from regular snow spatial distribution data years. This may suggest that wind is not an important causal factor in snow spatial distributions. Alternatively, the more defined differences at Juvvasshøe suggest that wind is important in affecting snow spatial distributions, in agreement with numerous researchers (Lehning *et* al., 2011; 2009; Erickson *et al*., 2005). The high degree of exposure at Juvvasshøe may produce higher wind speed values than at that at Gråsubreen and Hellstugubreen. Despite this, Juvvasshøe is considered more reflective of on glacier conditions than alternative WSs, owing to the similar elevation to the glaciers and site proximity. Reduced southerlies and increased westerlies can be tentatively put forward as a mechanism for irregular snow spatial distribution, however, more detailed glacier specific data must be collected to further investigate this claim.

Largescale atmospheric circulation patterns such as the North Atlantic Oscillation (NAO), an oscillating pressure differential between the Icelandic low and the Azores high, have been linked to mass balance changes in Scandinavia (Øksendal, 2011; Nesje *et al*., 2000). The NAO may affect B_w by controlling westerly winds and precipitation levels, both increasing during positive phases with high pressure differentials. These atmospheric controls should be further researched regarding spatial snow distributions at Hellstugubreen and Gråsubreen.

4.5 Glacier geometry

4.5.1 Elevation change

Compiling data from different years on a changing glacier surface presents a problem in glacier geometry. Geometric changes of the glaciers in x and y axes are removed by clipping

all maps to the smallest of all overlapping extents. Peripheral areas that retreat are not included, thus avoiding the problem of limited overlap between data years spatial extents. Changes in the z axis are given in Table 4.5-1 and Table 4.5-2 for Hellstugubreen and Gråsubreen respectively (DTM perimeters are clipped to the smallest extent of all overlapping maps). These changes show moderate surface downwasting between 1968-1980/1984, before relative stability between 1980/1984-1997, followed by more intense downwasting after 1997. These time averaged results mask inter-annual changes, and analysis at specific parts of the glacier. In all cases, the snout at Hellstugubreen features extensive downwasting. At Gråsubreen, the northern edge of the glacier consistently downwasted, whereas the southern edge was more stable.

Table 4.5-1 Mean elevation changes at Hellstugubreen.

Hellstugubreen	
DTM interval	Mean elevation change (m)
1968 to 1980	-5.25
1980 to 1997	+0.22
1997 to 2009	-8.42

Table 4.5-2 Mean elevation changes at Gråsubreen.

Gråsubreen	
DTM interval	Mean elevation change (m)
1968 to 1984	-4.44
1984 to 1997	-0.05
1997 to 2009	-7.24

Downwasting is likely to have limited impacts on the topographical controls on snow distribution and redistribution relative to stable largerscale geological formations, and is therefore unlikely to adversely affect stability and reliability probing locations through time. Similarly, the bedrock is stable and causes glacier forms generally repeated from year to year (Jansson, 1999).

4.6 Outlook

The results in this thesis provide a detailed analysis of time stability, reliability of probing locations, and survey designs. The output maps are designed to assist future fieldworkers and analysts to better understand the nature of snow distribution patterns on Hellstugubreen and Gråsubreen. The ability to analyse B_w and snow distribution patterns is only possible due to the extensive and well archived data records held by NVE. Reductions in survey sampling designs are therefore not encouraged, since this inherently limits future snow distribution pattern observations, and effectively removes any checks that future surveys have maintained accuracy. The continued long-term LOP data collection technique is encouraged, especially given that short-term snow distribution records are limited by their series length, and have less dependable results (see Hirashima *et al*., 2004; König and Sturm, 1998). It is also important, where possible, to extend snow probings into the cirques on Hellstugubreen to increase the detail of data in these areas. The same applies for poorly covered glacier marginal areas.

Time stability data provided here may be used as a CSDP input data source for snow distribution modelling, as applied by Sturm and Wager (2010). Models may also expand on this study to further investigate the controls and causes of snow time stability.

4.6.1 Survey sample designs

Stability maps and representative probing location maps are designed to be useful as a form of prior knowledge for fieldworkers and researchers, and may be especially useful in future years where poor field conditions limit data collections. Survey design results suggest that the most representative data from a reduced survey design is to follow the suggested probing location in each 50 m elevation interval for the specific B_w quarter. The appropriate B_w quarter may first be assessed by limited probings and prior knowledge of past years of snow depths.

Under poor field conditions in past years, probing data has been collected only along a glacier centreline. This underestimates B_w, especially at Hellstugubreen due to its valley setting. It is thus recommended that multiple lateral transects are also made where possible.

4.7 Limitations

Original data are received from NVE, where both the contour and profile methods have been used to calculate B_w. Whilst Escher-Vetter *et al*. (2009) find good agreement in these methods, further researchers may homogenise the data to assess the level of agreement in B_w records using the different techniques at Hellstugubreen and Gråsubreen.

Stability maps are constructed using the range of normalised SWE values in a given cell. This range of values is the maximum variability of a cell's normalised SWE values. This technique does not examine the statistical characteristics of normalised SWE values in each cell, meaning that cells which are deemed unstable may be skewed by few irregular data years. Abnormal years are not identified in this method. The level of detail used gives a picture of total stability, regardless of frequencies of stable or unstable years. This methodology does, however, include all data, and is true to the range of normalised SWE values found in a data cell.

Representative probing locations are chosen based on the maximum number of data year layers overlying each other. A structured framework is used to select specific locations, whilst reducing subjectivity where possible. If two areas of the same number of data year layers are found, the largest area is given preference, as are areas away from glacier peripheries that may be at risk from future retreat. This technique is fully acknowledged, and is deemed both practical and acceptable. Some selected locations are unlikely to be able to be reached by fieldworkers, for example near cirque headwalls on Hellstugubreen. However, data is extracted at these locations for resampling to compute the reconstructed B_w. This is for the purposes of B_w reconstructions in the thesis only, and it is not expected that fieldworkers will visit these inaccessible locations.

4.7.1 Unprobed areas, and data interpolation and extrapolation

Some unprobed areas on the glaciers are used in stability and reliability maps and B_w reconstructions. This problem is most apparent for the cirque areas on Hellstugubreen. Here, probings have only been taken in a small fraction of all years, yet the area is used for mass balance calculations. This is deemed suitable, and indeed must be computed if data are to be compared to official records. This is because the NVE official record includes the cirque areas in all mass balance calculations, despite the limited data retrieved from these areas. Caution is given to the extrapolated data in these regions, which may not be well adjusted.

Peripheral areas on the glacier are also able to affect results. As demonstrated in section 4.3.3, centreline only probings may miss details at the glacier perimeter. Further, extrapolated data may underestimate the deep snow at glacier margins, reducing overall B_w figures, as suggested by Jannson (1999). Headwalls are also underestimated in the same manner, due to limited probings taken at the obscured or inaccessible glacier margins.

Crevasse areas are likely to be overestimated by data interpolation, due to their convex form causing a thin snowpack by exposure (Jansson, 1999). This effectively may reduce the accuracy of data in these areas, and the area averaged data in B_w reconstructions. However, crevasses found on Hellstugubreen cover only a small fraction of the overall glacier, limiting the adverse effects on results. At Gråsubreen, still fewer crevasses are found due to the cold ice. Multiple supraglacial meltwater channels are found at Gråsubreen, which may cause micro-scale differentiations in snow probings. NVE has historically included crevassed areas and supraglacial channel areas without differentiation in mass balance calculations. For comparative results, the same spatial coverage methodologies are applied here.

4.7.2 Wind frequency distribution data

Wind frequency distributions contribute information to the potential controls on snow spatial distributions. They are, however, problematic due to multiple data sources and time periods.

Four WSs are necessarily used to provide data for the long time series. This limits references to a known single data source. Owing to the data availability, only latter accumulation season months of data are used. This removes some of the snow accumulation period, however, maintains the latter period in which more snow-drift and redistribution is likely to take place, resulting in the final snow spatial distributions.

The WSs are at differing locations and elevations, and bear differing resemblances to glacier specific conditions. Wind data was variable at the different WSs, as also found by Giesen *et al*. (2009), producing difficulties in compiling multiple sources of wind data. Juvvasshøe is deemed most similar to the glacier conditions owing to its elevation and relative proximity to the glaciers, despite the enhanced exposure of the WS location. The same WSs are used for analysis of both glaciers, despite known differences in data years of snow spatial distributions between the glaciers. For more reliable data collection and analysis of snow spatial distributions, installing WSs on glaciers is recommended, and will produce more reliable data. Similar recommendations regarding the use of on glacier WSs to monitor local conditions are given by Giesen *et al*. (2009) and Andreassen *et al*. (2008).

5. Summary and conclusions

This thesis has explored time stability of snow distribution patterns, reliable and representative b_w probing locations, and reduced survey designs, on two glaciers in southern Norway. Throughout, data year categorisation by B_w quarters compared to all years of data has been evaluated.

The results showed generally time stable glaciers, with improvements in time stability maps and areas by categorising data by B_w quarters, as opposed to using all years of data simultaneously. Hellstugubreen exhibited lower variation of snow stability patterns between years. At Hellstugubreen, increasing overall B_w produced an increasingly stable snow distribution pattern. At Gråsubreen this was true of B_w quarters 2 through 4, with B_w quarter 1 also demonstrating good time stability. At Hellstugubreen, increased snow levels allowed increasingly stable snow spatial distribution patterns to form. Gråsubreen is more continental and at higher elevation, with a known central thin snowpack area causing strong snow spatial distribution time stability at even low precipitation levels. This pattern was limited in B_w quarter 2, afterwhich increasing snowfall levels again caused increases in the time stability of snow spatial distributions.

Different reduced survey designs using reliable and representative b_w probing locations were created and tested. These were based on either taking one probing at an index site to evaluate the B_w for the entire glacier, or taking one probing per 50 m elevation interval. Both methods were created and tested using all years of data, or using B_w quarters. All survey designs were tested relative to the official B_w record. At Hellstugubreen, the RMSEs were all <0.10 m w.e. and the mean errors were all <6.2 %. At Gråsubreen, the respective values were <0.15 m w.e. and < 13.7 %. These show good alignment with official results, and fit well with error estimates of reduced survey designs presented by Jansson and Pettersson (2007) and Jansson (1999). Results highlighted that Gråsubreen is not as time stable as Hellstugubreen. Representative probing locations at Gråsubreen produced worse final results in comparison to official B_w values, than at Hellstugubreen. Generally, the best results were found using one probing location per 50 m elevation interval, and using complied B_w quartered data.

When centreline only b_w probings were considered in calculating B_w, there was significant underestimation of the official B_w record. This was magnified at Hellstugubreen, where the valley type glacier is likely to cause a thin snowpack along the convex centreline region on the ablation zone dominated glacier. Gråsubreen is more exposed, and has a less dominant valley form, limiting this effect. In years of reduced probings, care should be taken to try to expand probing locations beyond only the centreline.

For all analyses, a small number of irregular snow distribution years created significant differences both in time stable snow spatial distribution patterns, and errors in B_w reconstructions relative to the official B_w record. These limited irregular years support similar findings by Sturm and Wagner (2010) and Jansson and Pettersson (2007). Wind fields are tentatively suggested as a cause of irregular snow spatial distributions, in particular during years of reduced southerlies and increased westerlies. This suggestion is hindered by poor data specificity, and is an area where further glacier specific research is encouraged. Whilst a data year may in general conform with the snow distribution patterns of other data years, using a reduced probing survey design has the potential to magnify errors by increasing percentage importance of each probing value.

This thesis suggests that the current snow sampling method is continued, in order to evaluate future snow distribution patterns. Additionally, increasing spatial coverage of cirque and marginal glacier zones will add detail to future snow distribution analyses. Caution should be taken if only centreline probings are taken due to poor field conditions, and lateral transects are encouraged where possible. Where necessary, the sampling design can be reduced, however, attention must be given to the potential for irregular snow distribution years.

6. References

Alfnes, E., Andreassen, L., Engeset, R., Skaugen, T. and Udnaes, H. (2004). Temporal variability in snow distribution. *Annals of Glaciology*, 38(1), pp.101-105.

Andreassen, L. M. and Winsvold, S. (2012). (Eds.) *Inventory of Norwegian Glaciers*. Rapport 38-2012. Norwegian Water Resources and Energy Directorate: Oslo

Andreassen, L. M. (2011a). 'Hellstugubreen' in Bjarne Kjøllmoen (Ed.), Liss M. Andreassen, Hallgeir Elvehøy, Miriam Jackson and Rianne H. Giesen, 2011: *Glaciological investigations in Norway in 2010. NVE Report 3 2011*, 89 pp. +app.

Andreassen, L. M. (2011b). 'Gråsubreen' in Bjarne Kjøllmoen (Ed.), Liss M. Andreassen, Hallgeir Elvehøy, Miriam Jackson and Rianne H. Giesen, 2011: *Glaciological investigations in Norway in 2010. NVE Report 3 2011*, 89 pp. +app.

Andreassen, L. M. and Oerlemans, J. (2009). Modelling long-term summer and winter balances and the climate sensitivity of Storbreen, Norway. *Geografiska Annaler: Series A, Physical Geography*, 91(4), pp.233-251.

Andreassen, L. M., Van Den Broeke, M., Giesen, R. and Oerlemans, J. (2008). A 5 year record of surface energy and mass balance from the ablation zone of Storbreen, Norway. *Journal of Glaciology*, 54(185), pp.245-258.

Andreassen, L. M., Elvehøy, H., Kjøllmoen, B., Jackson, M. and Engeset, R. V. (2007). Long term observations of glaciers in Norway. In Orlove *et al.*: *The Darkening Peaks: Glacial Retreat in Scientific and Social Context.* pp.100-110.

Andreassen, L. M., Elvehøy, H., Kjøllmoen, B., Engeset, R. and Haakensen, N. (2005). Glacier mass-balance and length variation in Norway. *Annals of Glaciology*, 42(1), pp.317-325.

Andreassen, L. M., Elvehøy, H. and Kjøllmoen, B. (2002). Using aerial photography to study glacier changes in Norway. *Annals of Glaciology*, 34(1), pp.343-348.

Anonymous. (1969). Mass-balance terms, *Journal of Glaciology*, 8(52), pp.3-7.

Balk, B. and Elder, K. (2000). Combining binary decision tree and geostatistical methods to estimate snow distribution in a mountain watershed. *Water Resources Research*, 36(1), pp.13-26.

Bamber, J. and Rivera, A. (2007). A review of remote sensing methods for glacier mass balance determination. *Global and Planetary Change*, 59(1-4), pp.138-148.

Bormann, K., Westra, S., Evans, J. and McCabe, M. (2013). Spatial and temporal variability in seasonal snow density. *Journal of Hydrology*, 484, pp.63-73.

Braithwaite, R. (2002). Glacier mass balance: the first 50 years of international monitoring. *Progress in Physical Geography*, 26(1), pp.76-95.

Carrivick, J., Smith, M., Quincey, D. and Carver, S. (2013). Developments in budget remote sensing for the geosciences. *Geology Today*, 29(4), pp.138-143.

Cogley, J. G. , Hock, R. , Rasmussen, L. A. , Arendt, A. A. , Bauder, A. , Braithwaite, R. J. , Jansson, P. , Kaser, G. , Möller, M. , Nicholson, L. , and Zemp, M . (2012). *Glossary of Glacier Mass Balance and Related Terms*, IHP-VII Technical Documents in Hydrology No. 86, IACS Contribution No. 2. UNESCOIHP, Paris.

Cogley, J. (1999). Effective Sample Size for Glacier Mass Balance. *Geografiska Annaler A*, 81(4), pp.497-507.

Dadic, R., Mott, R., Lehning, M. and Burlando. P. 2010a. Parameterization for wind–induced preferential deposition of snow. *Hydrological Processes*. 24, pp.1994-2006.

Dadic, R., Mott, R., Lehning, M. and Burlando. P. 2010b. Wind influence on snow depth distribution and accumulation over glaciers. *Journal of Geophysical Research.* 115.

Deems, J., Fassnacht, S. and Elder, K. (2008). Interannual Consistency in Fractal Snow Depth Patterns at Two Colorado Mountain Sites. *Journal of Hydrometeorology*, 9(5), pp.977-988.

Doorschot, J. J. J. and Lehning, M. (2002). Equilibrium saltation: Mass fluxes, aerodynamic entrainment, and dependence on grain properties. *Boundary-Layer Meteorology*. 104, pp.111-130.

eKlima. (2015) *eKlima download webportal*. http://sharki.oslo.dnmi.no/portal/page?_pageid=73,39035,73_39049&_dad=portal&_schema=PORTAL. Accessed on 20/05/2015.

Elder, K., Dozier, J. and Michaelsen, J. (1991). Snow accumulation and distribution in an Alpine Watershed. *Water Resources Research*. 27(7), pp.1541-1552.

Erickson, T. A. and Williams, M. W. 2005. Persistence of topographic controls on the spatial distribution of snow in rugged mountain terrain, Colorado, United States. *Water Resources Research*. 41.

Escher-Vetter, H., Kuhn, M. and Weber, M. (2009). Four decades of winter mass balance of Vernagtferner and Hintereisferner, Austria: methodology and results. *Annals of Glaciology*, 50(50), pp.87-95.

Flach, P. (2012). *Machine learning: the Art and Science of Algorithms that Make Sense of Data*. Cambridge University Press: Cambridge.

Foreman, E. (1991). *Survey sampling principles*. M. Dekker: New York.

Fountain, A. and Vecchia, A. (1999). How many Stakes are Required to Measure the Mass Balance of a Glacier? *Geografiska Annaler A*, 81(4), pp.563-573.

Funk, M., R. Morelli and W. Stahel. (1997). Mass balance of Griesgletscher 1961–1994: different methods of determination. *Z. Gletscherkd. Glazialgeol*., 33(1), pp.41-55.

Giesen, R., Andreassen, L. M., van den Broeke, M. and Oerlemans, J. (2009). Comparison of the meteorology and surface energy balance at Storbreen and Midtdalsbreen, two glaciers in southern Norway. *The Cryosphere*, 3(1), pp.57-74.

Grayson, R., Blöschl, G., Western, A. and McMahon, T. (2002). Advances in the use of observed spatial patterns of catchment hydrological response. *Advances in Water Resources*, 25(8-12), pp.1313-1334.

Grünewald, T., Schirmer,M., Mott, R. and Lehning, M. (2010). Spatial and temporal variability of snow depth and ablation rates in a small mountain catchment. *The Cryosphere*. 4: pp.215-225.

Haakensen, N. (1986). Glacier mapping to confirm results from mass-balance measurements. *Annals of Glaciology*, 8 pp.97-77.

Hawkins, D. (1981). A New Test for Multivariate Normality and Homoscedasticity. *Technometrics*, 23(1), pp.105.

Hirashima, H., T. Ohata, Y. Kodama, H. Yabuki, N. Sato, and A. Georgiadi (2004). Nonuniform distribution of tundra snow cover in eastern Siberia, *Journal of Hydrometeorology*, 5(3), pp.373–389, doi:10.1175/1525-7541

Hock, R. (2005). Glacier melt: a review of processes and their modelling. *Process in Physical Geography.* 29(3), pp.362-391.

Hock, R. and Jensen, H. (1999). Application of Kriging Interpolation for Glacier Mass Balance Computations. *Geografiska Annaler A*, 81(4), pp.611-619.

Hodgkins, R., Cooper, R., Wadham, J. and Tranter, M. (2006). Interannual variability in the spatial distribution of winter accumulation at a high-Arctic glacier (Finsterwalderbreen, Svalbard), and its relationship with topography. *Annals of Glaciology*. 42.

Holmlund, P., Jansson, P. and Pettersson, R. (2005). A re-analysis of the 58 year mass-balance record of Storglaciären, Sweden. *Annals of Glaciology*, 42(1), pp.389-394.

Huss, M., Bauder, A. and Funk, M. (2009). Homogenization of long-term mass-balance time series. *Annals of Glaciology*, 50(50), pp.198-206.

IPCC. (2013). *Climate Change 2013: The Physical Science Basis . IPCC Working Group I Contribution to the Fifth Assessment Report of the Intergovernmental Panel on Climate Change*. Cambridge University Press, Cambridge, United Kingdom and New York, NY, USA, 1132 pp.

Isaksen, K., Hauck, C., Gudevang, E., Ødegård, R. and Sollid, J. (2002). Mountain permafrost distribution in Dovrefjell and Jotunheimen, southern Norway, based on BTS and

DC resistivity tomography data. *Norsk Geografisk Tidsskrift - Norwegian Journal of Geography*, 56(2), pp.122-136.

Jansson, P. (1999). Effect of Uncertainties in Measured Variables on the Calculated Mass Balance of storglaciaren. *Geografiska Annaler A*, 81(4), pp.633-642.

Jansson, P. and Pettersson, R. (2007). Spatial and Temporal Characteristics of a Long Mass Balance Record, Storglaciären, Sweden. *Arctic, Antarctic, and Alpine Research*, 39(3), pp.432-437.

Klemsdal, T. (1970). A glacio-meteorological study of Gråsubreen, Jotunheimen, in *Norsk Polarinstitutt - Årbok 1968*, Norsk Polarinstitutt, Oslo, Norway, pp.58–74.

Krivoruchko, K. (2012). *Empirical Bayesian Kriging: Implemented in ArcGIS Geostatistical Analyst.* Esri.com.

Kronholm, K. and Birkeland, K. (2007). Reliability of sampling designs for spatial snow surveys. *Computers & Geosciences*, 33(9), pp.1097-1110.

König, M. and Sturm, M. (1998). Mapping snow distribution in the Alaskan Arctic using aerial photography and topographic relationships, *Water Resources Research,* 34(12), pp.3471–3483, doi:10.1029/98WR02514.

Lehning, M., Grünewald, T. and Schirmer, M. (2011). Mountain snow distribution governed by an altitudinal gradient and terrain roughness. *Geophysical Research Letters*. 38.

Lehning, M., Löwe, H., Ryser, M. and Raderschall, N. (2008). Inhomogeneous precipitation distribution and snow transport in steep terrain. *Water Resources Research*. 44.

López-Moreno, J., Fassnacht, S., Beguería, S. and Latron, J. (2011). Variability of snow depth at the plot scale: implications for mean depth estimation and sampling strategies. *The Cryosphere Discussions*, 5(3), pp.1627-1653.

Machguth, H., Eisen, O., Paul, F. and Hoelzle, M. (2006). Strong spatial variability of snow accumulation observed with helicopter-borne GPR on two adjacent Alpine glaciers. *Geophysical Research Letters*, 33(13).

McKay, D. M. and Gray, D. H. (2004). in (eds.) McKay, D. M. and Gray, D. H. *Handbook of Snow: Principles, Processes, Management & Use*. Blackburn Press: Caldwell

Messel, S. (1985). Energibalanse-undersøkelser på breer i Norge 1954-1981, in: *Glasiologiske undersøkelser i Norge 1982*, NVE rapport Nr. 1–85, (eds.) Roland, E. and Haakensen, N., Norwegian Water Resources and Energy Directorate, Oslo, Norway, pp45–59.

Mizukami, N. and Perica, S. (2008). Spatiotemporal Characteristics of Snowpack Density in the Mountainous Regions of the Western United States, *Journal of Hydrometeorology*. 9, pp.1416–1426.

Mott, R., Faure, F., Lehning, M., Löwe, H., Hynek, B., Michlmayer, G., Prokop, A. and Schöner, W. (2008). Simulation of seasonal snow-cover distribution for glacierized sites on Sonnblick, Austria, with the Alpine3D model. *Annals of Glaciology.* 49, pp.155-160.

Nesje, A., Lie, Ø. and Dahl, S. (2000). Is the North Atlantic Oscillation reflected in Scandinavian glacier mass balance records? *Journal of Quaternary Science*, 15(6), pp.587-601.

Neyman, J. (1934). On the Two Different Aspects of the Representative Method: The Method of Stratified Sampling and the Method of Purposive Selection. *Journal of the Royal Statistical Society*, 97(4), pp.558.

NVE. (2015). Hellstugubreen Climate Indicators. *NVE Climate Indicator Products*. Available at: http://glacier.nve.no/viewer/CI/en/nve/ClimateIndicatorInfo/2768. Accessed on 03/06/2015.

Oerlemans, J. (1992). Climate sensitivity of glaciers in southern Norway: application of an energy-balance model to Nigardsbreen, Hellstugubreen and Alfotbreen. *Journal of Glaciology*, 38, pp.223-232.

Pelto, M. (2000). The impact of sampling density on glacier mass balance determination. *Hydrological Processes.* 14(18), pp.3215-3225.

Pilz, J. and Spöck, G. (2007). Why do we need and how should we implement Bayesian kriging methods. *Stochastic Environmental Research and Risk Assessment.* 22(5), pp.621-632.

Pytte, R. (1964). *Hellstugubreen: En glasiologisk undersøkelse.* Hovedoppgåve i geografi, Universitetet i Oslo.

Rasmussen, L. and Andreassen, L. (2005). Seasonal mass-balance gradients in Norway. *Journal of Glaciology*, 51(175), pp.601-606.

Razali, N. M. and Wah, Y. B. (2011). Power comparisons of Shapior-Wilk, Kolmogorow-Smirnov, Lilliefors and Anderson-Darling tests. *Journal of Statistical Modelling and Analytics*, 2(1) pp.21-33.

Scheffran, J. and Battaglini, A. (2010). Climate and conflicts: the security risks of global warming. *Regional Environmental Change*, 11(S1), pp.27-39.

Schirmer, M., Wirz, V., Clifton, A, and Lehning, M. (2011). Persistence in intra-annual snow depth distribution: 1. Measurements and topographic control. *Water Resources Research*. 47.

Skaugen, T. (2007). Modelling the spatial variability of snow water equivalent at the catchment scale. *Hydrology and Earth System Sciences*, 11(5), pp.1543-1550.

Sturm, M. and Wagner, A. (2010). Using repeated patterns in snow distribution modeling: An Arctic example. *Water Resources Research.* 46(12).

Sørdal, I. (2013). *Kartlegging av temperaturtilhøva i Gråsubreen og Juvfonne.* Masteroppgåve i geofag, Institut for Geofag, Matematisk-naturvitskapleg fakultet, Universitetet i Oslo.

Tarboton, D. G., Blöschl, G., Cooley, K., Kirnbauer, R. and Luce, C. (2000), "Spatial Snow Cover Processes at Kühtai and Reynolds Creek," Chapter 7 in *Spatial Patterns in Catchment Hydrology: Observations and Modelling*, (Eds) Grayson, R and Blöschl, G. Cambridge University Press: Cambridge, pp.158-186.

Tedesco, M. (2015) (Eds). *Remote sensing of the cryosphere*. John Wiley & Sons: Oxford

Thibert, E., Vincent, C., Blanc, R., Eckert, N. (2008) Glaciological and volumetric mass-balance measurements: error analysis over 51 years, Sarennes Glacier, French Alps. *Journal of Glaciology*, Vol. 54 (186).

Wackernagel, H. (2003). *Multivariate geostatistics: An Introduction with Applications*. (3rd Edition). Springer: Berlin.

Wang, P. (2011). (Eds.) *Pattern recognition, machine intelligence and biometrics*. Higher Education Press Beijing

Watson, F., Anderson, T., Newman, W., Alexander, S. and Garrott, R. (2006). Optimal sampling schemes for estimating mean snow water equivalents in stratified heterogeneous landscapes. *Journal of Hydrology*, 328(3-4), pp.432-452.

WGMS (2013). *Glacier Mass Balance Bulletin No. 12 (2010–2011)*. Zemp, M., Nussbaumer, S. U., Naegeli, K., Gärtner-Roer, I., Paul, F., Hoelzle, M., and Haeberli, W. (eds.), ICSU(WDS)/IUGG(IACS)/UNEP/UNESCO/WMO, World Glacier Monitoring Service, Zurich, Switzerland.

Winstral, A. and Marks, D. (2014). Long-term snow distribution observations in a mountain catchment: Assessing variability, time stability, and the representativeness of an index site. *Water Resources Research.* 50(1), pp.293-305.

Zemp, M., Hoelzle, M. and Haeberli, W. (2009). Six decades of glacier mass-balance observations: a review of the worldwide monitoring network. *Annals of Glaciology*, 50(50), pp.101-111.

Zemp, M., Jansson, P., Holmlund, P., Gärtner-Roer, I., Koblet, T., Thee, P. and Haeberli, W. (2010). Reanalysis of multi-temporal aerial images of Storglaciären, Sweden (1959–99) – Part 2: Comparison of glaciological and volumetric mass balances. *The Cryosphere*, 4(3), pp.345-357.

Zemp, M., Thibert, E., Huss, M., Stumm, D., Rolstad Denby, C., Nuth, C., Nussbaumer, S., Moholdt, G., Mercer, A., Mayer, C., Joerg, P., Jansson, P., Hynek, B., Fischer, A., Escher-Vetter, H., Elvehøy, H. and Andreassen, L. M. (2013). Reanalysing glacier mass balance measurement series. *The Cryosphere*, 7(4), pp.1227-1245.

Øksendal, T. (2011). *En analyse av massebalansemålinger på Storbreen, Jotunheimen.* Masteroppgåve i geofag, Institut for Geofag, Matematisk-naturvitskapleg fakultet, Universitetet i Oslo.

Østrem, G. & M. Brugman (1991). Glacier mass-balance measurements. A manual for field and office work. National Hydrology Research Institute, *Scientific Report, No. 4.* Environment Canada, N.H.R.I., Saskatoon and Norwegian Water Resources and Energy Directorate, Oslo.

Østrem, G. (1961). Breer og morener i Jotunheimen. Norsk Geografisk Tidsskrift, 17(5-8) pp. 210-243.

6.1 NVE Glaciological Investigations in Norway

Bjarne Kjøllmoen (Ed.), Liss M. Andreassen, Hallgeir Elvehøy, Miriam Jackson and Rianne H. Giesen,(2011). *Glaciological investigations in Norway in 2010.* NVE Report 3 2011, 89 p. +app.

Bjarne Kjøllmoen (Ed.), Liss M. Andreassen, Hallgeir Elvehøy, Miriam Jackson and Rianne H. Giesen, (2010). *Glaciological investigations in Norway in 2009*. NVE Report 2 2010, 85 p. +app.

Bjarne Kjøllmoen (Ed.), Liss M. Andreassen, Hallgeir Elvehøy, Miriam Jackson, Rianne H. Giesen and Arve M. Tvede, (2009). *Glaciological investigations in Norway in 2008*. NVE Report 2 2009, 80 p. 6.

Bjarne Kjøllmoen (Ed.), Liss M. Andreassen, Hallgeir Elvehøy, Miriam Jackson, Rianne H. Giesen and Stefan Winkler, (2008). *Glaciological investigations in Norway in 2007*. NVE Report 3 2008, 91 p.

Bjarne Kjøllmoen (Ed.), Liss M. Andreassen, Hallgeir Elvehøy, Miriam Jackson, Arve M. Tvede, Tron Laumann and Rianne H. Giesen, (2007). *Glaciological investigations in Norway in 2006*. NVE Report 1 2007, 99 p.

Bjarne Kjøllmoen (Ed.), Liss M. Andreassen, Rune V. Engeset, Hallgeir Elvehøy, Miriam Jackson and Rianne H. Giesen, (2006). *Glaciological investigations in Norway in 2005*. NVE Report 2 2006, 99 p.

Bjarne Kjøllmoen (Ed.), (2005). *Glaciological investigations in Norway in 2004.* NVE Report 2 2005, 90 p.

Bjarne Kjøllmoen (Ed.), (2004). *Glaciological investigations in Norway in 2003.* NVE Report 4 2004, 97 p.

Bjarne Kjøllmoen (Ed.), (2003). *Glaciological investigations in Norway in 2002.* NVE Report 3 2003, 100p.

Bjarne Kjøllmoen (Ed.), (2003). *Glaciological investigations in Norway in 2001*. NVE Report 1 2003, 103 p.

Bjarne Kjøllmoen (Ed.), (2001). *Glaciological investigations in Norway in 2000*. NVE Report 2 2001, 122 p.

Bjarne Kjøllmoen (red.), (2000). *Glasiologiske undersøkelser i Norge 1999*. NVE rapport 2 2000, (140 s).

Bjarne Kjøllmoen (red.), (1999). *Glasiologiske undersøkelser i Norge 1998*. NVE rapport 5 1999 (119 s).

Bjarne Kjøllmoen (red.), (1998). *Glasiologiske undersøkelser i Norge 1996 og 1997*. NVE rapport 20 1998 (134 s).

Hallgeir Elvehøy, Nils Haakensen, Mike Kennett, Bjarne Kjøllmoen, Jack Kohler og Arve M.Tvede, (1997). *Glasiologiske undersøkelser i Norge 1994 og 1995.* NVE publikasjon 19 1997 (197 s.)

Nils Haakensen (red.), (1995). *Glasiologiske undersøkelser i Norge 1992 og 1993*. NVE Publikasjon nr 08 1995 (139 s.)

Hallgeir Elvehøy og Nils Haakensen (red.), (1992). *Glasiologiske undersøkelser i Norge 1990 og 1991*. NVE Publikasjon nr 03 1992 (103 s.)

Gunnar Østrem, Nils Haakensen, Bjarne Kjøllmoen, Tron Laumann og Bjørn Wold, (1991). *Massebalansemålinger på norske breer 1988 og 1989*. NVE Publikasjon nr 11 1991 (78 s.)

Tron Laumann, Nils Haakensen og Bjørn Wold, (1988). *Massebalansemålinger på norske breer 1985, 1986 og 1987*. NVE Publikasjon nr V 13 1988 (46 s.)

Ola Kjeldsen (red.), (1987). *Glasiologiske undersøkelser i Norge 1984*. NVE V-Publikasjon nr 01 1987 (70 s.)

Erik Roland og Nils Haakensen (red.), (1986). *Glasiologiske undersøkelser i Norge 1983*. NVE rapport nr 01 1986 (52 s.)

Erik Roland og Nils Haakensen (red.), (1985). *Glasiologiske undersøkelser i Norge 1982.* NVE rapport nr 01 1985 (102 s.)

Nils Haakensen (red.), (1984). *Glasiologiske undersøkelser i Norge 1981*. NVE rapport nr 01 1984 (79 s.)

Nils Haakensen (red.), (1982). *Glasiologiske undersøkelser i Norge 1980*. NVE rapport nr 01 1982 (87 s.)

Nils Haakensen og Bjørn Wold (red.), (1981). *Glasiologiske undersøkelser i Norge 1979*. NVE rapport nr 03 1981 (80 s.)

Bjørn Wold og Kjell Repp (red.), (1979). *Glasiologiske undersøkelser i Norge 1978.* NVE rapport nr 04 1979 (71 s.)

Bjørn Wold og Nils Haakensen (red.), (1978). *Glasiologiske undersøkelser i Norge 1977.* NVE rapport nr 03 1978 (54 s.)

Jon Ove Hagen (red.), (1977). *Glasiologiske undersøkelser i Norge 1976*. NVE rapport nr 07 1977 (94 s.)

Bjørn Wold og Jon Ove Hagen (red.), (1977). *Glasiologiske undersøkelser i Norge 1975.* NVE rapport nr 02 1977 (66 s.)

Arve M. Tvede, Bjørn Wold og Gunnar Østrem (red.), (1975). *Glasiologiske undersøkelser i Norge 1974*. NVE rapport nr 05 1975 (71 s.)

Arve M. Tvede (red.), (1975). *Glasiologiske undersøkelser i Norge 1973*. NVE rapport nr 01 1975 (72 s.)

Arve M. Tvede (red.), (1974). *Glasiologiske undersøkelser i Norge 1972.* NVE rapport nr 01 1974 (99 s).

Arve M. Tvede (red.), (1973). *Glasiologiske undersøkelser i Norge 1971*. NVE rapport nr 02 1973 (110 s).

Arve M. Tvede (red.), (1971). *Glasiologiske undersøkelser i Norge 1970*. NVE rapport nr 02 1971 (111 s).

Randi Pytte (red.), (1970*). Glasiologiske undersøkelser i Norge 1969*. NVE rapport nr 05 1970 (96 s).

Randi Pytte (red.), (1969). *Glasiologiske undersøkelser i Norge 1968*. NVE rapport nr 05 1969 (149 s).

Randi Pytte (red.), (1967). *Glasio-hydrologiske undersøkelser i Norge 1966.* NVE rapport nr 02 1967 (83 s).

Randi Pytte og Olav Liestøl (red.), (1966). *Glasio-hydrologiske undersøkelser i Norge 1965*. NVE årsrapport fra Brekontoret (64 s).

7. Appendix

7.1 Winter balance data distributions

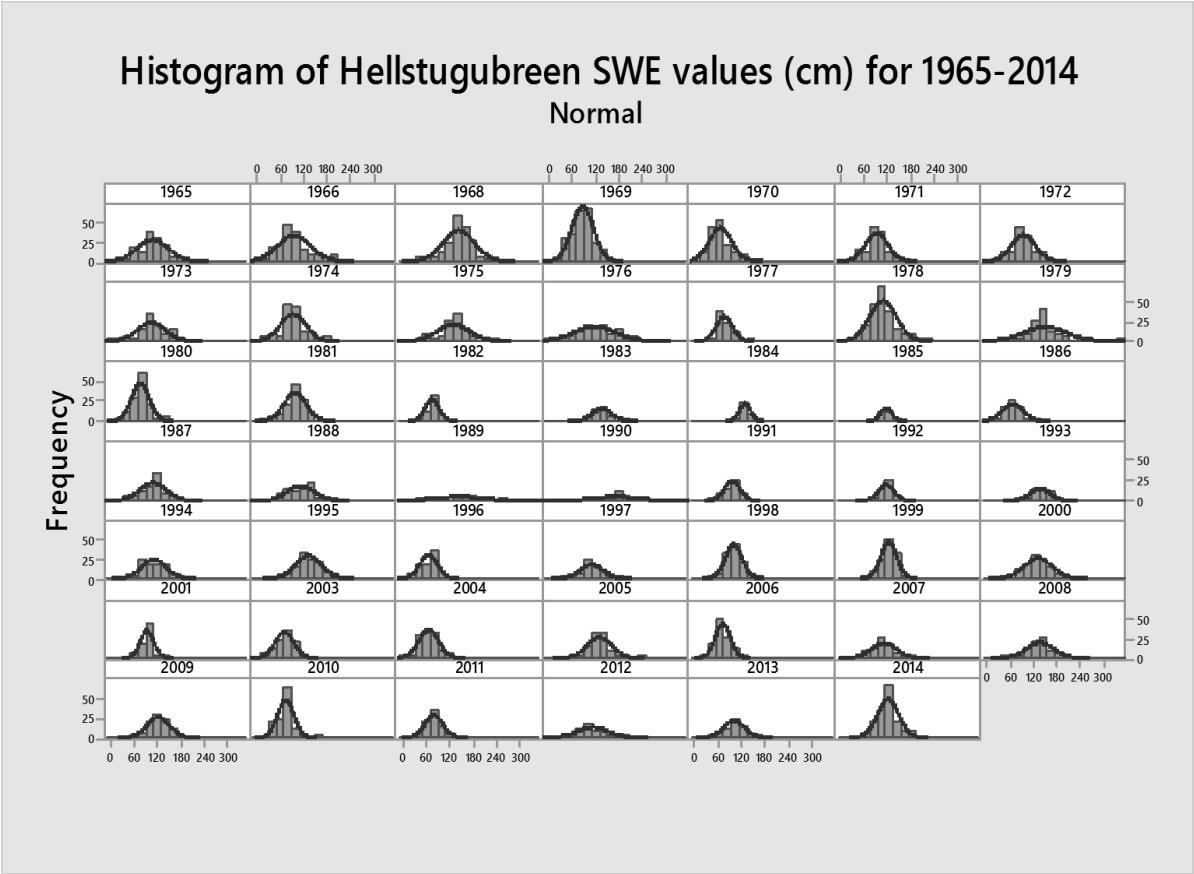

Figure 7.1.1 Histograms of Hellstugubreen SWE values, showing expected normal distribution curves. Note that all histrograms are presented at the same scale.

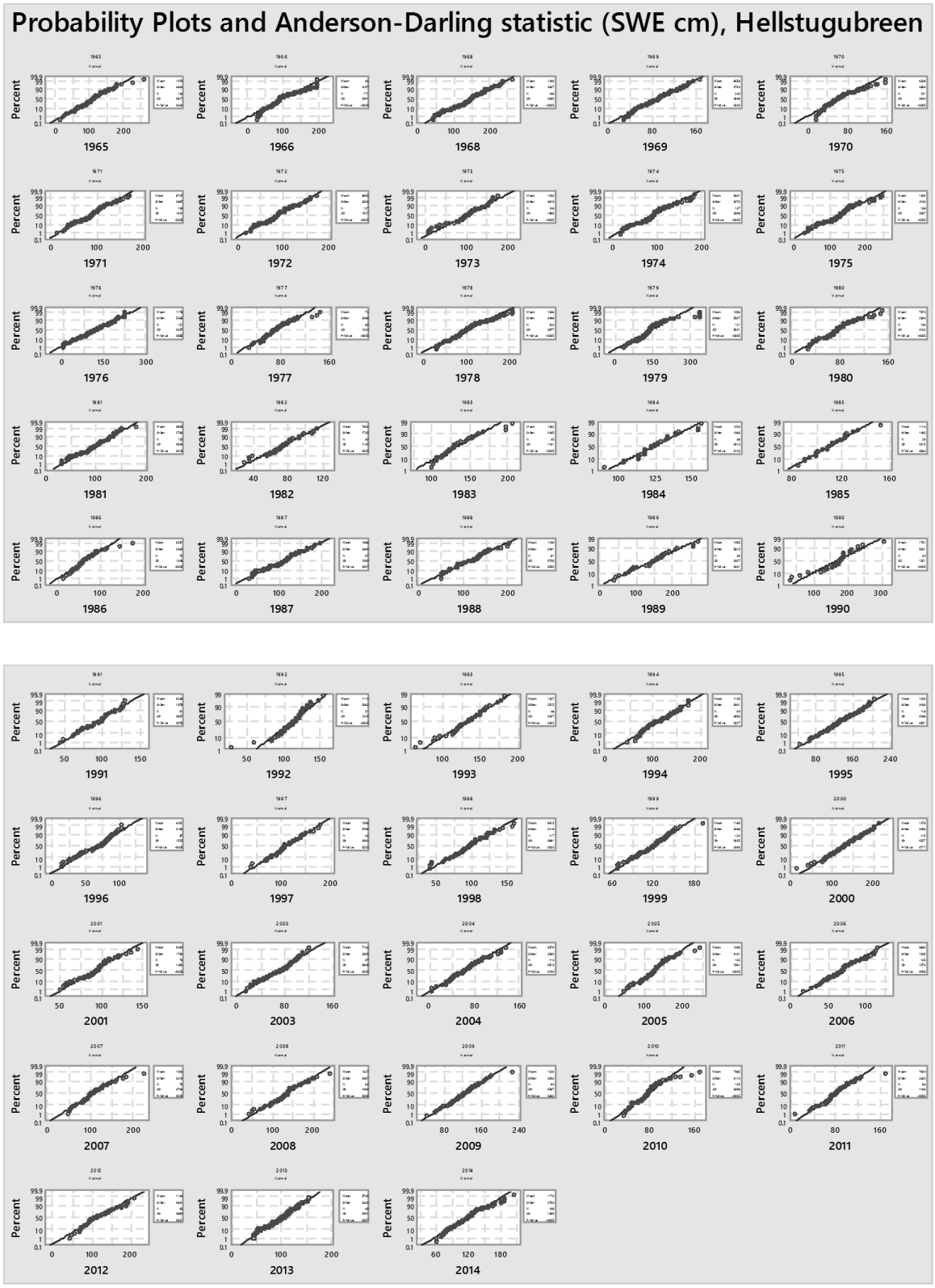

Figure 7.1.2 Probability Plots of SWE values for data years, Hellstugubreen.

Table 7.1-1 Anderson-Darling normality test P values,B_w and number of probings, Hellstugubreen. Note, greyed values denote non-normally distributed data years.

Year	Anderson-Darling normality test P value, Hellstugubreen	B_w	Number of probings
1965	0.034	1.27	136
1966	<0.005	0.94	171
1968	<0.005	1.38	198
1969	0.029	0.95	240
1970	<0.005	0.69	151
1971	<0.005	1.1	129
1972	<0.005	0.91	127
1973	<0.005	1.17	106
1974	<0.005	0.97	137
1975	<0.005	1.32	108
1976	0.585	1.12	121
1977	<0.005	0.67	80
1978	<0.005	1.04	223
1979	<0.005	1.4	121
1980	<0.005	0.78	136
1981	0.018	1.05	125
1982	0.005	0.83	60
1983	<0.005	1.43	45
1984	0.103	1.2	38
1985	0.833	1.09	29
1986	<0.005	0.73	70
1987	0.007	1.12	97
1988	0.05	1.22	81
1989	0.331	1.58	35
1990	<0.005	1.77	34
1991	0.078	0.95	61
1992	<0.005	1.16	51
1993	0.302	1.24	48
1994	0.027	1.22	94
1995	0.901	1.38	118
1996	<0.005	0.63	87
1997	0.252	1.14	62
1998	0.023	1.02	117
1999	0.096	1.22	122
2000	0.717	1.27	115
2001	<0.005	0.85	76
2003	0.035	0.72	97
2004	0.19	0.65	114
2005	<0.005	1.34	102

2006	0.008	0.73	105
2007	0.045	1.03	76
2008	0.008	1.41	84
2009	0.362	1.3	94
2010	<0.005	0.74	125
2011	<0.005	0.83	83
2012	0.021	1.21	63
2013	0.267	1.05	69
2014	<0.005	1.16	168

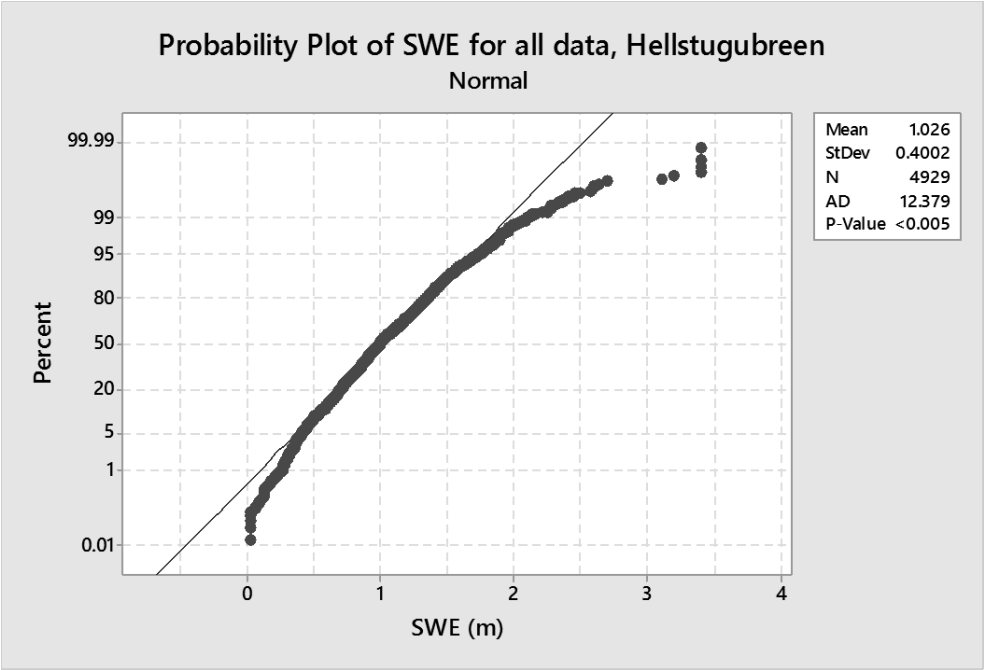

Figure 7.1.3 Probability plot of merged normalised SWE data for all years, Hellstugubreen.

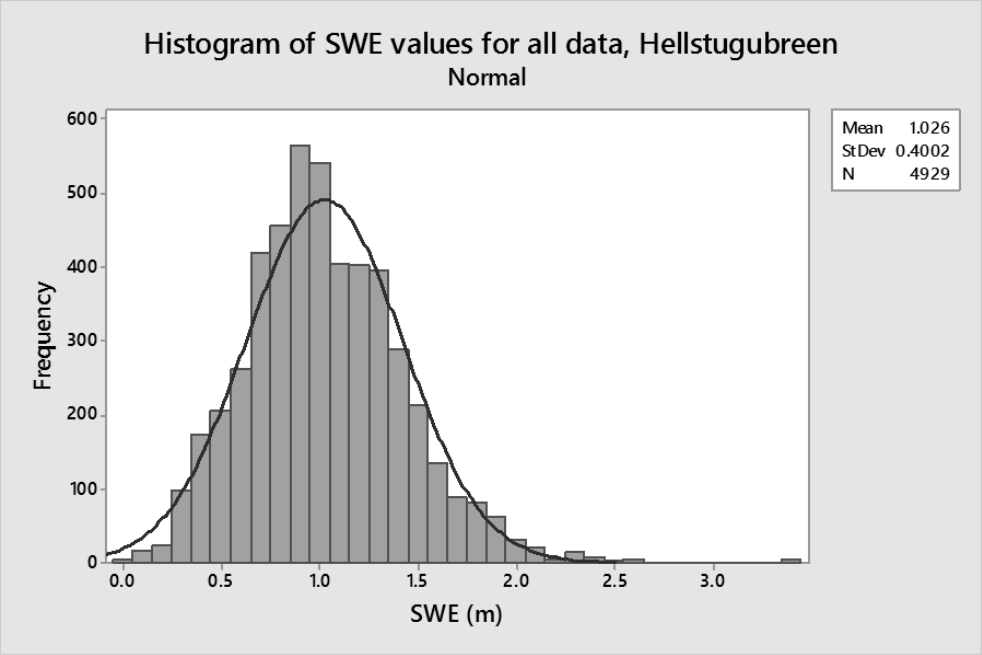

Figure 7.1.4 Histogram of merged normalised SWE data for all years, Hellstugubreen.

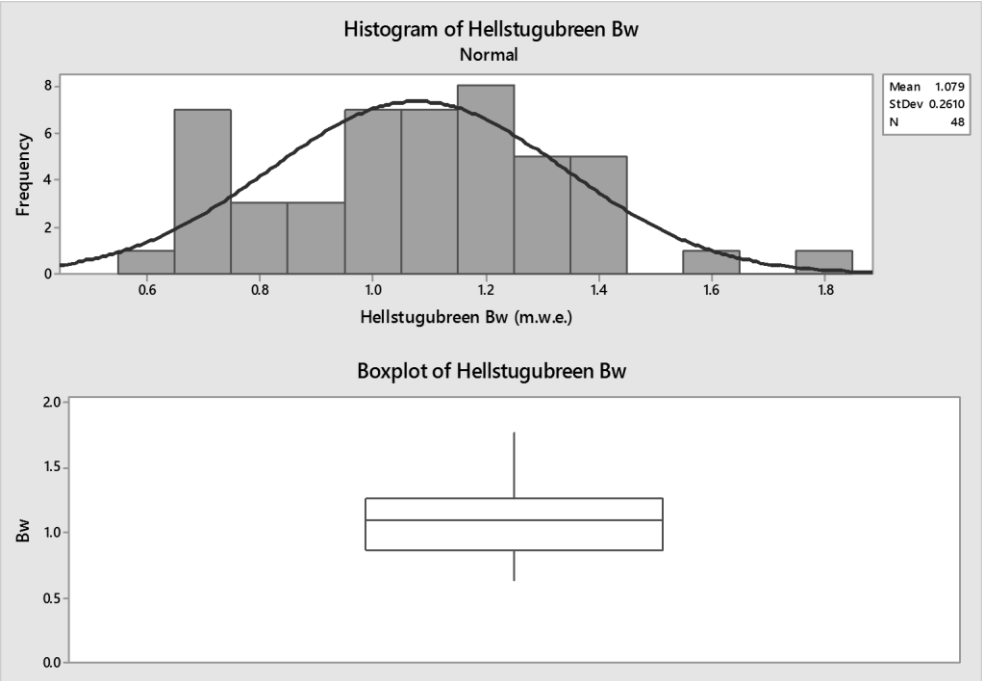

Figure 7.1.5 Distribution of overall B_w values shown as a histogram and boxplot, Hellstugubreen.

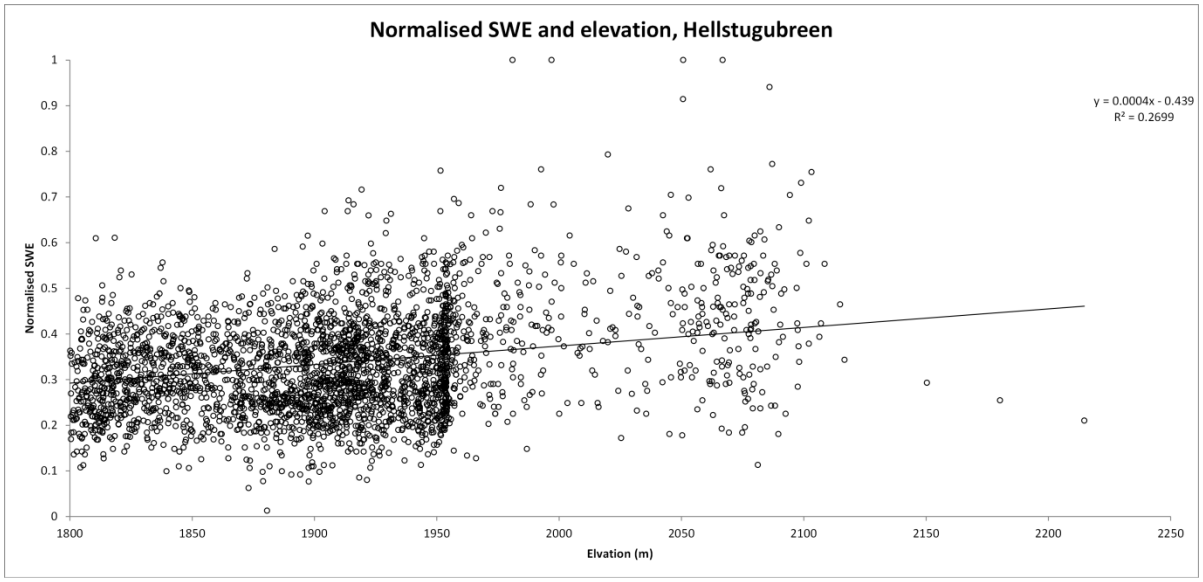

Figure 7.1.6 Scatterplot of normalised B_w for all years and elevation, Hellstugubreen

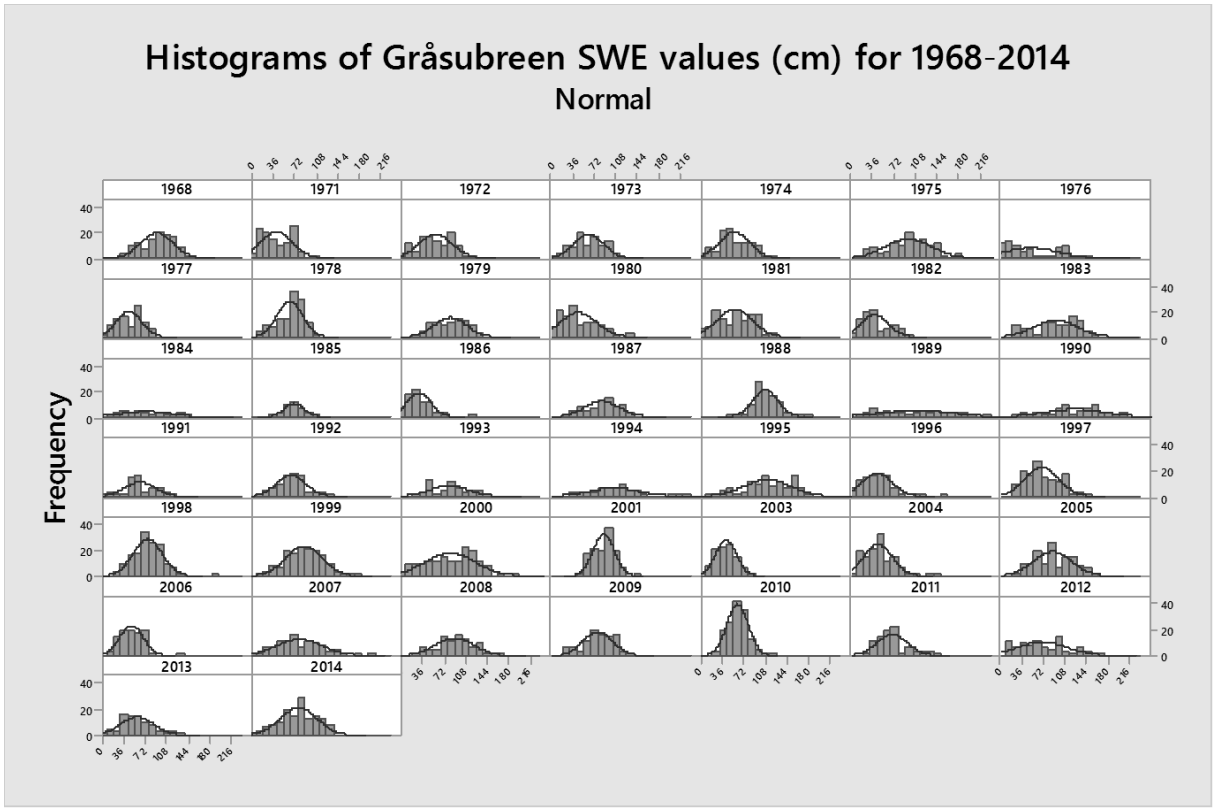

Figure 7.1.7 Histograms of Gråsubreen SWE values, showing expected normal distribtion curves. Note that all histograms are presented at the same scale.

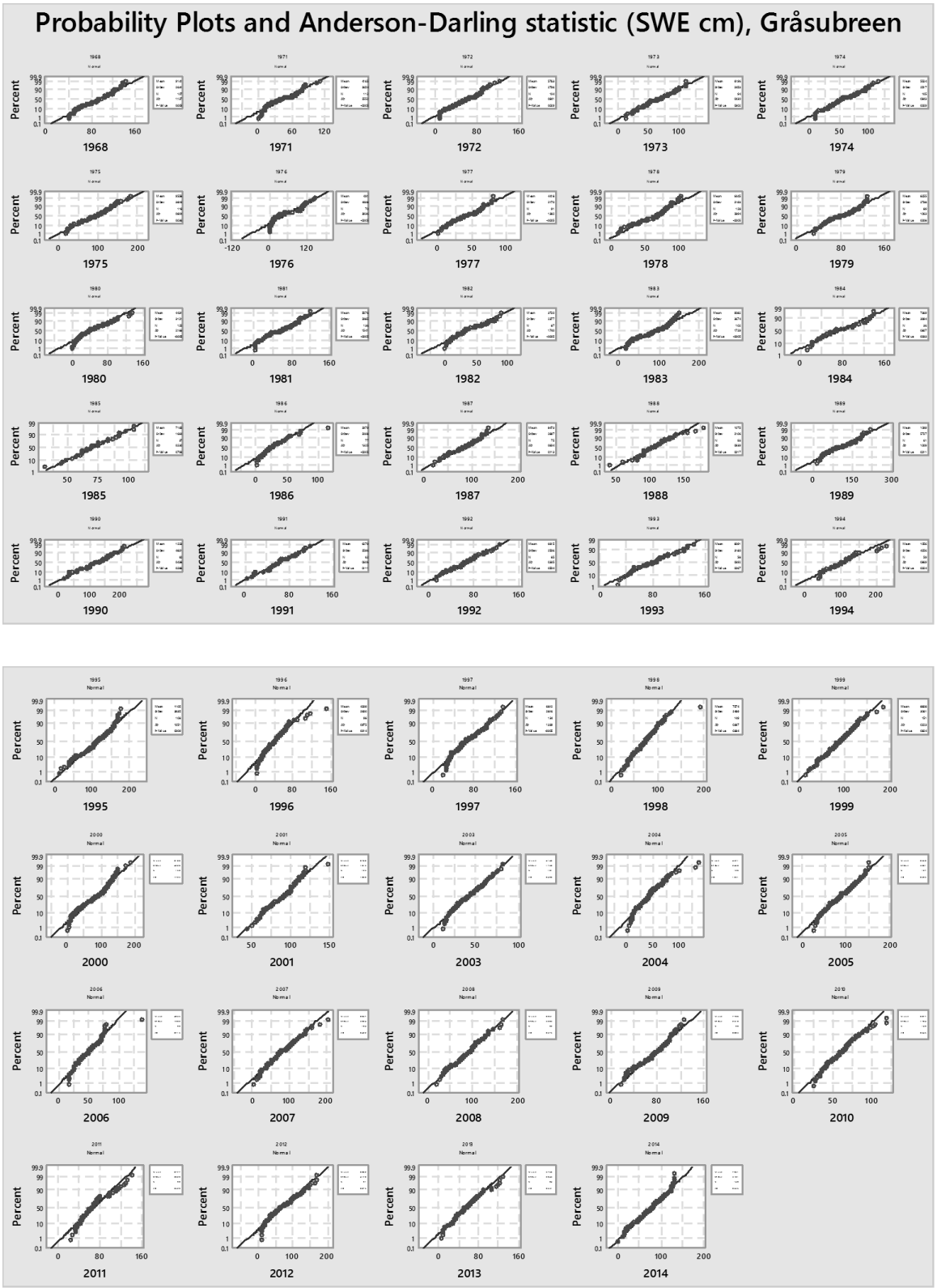

Figure 7.1.8 Probability Plots of SWE values for data years, Gråsubreen.

Table 7.1-2 Anderson-Darling normality test P values, B_w and number of probings, Gråsubreen. Note, greyed values denote non-normally distributed data years.

year	Anderson-Darling normality test P value, Gråsubreen	B_w	Number of probings
1968	0.005	1.03	107
1971	<0.005	0.49	112
1972	0.029	0.66	104
1973	0.302	0.72	94
1974	0.029	0.59	105
1975	0.036	0.91	118
1976	<0.005	0.62	70
1977	<0.005	0.51	91
1978	<0.005	0.67	128
1979	0.008	0.91	89
1980	<0.005	0.43	125
1981	<0.005	0.6	136
1982	<0.005	0.5	87
1983	<0.005	0.92	102
1984	0.033	0.96	36
1985	0.793	0.74	37
1986	<0.005	0.41	77
1987	0.113	0.93	75
1988	0.017	1.08	93
1989	0.011	1.09	61
1990	0.286	1.33	60
1991	0.111	0.66	62
1992	0.504	0.7	85
1993	0.067	0.92	58
1994	0.024	1.15	59
1995	0.009	1.17	108
1996	0.014	0.52	98
1997	<0.005	0.67	134
1998	0.384	0.77	149
1999	0.824	0.9	151
2000	<0.005	0.87	158
2001	0.008	0.8	123
2003	0.209	0.44	101
2004	<0.005	0.48	126
2005	0.118	0.83	127
2006	0.06	0.51	98
2007	0.316	0.61	104
2008	0.406	0.95	92
2009	0.023	0.8	98

2010	0.158	0.54	149
2011	<0.005	0.67	90
2012	0.024	0.6	91
2013	0.17	0.67	84
2014	0.168	0.86	140

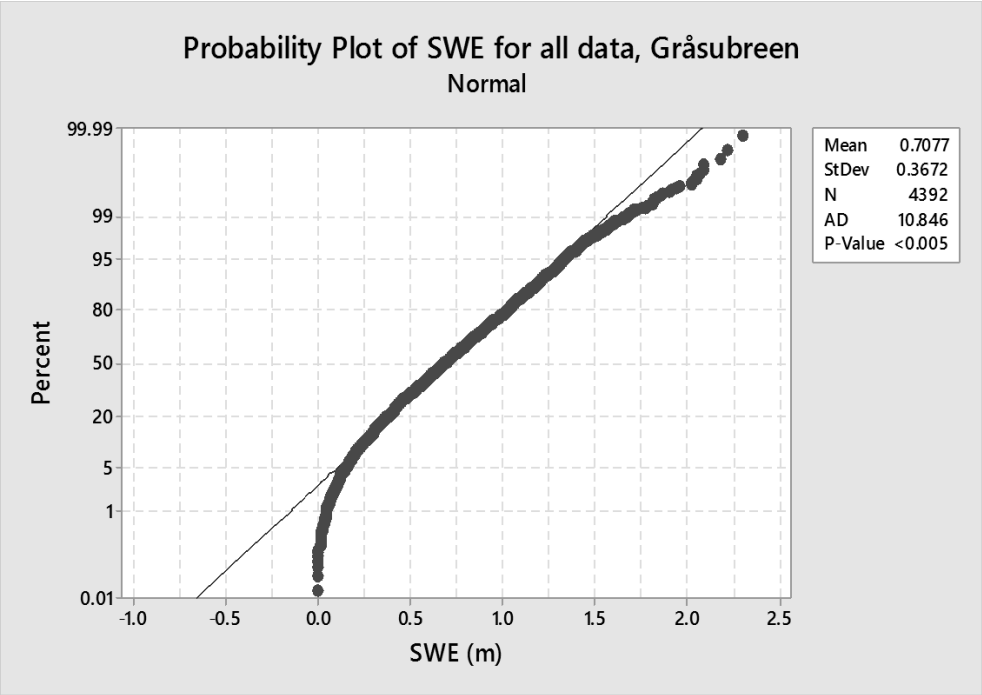

Figure 7.1.9 Probability plot for merged normalised SWE data for all years, Gråsubreen.

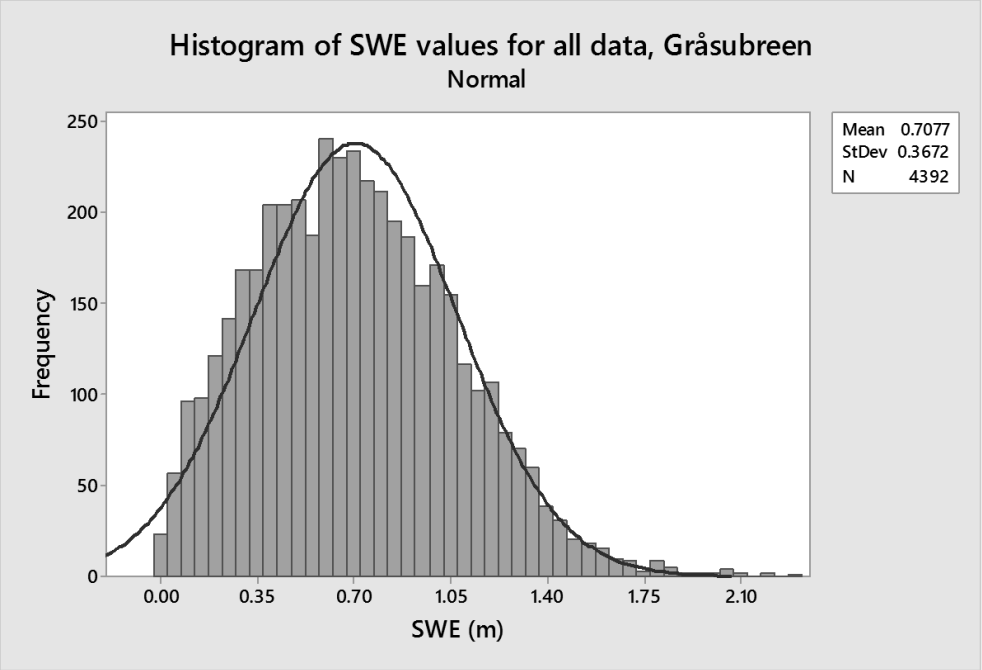

Figure 7.1.10 Histogram of merged normalised SWE data for all years, Gråsubreen.

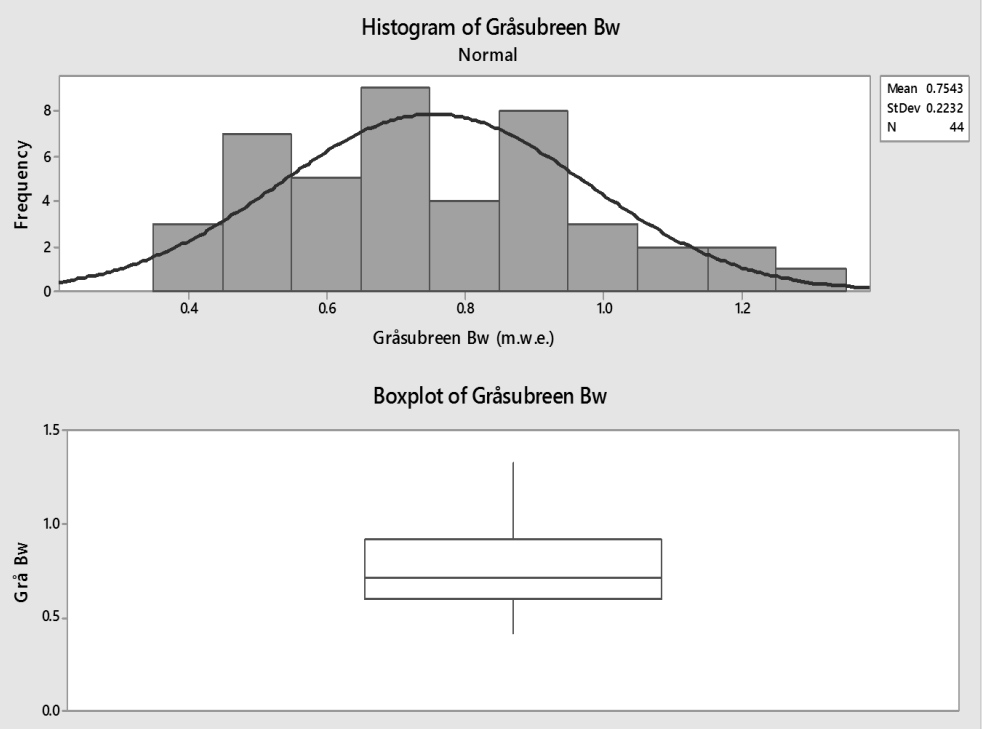

Figure 7.1.11 Distribution of overall B_w values shown as a histogram and boxplot, Gråsubreen.

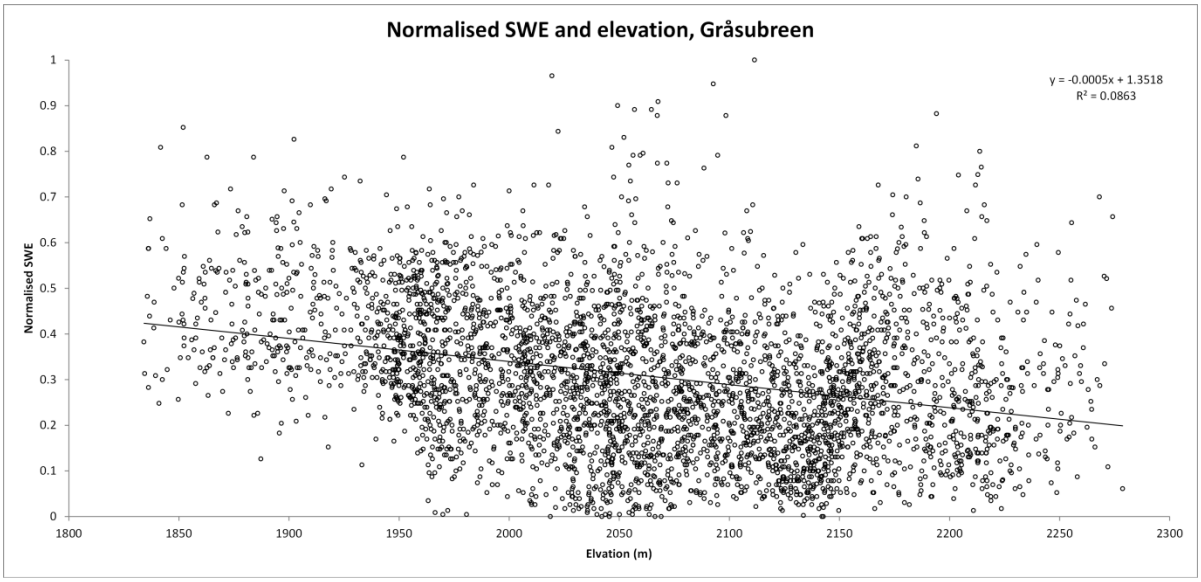

Figure 7.1.12 Scatterplot of normalised B_w for all years and elevation, Gråsubreen.

7.2 Wind frequency data distributions

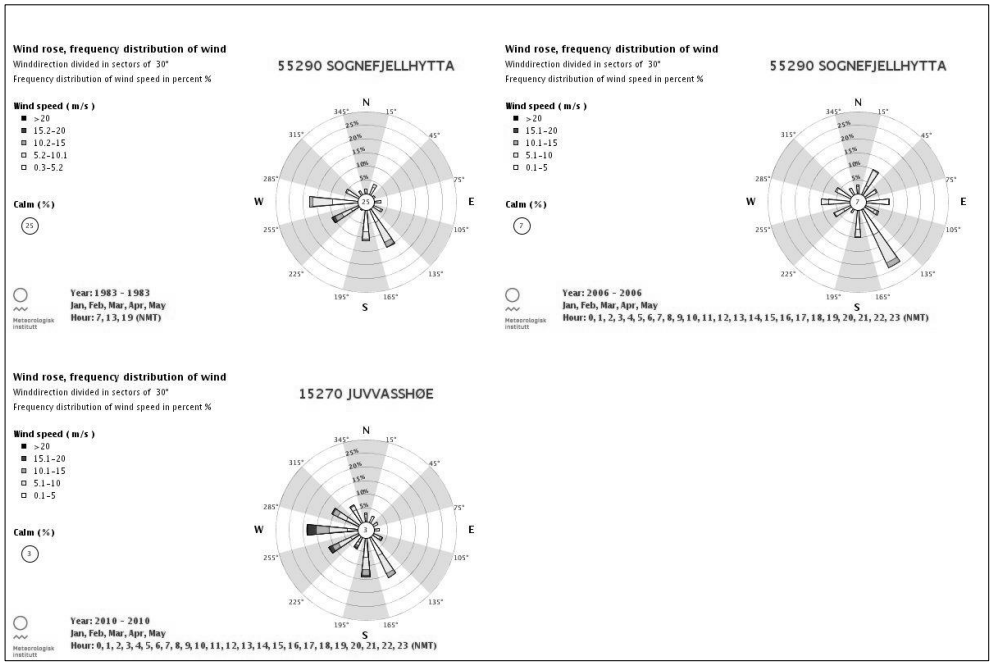

Figure 7.2.1 Wind frequency distributions for high RMSE years, at Hellstugubreen.

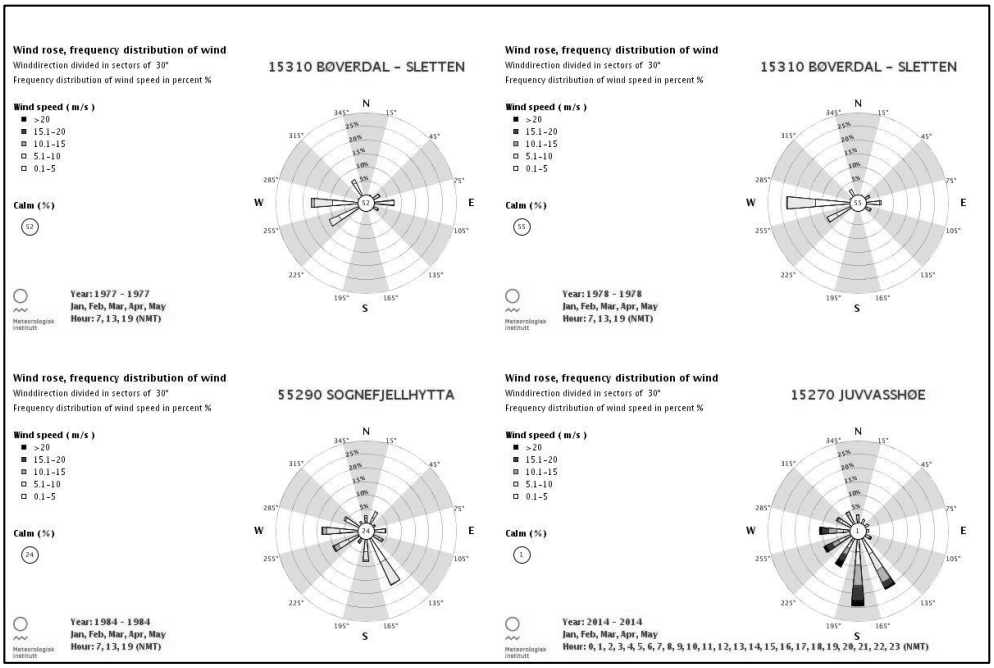

Figure 7.2.2 Wind frequency distributions for high RMSE years, at Gråsubreen.

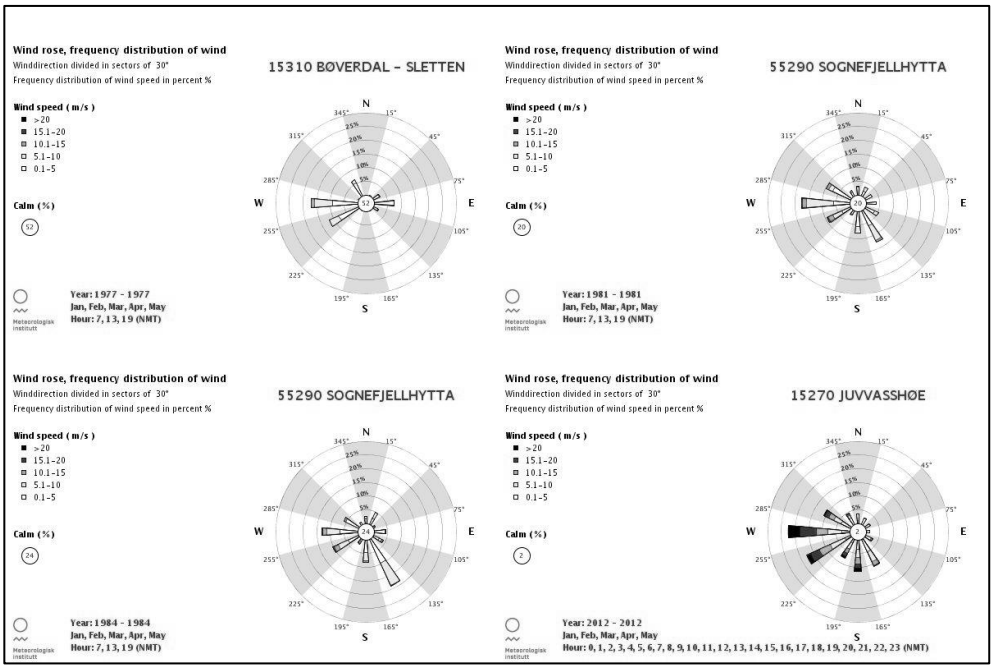

Figure 7.2.3 Wind frequency distributions for low correlation years, at Hellstugubreen.

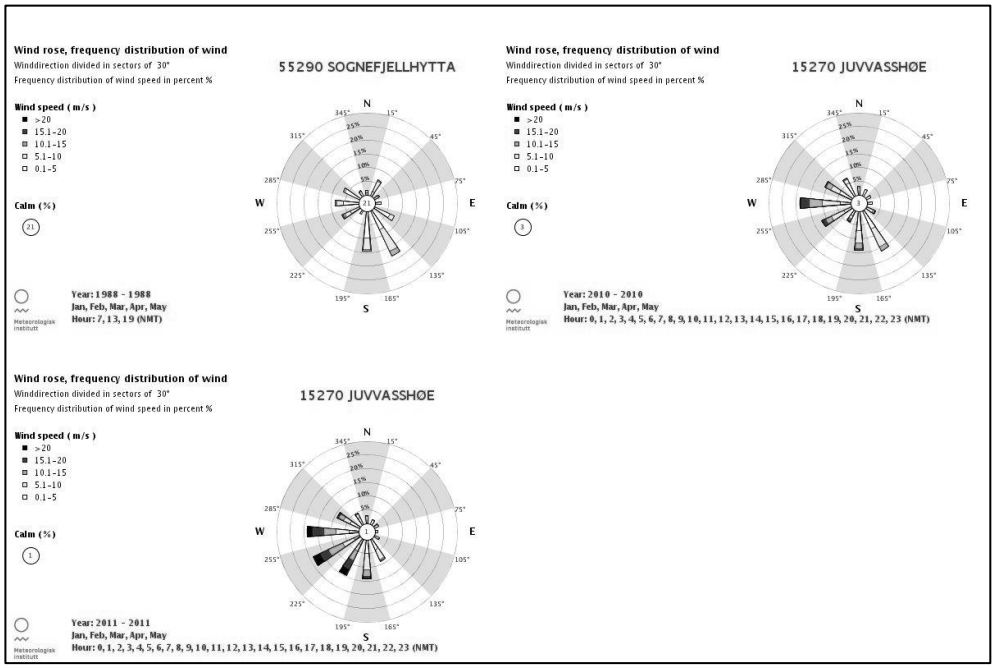

Figure 7.2.4 Wind frequency distributions for low correlation years, at Gråsubreen.

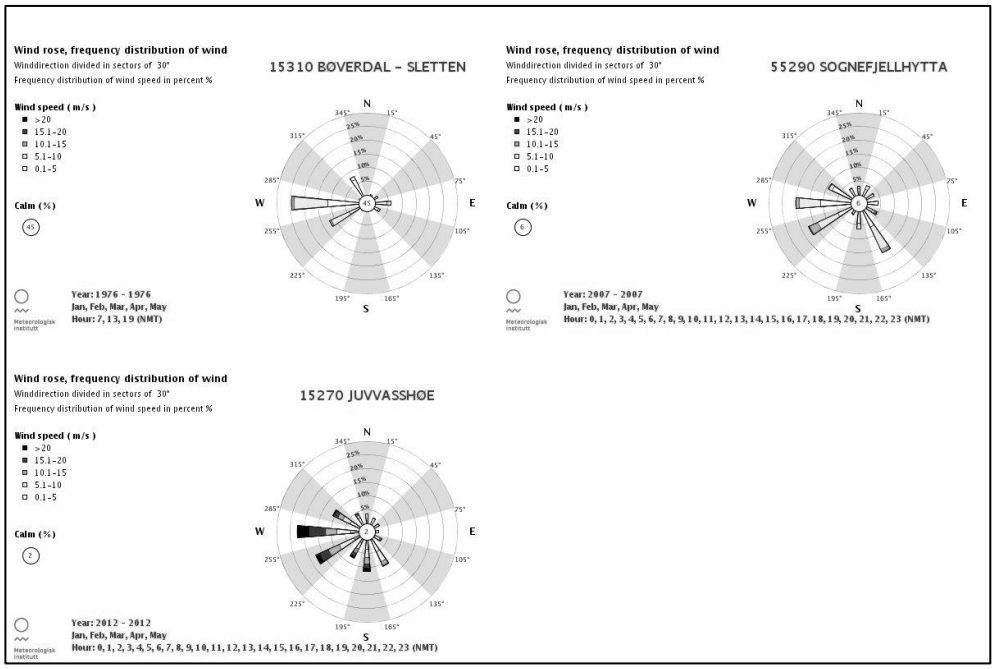

Figure 7.2.5 Wind frequency distributions for high error years, at Gråsubreen